Spring 2010

Lacustrine Sediment Record of Multiple Quaternary Lava Dams on the Owyhee River, Southeastern Oregon

Caitlin Anne Orem
Central Washington University

LACUSTRINE SEDIMENT RECORD OF MULTIPLE QUATERNARY LAVA DAMS

ON THE OWYHEE RIVER, SOUTHEASTERN OREGON

A Thesis

Presented to

The Graduate Faculty

Central Washington University

In Partial Fulfillment

of the Requirements for the Degree

Master of Science

Geology

---

by

Caitlin Anne Orem

May 2010

CENTRAL WASHINGTON UNIVERSITY

Graduate Studies

We hereby approve the thesis of

Caitlin Anne Orem

Candidate for the degree of Master of Science

APPROVED FOR THE GRADUATE FACULTY

______________ ______________________________
Dr. Lisa Ely, Committee Chair

______________ ______________________________
Dr. Beth Pratt-Sitaula

______________ ______________________________
Dr. Marie Ferland

______________ ______________________________
Dean of Graduate Studies

ABSTRACT

LACUSTRINE SEDIMENT RECORD OF MULTIPLE QUATERNARY LAVA DAMS ON THE OWYHEE RIVER, SOUTHEASTERN OREGON

by

Caitlin Anne Orem

May 2010

Multiple lava dams and correlating lakes impacted the Quaternary evolution of the Owyhee River. Sediment records from lava-dammed lakes were investigated to understand effects of the West Crater (WC) lava dam (~70 ka), the Saddle Butte 2 lava dam (~144 ka), and the Bogus Rim lava dam (~1.9 Ma). Evidence from the WC lava dam and related features indicates that dam duration consisted of five stages (1) dam and lake formation at ~70 ka; (2) dam overflow and lake sedimentation from ~70–46 ka; (3) removal of lava dam and lake termination from ~46 ka to at least 36 ka; (4) incision of underlying units from ~36–15 ka; and (5) incision to modern river level from ~15–0 ka. The WC lava dam lasted ~24,000 yrs and ~31,000 yrs of incision was needed to reestablish the river. This information gives perspective on the effects of lava dams on fluvial landscapes.

ACKNOWLEDGMENTS

Financial assistance was provided by the NSF grant EAR-0617234, the NSF GK-12 WATERS grant, the CWU Department of Geology, and the CWU Graduate Studies and Research. A special thank you to the participants in the Owyhee River Project (ORIGIN) including Lisa Ely, Kyle House, Jim O'Connor, Liz Safran, Duane Champion, Cooper Brossy, Gordon Grant, Terri Garside, Nichole Knepparth and Natalia Deligne. This project would not have existed or been completed without them and their discussions and help in the field. Thanks to the UNR geology field camp class of 2009, Anya Shultz, Chris Markley, Delaney Paullus, and Jordon Bright for their backbreaking work as field assistants.

At CWU I was fortunate to have knowledgeable staff to answer questions and fix technical glitches, including Jocelyn Robinette, Linda Shepard, Craig Scrivner, and Andy Miner. I am also greatly indebted to the Department of Geology faculty members and my fellow graduate students for their assistance and friendship.

I'd also like to thank those outside of CWU for their help. Nick Foit at the WSU GeoAnalytical Lab completed the tephrochronology analyses. OSL samples were analyzed and dated at Utah State University by Tammy Rittenour. Dr. Scott Starratt at the USGS, Menlo Park, was kind enough to analyze diatom samples.

My committee members Beth Pratt-Sitaula, and Marie Ferland were very helpful during field and laboratory research, as well as thesis writing. Lastly, I would like to thank my advisor Lisa Ely who provided guidance and support through this project and many other ventures during my time at CWU.

TABLE OF CONTENTS

TABLE OF CONTENTS (continued)

Chapter Page

LIST OF TABLES

LIST OF FIGURES

LIST OF FIGURES (continued)

CHAPTER I

INTRODUCTION

The goal of this study is to use lacustrine sediments and fluvial terraces to quantify the effect of lava dams on the evolution of the Owyhee River, Oregon. The Owyhee River is located in the southeastern corner of Oregon (Fig. 1). Over the last 2 million years the river has been influenced by at least nine intracanyon lava flows, each with the potential to dam the river and form a lake. The three best-preserved lava dams and their correlating lakes are addressed in this study: the West Crater (WC) lava dam and lake (~70 ka; Bondre, 2006; Brossy, 2007), the Saddle Butte 2 (SB2) lava dam and lake (~144 ka; B. Turrin, unpublished data), and the Bogus Rim (BR) lava dam and lake (~1.9 Ma; Bondre, 2006). The primary focus of this study is the WC lava dam because it is the youngest lava dam and has the best-preserved lacustrine sediment sections.

The lacustrine sediment associated with each lava dam, and the terraces cut into them, may provide insight into the duration and incision of the lava dams and paleo-lake conditions. The five main objectives of this study are (1) locate and map lacustrine sediments and fluvial terraces in the vicinity of the lava dams; (2) date the lacustrine sediments to document the duration of the lakes and the lava dams; (3) thoroughly describe the lacustrine sediment for evidence of changes in river routing, discharge, and sedimentation in response to the lava dam; (4) correlate fluvial terraces to lava-damming events to understand the incision history of each dam; and (5) investigate the lacustrine sediments for microfauna and organic material that may provide additional information about the paleo-lake environments.

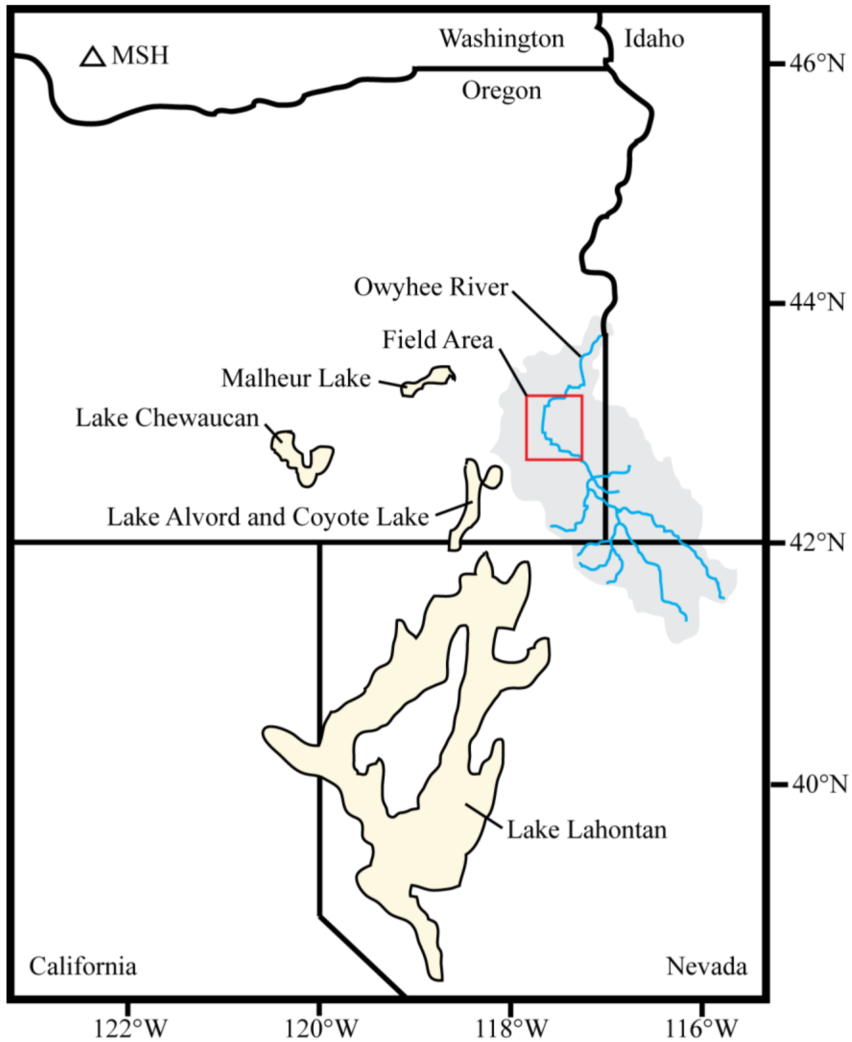

Figure 1. Map showing the field area (red box, detailed in Figure 2) and the Owyhee River and drainage basin (gray shading). Also shown are the locations and possible extents of Lake Chewaucan, Malheur Lake, Lake Alvord, Coyote Lake, and Lake Lahontan during the Last Glacial Maximum (20–15 ka). Mount St. Helens (MSH) is also pictured.

This thesis is one of the first studies that uses lacustrine sediments to form a detailed record of lava-damming events. There have only been a limited number of studies on lava dams and few of these studies have utilized the lacustrine sediment record deposited behind lava dams. Lacustrine sediment deposits resulting from lava-damming events, and terraces cut into those sediments during subsequent incision, can provide useful information about the duration of the lava dam, its incision, and the effects it had on the landscape. Lacustrine sediment also acts as a "snapshot" of the paleohydrology, paleotopography, and paleoenvironment at the time of the lava-damming event. The most notable study on lava-dammed lacustrine sediments was by Malde (1982) who described the Yahoo Clay, a lacustrine sediment unit behind the McKinney Basalt lava dam (~52 ka; Tauxe et al., 2004) on the Snake River. In Malde's (1982) Yahoo Clay study, the lacustrine sediments were described and some paleo-lake conditions were inferred, but no geochronological constraints were provided. Other studies have used lacustrine sediments to describe the effects of landslide dams and paleo river conditions on the Rio Grande in New Mexico (Reneau and Dethier, 1996) and the Marsyangdi River in the Himalayas (Pratt-Sitaula et al., 2007).

Lava dams can impact river systems in significant ways. When a lava dam blocks a river it can divert the channel around the dam, eroding an epigenetic gorge into the adjacent rock (Ouimet et al., 2008) and widen the valley or canyon. The extent of channel diversion can be limited in incised canyons, but may be larger when rivers are not constrained by topography. Both diversion and valley widening can affect river profiles and stream morphology on a reach scale. On the Owyhee River, lava dams may have impacted the evolution of the river channel by impinging on the lateral migration area of the river, causing the migration area to become smaller over time. This limit on lateral migration and erosion may have been partially responsible for increased vertical erosion and incision of the Owyhee River Canyon. After the Owyhee River Canyon was incised many events, including the WC and SB2 lava dams, continued to influence the river channel. Potential constraints on lava dam and lake duration from this study may quantify the amount of time the Owyhee River required to return to equilibrium following emplacement of a lava dam. Estimates have been made for lava dams that catastrophically failed, but such quantification would be the first of its kind for incised lava dams.

Another effect of lava dams on rivers is sedimentation behind the dam and a limiting of sediment supply to lower reaches. This limiting of sediment supply can impede abrasion and incision downstream, including over the dam surface. If abrasion is one of the processes eroding the dam, tools must be available on the surface of the dam. Lava dams can be eroded through abrasion if sediment is carried over the dam after sediment fills the lake basin, but may also occur without sediment accumulating to the top of the dam if ample material is already available on the dam surface. Lava dams also may be removed by catastrophic failure of the dam or surrounding units (Fenton et al., 2004; Fenton et al., 2006) or by knickpoint migration processes.

The Owyhee River and the surrounding area are not well studied due to its isolated location and complex geology. Lacustrine sediments accumulated behind the lava dams on the Owyhee River may provide information pertaining to Quaternary environments and climate, which are locally unknown. Additionally, the lacustrine sediments in the Owyhee River canyon can act as an analog for understanding sedimentation in other natural lakes and man-made reservoirs. Quantitative and qualitative information from this study can be used in future landscape evolution models and studies in similar settings. Understanding the interaction between volcanism and the Owyhee River is imperative to fully comprehend the evolution of this drainage system.

Regional and Geologic Setting

The field area is located along the middle section of the Owyhee River between the town of Rome, Oregon and the geographical feature of Iron Point, Oregon (Fig.2). The Owyhee River drains ~28,360 km^2 including parts of Idaho, Oregon, and Nevada (Craft et al., 2000). Within the Owyhee River drainage basin are the Owyhee Mountains, the Santa Rosa Range, the Tuscarora Mountains, the Independence Mountains, the Mahogany Mountains, and the Crooked Creek Range. The Owyhee River carries water from these mountain ranges through the sagebrush steppe of the Owyhee Desert to join the Snake River near the town of Owyhee, Oregon. Modern mean discharge for the Owyhee River at Rome, Oregon is 26.4 $m^3\ s^{-1}$ (1950-2008; USGS, 2008).

Bedrock in the field area includes interbedded basalt flows, rhyolite flows, and fluvial and lacustrine sediments of late Tertiary and Quaternary age (Hart and Mertzman, 1983; Cummings et al., 2000). The late Tertiary bedrock units are related to the Oregon-Idaho graben. The Oregon-Idaho graben is a north-south aligned, synvolcanic graben that formed after the emplacement of the Columbia River Basalt Group ~16 Ma (Cummings et al., 2000). The Oregon-Idaho graben was formed between 15.3 and 10.5 Ma with distinctive types of volcanism and fluvial-lacustrine deposition occurring at different times throughout formation (Cummings et al., 2000). Active formation and subsidence of the Oregon-Idaho graben stopped at approximately the same time as volcanism in the Snake River Plain started (~11 Ma; Cummings et al., 2000). Many fluvio-lacustrine

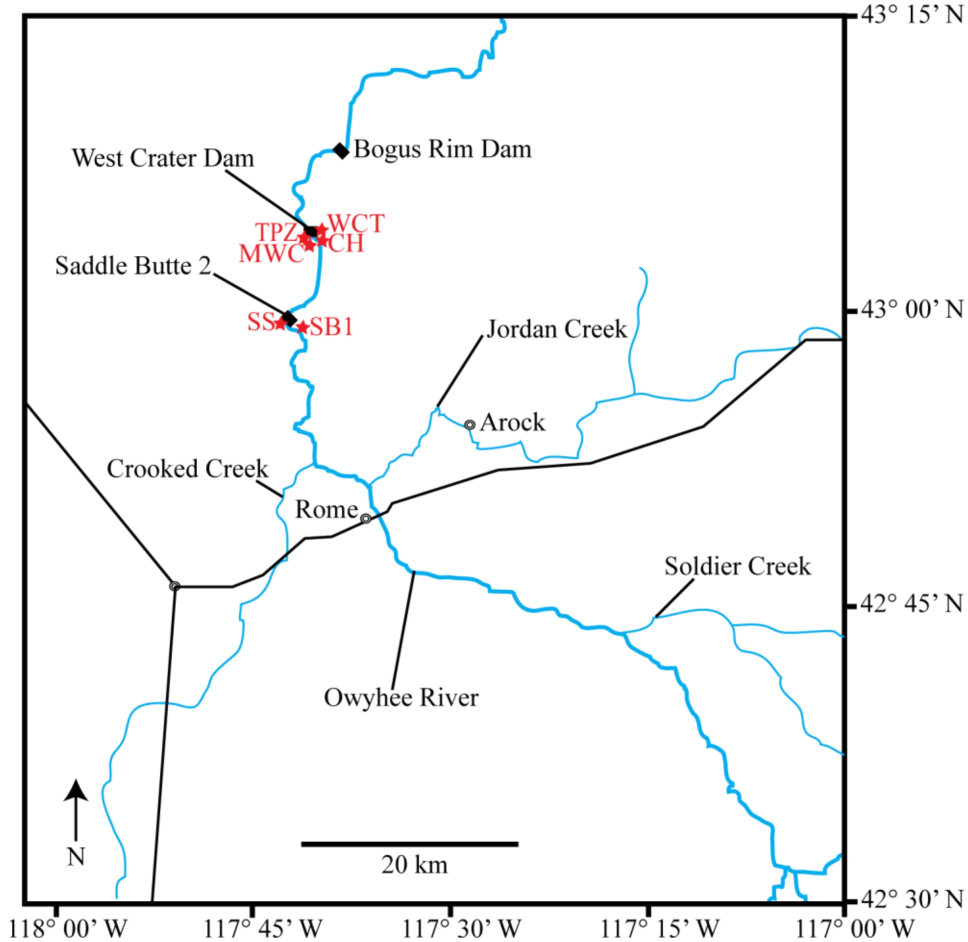

Figure 2. Map of field area including the Owyhee River and its tributaries Jordan Creek, Crooked Creek, and Soldier Creek. Red stars and text indicate the location of the six main Quaternary lacustrine sediment sections described in this study and black dashes indicate the three lava dams focused upon in this study. Location of Iron Point is the same as the Bogus Rim Dam.

units, including those connected with the Oregon-Idaho graben, are present in the field area (Ferns et al., 1993). Sediments not associated with the Oregon-Idaho graben were deposited in extensional basins between 4 and 4.5 Ma and may correlate to the Glenns Ferry and Upper Chalk Butte Formations of the Snake River Plain (Hart and Mertzman, 1983). These sediments also include the Rome Beds in the vicinity of Rome, Oregon (Wolf and Ellison, 1971). The Tertiary fluvio-lacustrine sediments that line the Owyhee

River Canyon are important due to their role as sediment sources for the Quaternary lacustrine sediments and because they are the supporting units for the lava dams.

An age estimate of ~7 Ma exists for the inception of the Owyhee River. Beranek et al. (2006) completed detrital zircon work on sediment within the Owyhee River and Snake River. They found zircons with signatures matching volcanic events in northern Nevada in the fluvial deposits of the Snake River dating to ~7 Ma. This indicates that the Owyhee River was an integrated river flowing from northern Nevada to the Snake River sometime after 7 Ma.

As many as nine intra-canyon lava flows have entered the Owyhee River Canyon during the last ~2 million years. Descriptions of many of the lava dams caused by these intra-canyon flows can be found in Brossy (2007). Lacustrine sediments impounded behind the intra-canyon lava flows are present in the field area upstream of the various dam sites and are the primary focus of this study. Gravel deposits that overlay the lacustrine sediments and the terrace surfaces cut into them are also investigated.

Background on Lava Dams and Lacustrine Records

Lava dams have affected many rivers in the western United States (Howard et al., 1982), although cases from other parts of the world have also been documented (Nott et al., 1996; Freeth and Rex, 2000, Huscroft et al., 2004; Komatsu et al., 2008). Examples of lava-dammed rivers in the western U.S. and Canada include the Colorado River (Hamblin, 1994; Fenton et al., 2000; Fenton et al., 2006; Crow et al., 2008), the Little Colorado River (Duffield et al., 2006), the Columbia River (Waters, 1973), the Crooked River (Peterson and Groh, 1970), the Snake River (Trimble and Carr, 1961; Malde, 1982;

Malde, 1987; Brand and White, 2007), the Boise River (Howard et al., 1982), the Yukon River (Huscroft et al., 2004), the Bear River (Bouchard et al., 1998), and the Truckee River (Birkeland, 1963).

The emplacement, duration, and removal style of lava dams varies from site to site. The most well-studied lava dams are those in the western Grand Canyon. In 1974, Hamblin described and classified 13 lava dams and the lake sediments behind them in the Grand Canyon (Hamblin, 1994). Most of these dams are thought to have lasted less than 20,000 yrs (Hamblin, 1994). The lakes behind these dams may have filled with water within days to a few decades, and filled with lacustrine sediment in as little as 3000 yrs (Hamblin, 1994). Today, some of the lacustrine sediments Hamblin referred to have been explained by different means (Kaufman et al., 2002) and no conclusive evidence for sedimentation by the large lakes invoked by Hamblin (1994) exists. Other studies have shown that at least five Grand Canyon lava dams failed catastrophically (Fenton et al., 2004) due to undermining and flow at the base or abutments of the dams (Fenton et al., 2000). These failures created very large outburst floods (Fenton et al., 2006). Fenton et al. (2000) found no trace of lacustrine sediments in any of the outburst deposits, but the lava-dammed lakes must have filled with large volumes of water to create such large-scale outburst floods.

Lava dams on the Owyhee River can be compared to other lava-damming events in the Great Basin and Snake River Plain Provinces due to similar geomorphology, volcanism, and climate. Lava dams on the Snake River and Boise River are perhaps the best comparisons. Howard et al. (1982) described evidence for numerous lava dams on the Boise River during the Quaternary. Pillow structures in the Smith Prairie Basalt suggest that the lake created by this lava dam filled very quickly (< 6 months) and water was able to interact with the later lobes of the lava flow that formed the lava dam. Another lava-dam, formed by the Steamboat Rock Basalt, created a lake that lasted long enough to deposit a lacustrine unit. Howard et al. (1982) noted but did not describe the lacustrine sediments associated with these lava dams described on the Boise River.

Lacustrine sediments impounded behind lava dams have been utilized to understand lava dam structural integrity and incision, paleoclimate, and paleotopography (Malde, 1982; Nott et al., 1996). For example, Malde (1982) investigated the Yahoo Clay, the lacustrine sediment unit deposited behind the late Pleistocene McKinney Basalt lava dam on the Snake River. The Yahoo Clay filled a 183 m-deep basin behind the McKinney lava dam. Malde (1982) speculated that the dam persisted longer than usual because of water leakage through conduits in the dam and through the subsurface, which allowed for the large amount of sediment to be impounded behind the dam. Stream discharge and sedimentation rates during the deposition of the Yahoo Clay may have been much higher due to cool, moist conditions during the damming of the lake, as indicated by the microfauna and pollen present in the lake sediments (Malde, 1982). The Snake River eventually bypassed the McKinney lava dam by incising an epigenetic gorge into the canyon wall made up of Glenns Ferry Formation. This created the modern canyon, which is very similar to the paleo-canyon outlined by the McKinney Basalt. The Yahoo Clay is not well preserved due to incision of the Snake River and Lake Bonneville outburst floods. The Yahoo Clay is typically found in tributary canyons and makes up terraces, sometimes being found in sections up to 28 m thick along the Snake River Canyon.

Modern Lake Owyhee

Although no intact lava dams exist on the Owyhee River, the modern Lake Owyhee is an analog for the lava-dammed lakes. Lake Owyhee is the reservoir behind the Owyhee Dam located approximately 80 km downstream of the field area. Lake Owyhee is the largest reservoir in the state of Oregon at a surface area of 51.5 km^2 and a typical volume of 8.82×10^8 m^3 (Craft et al., 2000). Lake Owyhee stretches approximately 60 km from the inflow of the Owyhee River to the Owyhee Dam (Craft et al., 2000).

Lakes created by lava dams are more similar to man-made dams built in stream restrictions than natural lakes formed in depressions (Hamblin, 1994). The Owyhee Dam was built geologically instantaneously in a deeply incised canyon and immediately began to form Lake Owyhee as the Owyhee River filled the canyon to near the crest of the dam. The intracanyon lava flows on the Owyhee River would have created lakes in a similar way. Lake Owyhee filled and became a long, narrow lake much like the lakes that would have formed behind the lava dams. Like Lake Owyhee, the main inflow to the lava-dammed lakes was the Owyhee River. The inflow point would have been located tens of kilometers upstream from the lava dam.

Craft et al. (2000) completed the most comprehensive study of Lake Owyhee to date. Lake Owyhee is characterized as eutrophic and experiences periodic algal blooms. Turnover in the reservoir is not well understood, but is believed to occur during the early spring. Thermal stratification increases with depth and distance from Owyhee River inflow, with the strongest stratification occurring in the summer. Low levels of dissolved oxygen (DO) occur throughout the water column and anaerobic conditions are common especially at depth and during long periods of stratification. The pH values ranged from approximately 7 to 10 over the reach and depth measured, and changed seasonally. Generally, pH did not follow stratification in the spring, but in the summer higher pH was measured in the epilimnetic region, while lower layers remained near or below neutral.

Perhaps the most extraordinary finding of Craft et al. (2000) was the continuous presence of suspended sediment in Lake Owyhee. Large sediment particles settle out over the first 0.8 km from the inflow point, but suspended sediment is seen throughout the reservoir. Wind mixing is cited as one explanation for the constant suspended sediment load observed in the epilimnetic layer.

Microfauna of the Owyhee River Region

The late Tertiary sedimentary units in southeastern Oregon are known for their fossil assemblages. The Deer Butte, Grassy Mountain, Owyhee Basalt, and Sucker Creek formations outcrop just north and northwest of the study area (Central Snake Project, 1994). These formations contain mammal, fish, mollusk, plant, ostracod, and diatom fossils of Miocene through Pliocene age (Krebs et al., 1987; Central Snake Project, 1994; Downing and Park, 1998).

In this study, diatoms are important when trying to reconstruct past lake conditions. Diatoms are found in the modern Owyhee River and are preserved in the Tertiary lacustrine sediment within the field area. Diatom faunas are controlled by water turbulence, nutrient availability, salinity, pH, light, and water temperature and therefore can be helpful in determining these variables for past environments (Abbott, 1972). The small size of diatoms increases the chance of preservation, but their fragility and silicic framework make compaction and high pH conditions detrimental to their preservation (Abbott, 1972).

Modern and Past Climates of Southern Oregon

Climate in the Owyhee River drainage basin is semi-arid and characterized by hot, dry summers and cold winters (Central Snake Projects, 1994; Craft et al., 2000). Temperatures in the Owyhee River region vary from 41.7°C to -26.7°C and average annual precipitation is 25 cm, with most of the precipitation being in the form of snow (Craft et al., 2000). Most precipitation is derived from winter storms originating in the west and northwest (Central Snake Projects, 1994). In general the area is windy, with the strongest winds usually come from the southwest or in association with large frontal storms (Central Snake Projects, 1994). Sagebrush, wheatgrass, saltbrush, and greasewood comprise more than 90% of the land cover in the Owyhee River drainage basin (Craft et al., 2000; Hardy et al., 2003).

Although climate can vary over relatively small areas (Mock and Bartlein, 1994), paleoclimate records from nearby locations may help to understand general temperature and precipitation conditions during the Quaternary in the Owyhee River drainage basin. Many of the paleoclimate records in the region are from Pleistocene pluvial lake sediments.

The position of the Laurentide ice sheet was a large factor affecting climate variations in the western United States during the Late Quaternary (Benson and

Thompson, 1987; Zielinski and McCoy, 1987; Hostetler and Benson, 1990; Hostetler et al., 1994; Benson et al., 1998; Licciardi, 2001). In the Western United States, the jet stream acts as the boundary between tropical warm air masses to the south and polar cold air masses to the north (Licciardi, 2001). The position of the jet stream may have been controlled by the extent of the Laurentide ice sheet and a high-pressure cell that formed over it (Benson and Thompson, 1987). When the Laurentide ice sheet was at its furthest extent, the jet stream may have been pushed south, creating a colder and wetter climate in the Great Basin and vice versa (Benson and Thompson, 1987, Zielinski and McCoy, 1987; Benson et al., 1998; Licciardi, 2001).

Although the position of the jet stream and Laurentide ice sheet may have been the major factors affecting climate variability during the Late Quaternary, in modern times and in paleo-records, variations between basins in close proximity to each other can be found (Zielinski and McCoy, 1987). Regional variations are harder to explain, but today many of these variations are linked to the El Nino-Southern Oscillation (ENSO) (Licciardi, 2001). Orogenic effects, elevation differences, and principal weather direction could also be causes of local variations (Zielinski and McCoy, 1987).

CHAPTER II

METHODS

Mapping and Elevation Measurements

Geologic mapping was completed in the field using USGS 7.5' topographic base maps. Aerial photography and Light Detection and Radar Digital Elevation Models (LiDAR DEM) of certain locations were used for identifying and mapping geologic features. Handheld GPS (Garmin 60csx), handheld eye levels, and a laser range finder were used to measure the elevation of specific points and terraces. River kilometers (Rkm) from Rome, Oregon were used to locate features along the river.

The LiDAR DEM data was analyzed using ArcMap 9.2 (ESRI, 2006) and Globalmapper 8.03 (2007). LiDAR DEM data was used to check field GPS measurements and to create cross sections. Volume and area measurements for the WC and SB2 lakes were calculated using LiDAR DEM data, USGS 10-m DEM data, and USGS 7.5' topographic maps. Cross sections of the Owyhee River Canyon were created every 1 km, from the dam sites to the lakes furthest extents upstream. Cross-sectional areas were calculated using LiDAR DEM data and Globalmapper software applications. Some cross sectional areas were calculated with topographic maps where LiDAR DEM date was not available. The lengths of the river canyon flooded by the WC and SB2 lakes were multiplied by the respective average cross sectional areas to find the volume of each lake. Lake volume was not calculated for the BR lake.

Stratigraphic Descriptions

Stratigraphic descriptions of Quaternary lacustrine sediments were completed at five locations: Caitlin’s Hill (CH) section, Main West Crater (MWC) section, West Crater (WCT) Top section, Sand Springs (SS) section, and Saddle Butte 1 (SB1) section (Table 1). These locations were the most well-preserved and largest exposures of Quaternary lacustrine sediment relating to the WC and SB2 lava dams. Other sections were identified and briefly described including the Trapezoid (TPZ), Bone Hill, (BH).

TABLE 1. STRATIGRAPHIC SECTION LOCATIONS

Stratigraphic Section	Latitude	Longitude	River Km
Caitlin’s Hill (CH)	43° 03.768’	-117° 41.173’	37.65 RR
Bone Hill (BH)	43° 03.824’	-117° 41.174’	37.80 RR
West Crater Top (WCT)	43° 04.120’	-117° 40.856’	38.00 RR
Trapezoid (TPZ)	43° 03.999’	-117° 41.784’	38.00 RL
Main West Crater (MWC)	43° 03.750’	-117° 41.674’	37.55 RL
Sand Springs (SS)	43° 00.842’	-117° 43.347’	30.50 RL
Saddle Butte 1 (SB1)	43° 00.206’	-117° 43.862’	27.65 RR

Descriptions of sections included approximate grain size, color, bedding and structures, sorting, estimates on induration, and weathering character. In total, ~70 vertical meters of section were cleared and described in detail. Sediment samples (approximately 500 mm^3) were collected at least every 0.5 m from the main sections, with some areas being sampled more thoroughly due to features of interest. A total of 250 samples were collected from the five primary stratigraphic sections (the CH, WCT, MWC, SS, and SB1 sections). Special attention was given to locating potential organic material for radiocarbon dating, tephra layers for tephrochronology, and clean sand layers for optically-stimulated luminescence (OSL) dating.

Grain Size Analysis

Forty-four representative samples from the five main sediment sections were analyzed for grain size using a Malvern Mastersizer 2000 laser diffractometer (Sperazza et al., 2004). Laser diffractometry measures the size of grains by detecting how each grain deflects the laser (Sperazza et al., 2004) and allows all three axes of a grain to be measured, unlike traditional sieving methods that only measure two axes.

The stirrer on the laser diffractometer was set at 750 rpm and the pump at 2100 rpm to check for a clean background reading. Samples were well mixed (dry) and added to the sonicating bath until the laser obscuration was within the correct range (Sperazza et al., 2004). Samples were sonicated at >80% strength and stirred at >800 rpm for approximately one minute to thoroughly mix and separate grains. Samples were then run with the sonicator turned off, the stirrer set at 750 rpm, and the pump set at 2100 rpm (Sperazza et al., 2004). Samples were run with the material refractive index set at 1.52 and the absorption set at 0.1. These values are the default setting, but also represent the sand and silt composition in the samples.

Each sample was measured three times during each run. The three results were averaged into a final result. Some clay-rich samples were problematic because of grains aggregating after sonication or during the analyses. Samples suffering from aggregation sometimes resulted in three dissimilar measurements. If aggregation was observed, or if the three runs were dissimilar, then the sediments were soaked in approximately 200 ml of deionized (DI) water with 5 g of sodium hexametaphosphate for one day (Sperazza et al., 2004) and reanalyzed.

Microfauna Analysis

Thirteen reconnaissance samples collected (August 2008) from the MWC and CH sections, and sediments related to the BR lava dam, and all 250 sediment samples collected from the five lacustrine sediment sections during this study, were checked for calcareous microfauna with dilute HCl acid. Those samples that effervesced (n = 9) were soaked in ~700 mL of water with 10 mg of sodium bicarbonate and 1 mg of sodium hexametaphosphate for 2 to 5 days. These samples were then wet sieved over a nested stack of 250 μm, 125 μm, and 45 μm sieves. The residue samples were air dried and scanned for specimens under 10x magnification.

All 75 samples from the CH section were also analyzed for the presence of silicic diatom frustules. Approximately 1 g of each sample was rinsed with DI water, agitated, and centrifuged for 5 minutes at 3500 rpm. Excess DI water was decanted off and a small amount of the remaining sediment was prepared as a smear slide. The smear slides were visually searched for diatom frustules and any other microfossil material at 40x magnification. Five of the most diatom-rich samples from the CH section (samples CH-3, CH-14, CH-41, CH-53, and CH-73) were sent to Dr. Scott Starratt at the USGS, Menlo Park, for diatom identification.

Geochronology

Prior to this study, ^{3}He cosmogenic, $^{40}Ar/^{39}Ar$, and paleomagnetic susceptibility dating methods were used to date fluvially carved surfaces, boulders, and lava flows. Information on these methods can be found in Brossy (2007). Additional dates on the lacustrine sediments were obtained during this study using geochemical tephra correlation and optically-stimulated luminescence (OSL) methods. Five light-colored airfall tephra deposits within the CH, MWC, TPZ, and BH sections were sampled. Tephra samples were sent to the School of Earth and Environmental Sciences GeoAnalytical Lab at Washington State University for electron beam analysis on tephra shard material. Tephra samples were analyzed under a microscope to identify key minerals for tephra identification. The major-element chemical compositions of the tephra shards were determined using a JEOL 8500F field emission electron microprobe. Dr. F.F. Foit correlated the major-element compositions to known tephra samples in the western U.S.A. tephrochronology database.

OSL samples were collected from sandy lenses within some lacustrine sediment sections including the MWC, CH, and SS sections. Samples were collected following instructions from the Utah State University Optically Stimulated Luminescence Laboratory (USU OSL Lab). Dr. Tammy Rittenour analyzed samples at the USU OSL Lab.

CHAPTER III

RESULTS

Five large sections of Quaternary lacustrine sediment were located through field observations (Figs. 2 and 3). Geomorphic relations, elevation, and sediment characteristics were used to distinguish Quaternary lacustrine sediments from older, pre-lava dam sediments. In general, the Quaternary lacustrine sediments were less indurated and contained fewer large clasts than the Tertiary sediment units. The Quaternary lacustrine sediments lack colorful horizons and are not interbedded with basalt flows as the Tertiary sediment units were.

It is important to understand the geomorphic relations between the Quaternary lacustrine sediments and other units in the field area to insure correct identification and interpretation. Caitlin's Hill (the location of the CH section) is located at Rkm 37.65 and sits near the modern river level immediately upstream from the WC lava dam (Fig. 4). The base of the section is not exposed, so it is unclear if the section sits on bedrock or alluvial deposits. The base of other sections, such as the MWC (Fig. 4) and the TPZ sections (Rkm 37.55 and 38 respectively), on lap the SB2 basalt flow and therefore are less ambiguous. The SS and SB1 sections (Rkm 30.5 and 27.65 respectively) (Figs. 5 and 6) are both located on top of the SB1 basalt flow. Smaller pods of Quaternary lacustrine sediments on lap and overlie the SB2 basalt flow in the vicinity of Sand Springs located at Rkm 30.5 and at another location at Rkm 36.5.

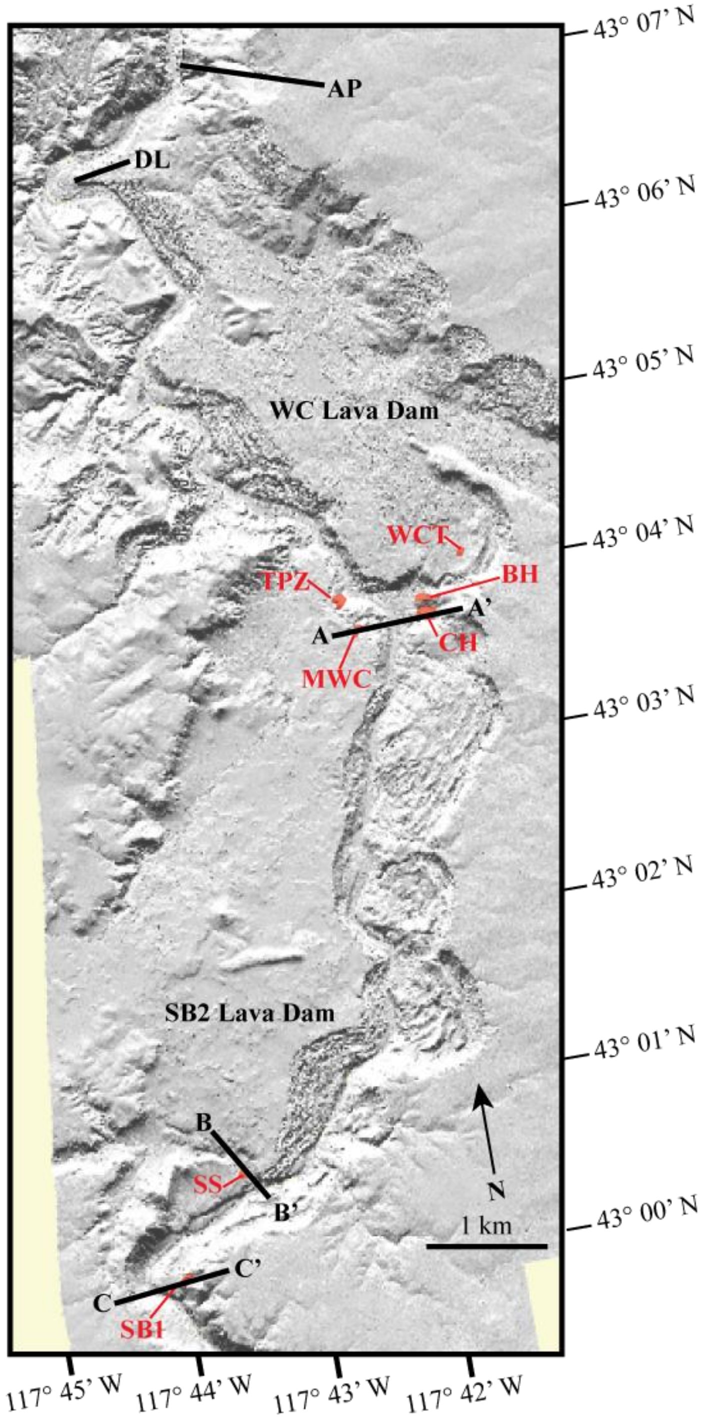

Figure 3. LiDAR imagery of the study reach including all stratigraphic section locations Stratigraphic sections are labeled in red; West Crater Top (WCT), Bone Hill (BH), Trapezoid (TPZ), Caitlin's Hill (CH), Main West Crater (MWC), Sand Springs (SS), and Saddle Butte 1 (SB1). Cross section lines are shown in black lines for Figures 4-6 are also shown. Dog Leg terraces (DL) and Airplane Point (AP) are also labeled.

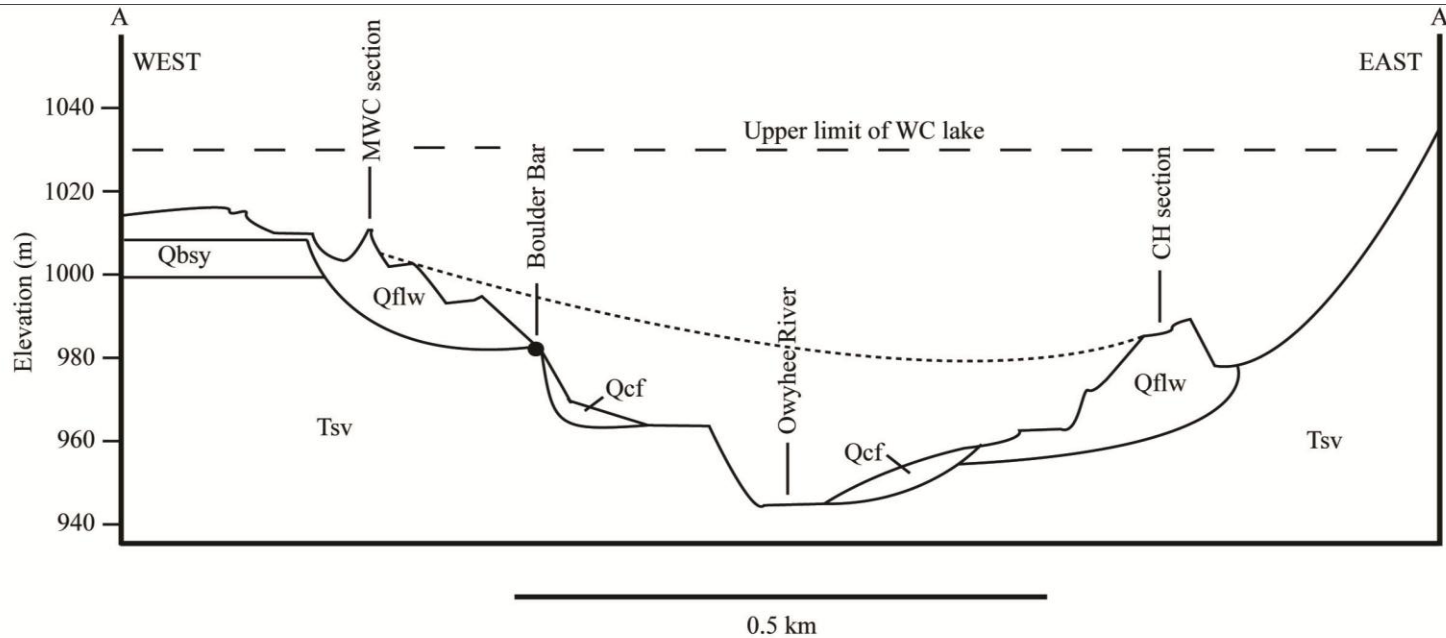

Figure 4. Cross-section from A to A' (Figure 4A) of the Main West Crater (MWC) and Caitlin's Hill (CH) sections and their relationship to the Owyhee River and other units. Units include Tsv (Tertiary sediments), Qbsy (Quaternary SB2 basalt flow), Qflw (Quaternary West Crater fluviolacustrine sediments), and Qcf (Quaternary colluvium and alluvium deposits). Maximum West Crater (WC) lake level is marked by a dashed line and is based on the elevation of the minimum overflow point on West Crater (WC) lava dam remnant. Dotted line marks possible tephra correlations between the Main West Crater and Caitlin's Hill sections and possible paleo-lake bathymetry. The very shallow dip of sediment layers in the Caitlin's Hill and Main West Crater sections indicate a depression in paleo-lake bathymetry near the location of the modern river level.

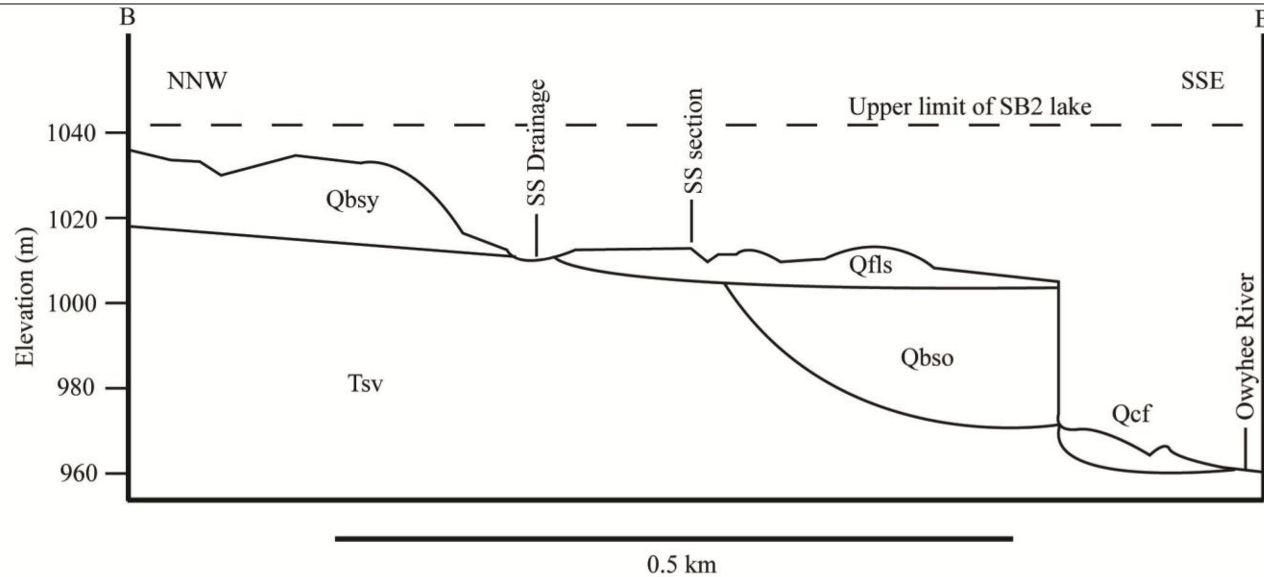

Figure 5. Cross-section from B to B’ (Figure 4B) of the Sand Springs (SS) section and its relationship to the Owyhee River, the Sand Springs Drainage, and other units. Units include Tsv (Tertiary sediments), Qbso (Quaternary SB1 basalt flow), Qbsy (Quaternary SB2 basalt flow), Qfls (Quaternary Saddle Butte 2 fluviolacustrine sediments), and Qcf (Quaternary colluvium and alluvium deposits). The maximum SB2 lake level is marked by the dashed line and based on the elevation of the minimum overflow point on Saddle Butte 2 (SB2) lava dam remnant.

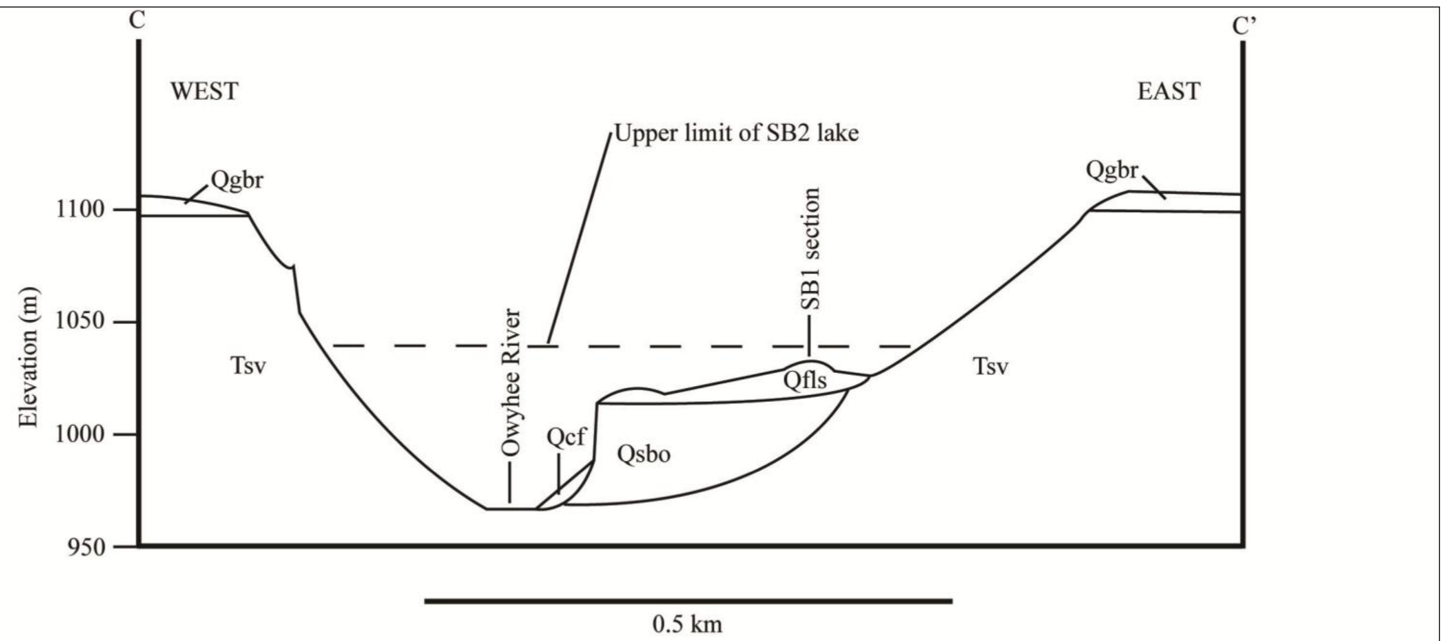

Figure 6. Cross-section from C to C’ (Figure 4B) of the SB1 section and its relationship to the Owyhee River and other units. Units include Tsv (Tertiary sediments), Qgbr (Quaternary BR gravel deposit), Qbso (Quaternary SB1 basalt flow), Qbsy (Quaternary SB2 basalt flow), Qfls (Quaternary Saddle Butte 2 fluviolacustrine sediments), and Qcf (Quaternary colluvium and alluvium deposits). Maxiumum Saddle Butte 2 (SB2) lake level is marked by dashed line and is based on the elevation of the minimum overflow point on Saddle Butte 2 (SB2) lava dam.

Lake Size and Extent

Lakes impounded by the WC, SB2, and BR lava dams varied in size. The WC and SB2 lakes both stayed within the confines of the Owyhee River Canyon and extended at least 29 km upstream based on dam crest height (Figs. 7 and 8). The BR lake formed before the Owyhee River Canyon was as deeply incised as it was during the emplacement of the WC and SB2 dams. The much shallower canyon during the BR time allowed for the impounded water to spill over the rim of the canyon and spread over a much larger surface area (Fig. 9).

Lacustrine sediments deposited in lava-dammed lakes can only accumulate as high as the dams that impounded them. This is sometimes helpful in distinguishing Tertiary sediment from the Quaternary sediments, but also may help to distinguish which lava dam each of the lacustrine sections may be related to. Additionally, the lacustrine sediments, and remnants bedrock, can help determine the pre-lava dam canyon topography. The CH section and the associated downstream WC lava dam remnants (Brossy, 2007) are located close to the modern river level. Therefore, it is likely that the pre-WC Owyhee River level was very close to the modern river level. Also, the elevations of the SB1 and SB2 lava dams are also near modern river level, again suggesting that the pre-SB1 and SB2 river level was similar to today's river level.

Stratigraphy of Lacustrine Sediments

Overall, Quaternary lacustrine sediments in the field area are characterized by massive to thinly laminated silts and clays with lenses of fine to medium-grained sand.

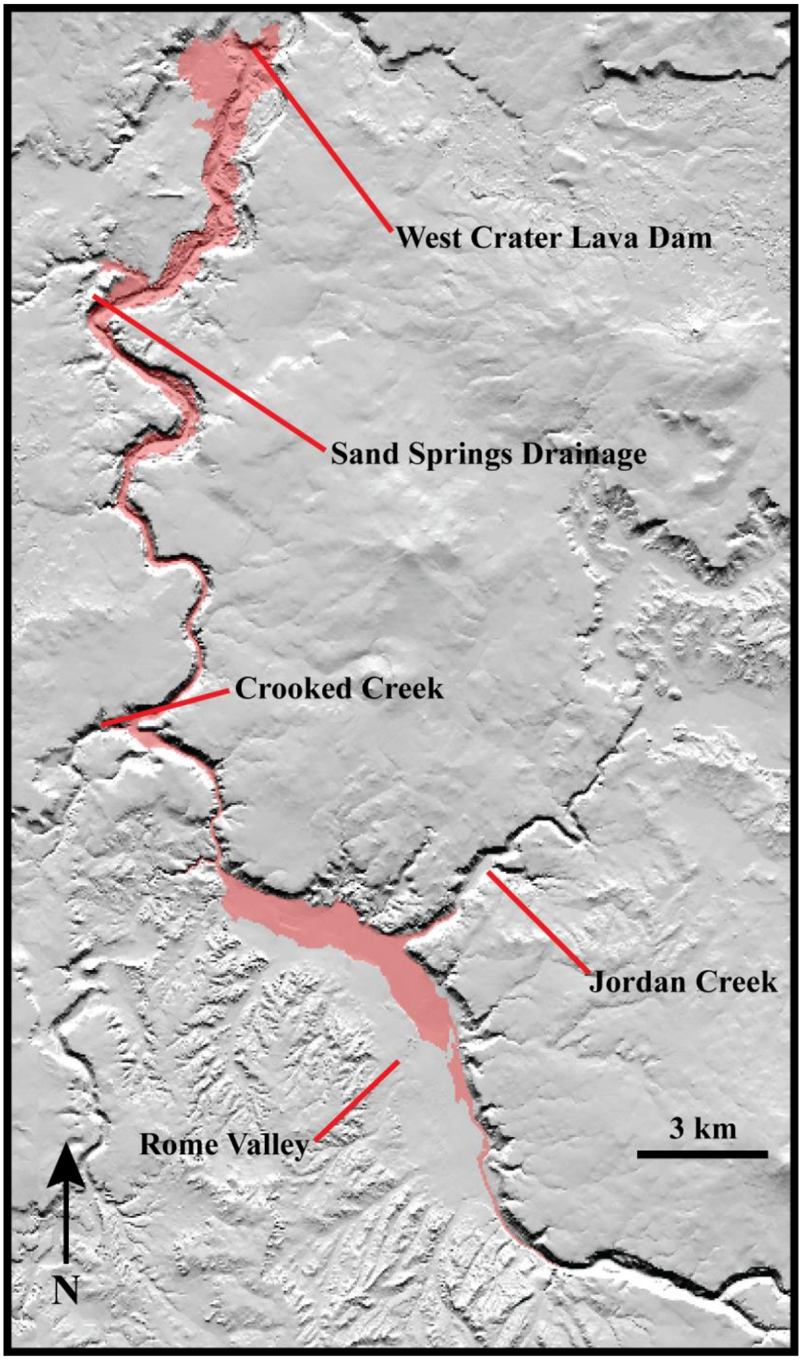

Figure 7. LiDAR imagery of the field area showing the extent of the West Crater lake when applied to modern topography. Topography at this time of the West Crater lava dam emplacement was very similar to the modern making this figure a good approximation of the extent of the West Crater lake.

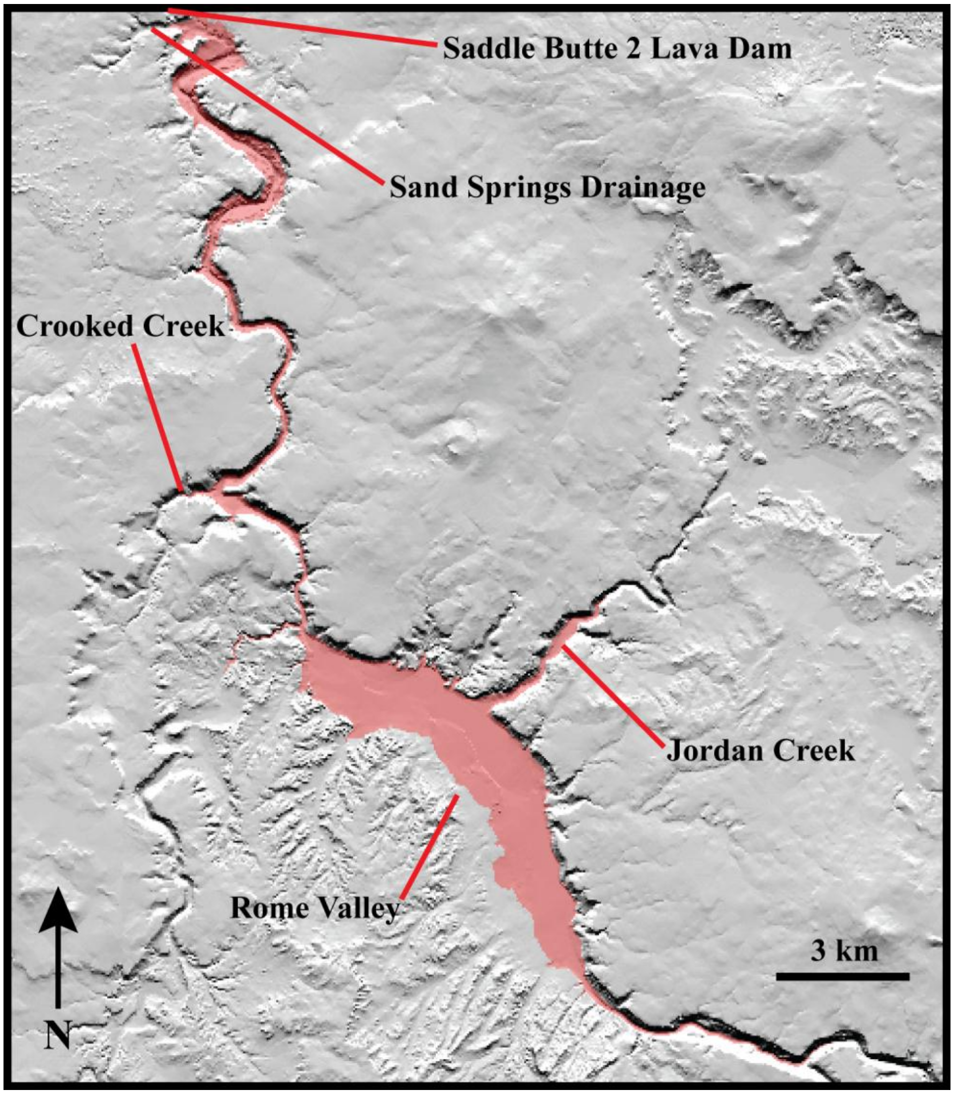

Figure 8. LiDAR imagery of the field area showing the extent of the Saddle Butte 2 lake when applied to modern topography. Topography at the time of the emplacement of the Saddle Butte 2 lava dam was similar to the modern in the Owyhee River Canyon, making this figure a good approximation of the extent of Saddle Butte 2 lake.

Detailed descriptions of all samples can be found in Appendix A. The results of the grain size analysis are listed in Table 2.

Caitlin's Hill (CH) Section

The CH Section is a 21.85 m-high section located on river right at Rkm 37.65, ~ 0.3 km upstream from the remnants of the WC lava dam (Fig. 10). The base of the

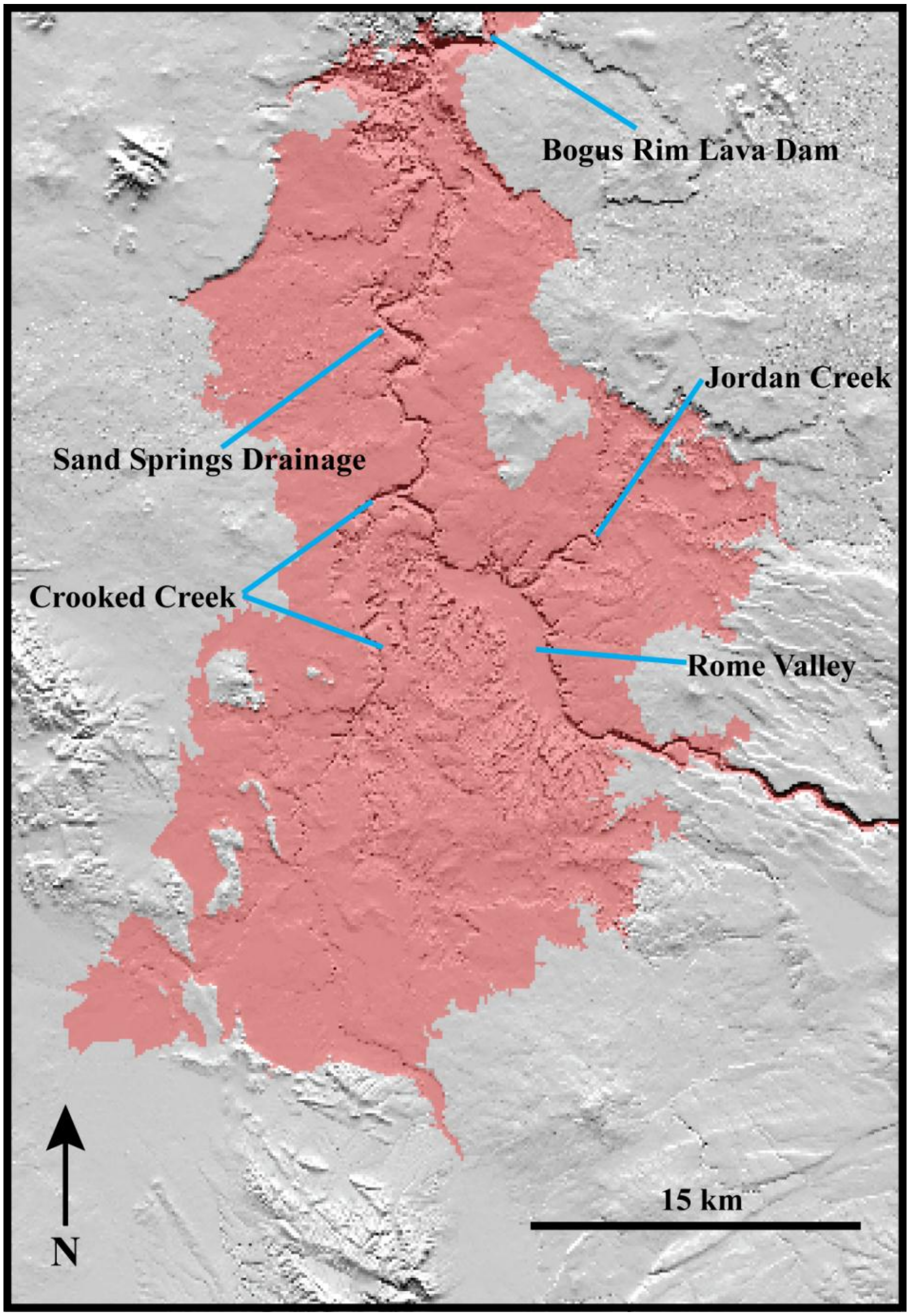

Figure 9. LiDAR imagery of the field area showing the extent of the Bogus Rim lake when applied to modern topography. Topography at the time of Bogus Rim lava dam emplacement was not similar to the modern. The Owyhee River Canyon was much shallower and the elevation of the surrounding landscape for this time is largely unknown, making this figure only a moderate to poor estimate of the Bogus Rim lake.

TABLE 2. AVERAGE GRAIN SIZE OF REPRESENTATIVE QUATERNARY LACUSTRINE SEDIMENT SAMPLES

Section	Sample	Height in Section (m)	Volume Weighted Mean (μm)	Size Fraction
Caitlin's Hill	CH-2	0.20–0.24	66.748	Very fine sand
	CH-8	1.40–1.45	182.443	Fine sand
	CH-16	2.92–2.96	73.199	Very fine sand
	CH-22	4.90–4.94	193.390	Fine sand
	CH-29	6.12–6.16	44.979	Silt
	CH-32	7.14–7.17	12.658	Silt
	CH-41	8.68–8.71	15.843	Silt
	CH-49	12.07–12.11	21.465	Silt
	CH-55	13.89–13.93	25.694	Silt
	CH-61	16.46–16.50	15.195	Silt
	CH-67	18.43–18.47	20.736	Silt
	CH-69	19.46–19.50	14.453	Silt
	CH-72	20.66–20.70	41.142	Silt
	CH-75	21.51–21.56	25.367	Silt
Main West Crater	MWC-4	0.40–0.42	465.488	Medium sand
	MWC-9	2.05–2.07	43.537	Silt
	MWC-12	2.92–2.96	18.348	Silt
	MWC-19	4.23–4.26	20.907	Silt
	MWC-26	5.14–5.17	74.377	Very fine sand
	MWC-31	6.12–6.15	99.123	Very fine sand
	MWC-40	7.40–7.43	37.877	Silt
	MWC-44	8.43–8.46	78.754	Very fine sand
	MWC-47	9.24–9.28	30.336	Silt
	MWC-50	9.88–9.92	239.980	Medium sand
	MWC-57	11.61–11.65	101.681	Very fine sand
	MWC-63	13.20–13.24	50.014	Silt

TABLE 2. (continued)

Section	Sample	Height in Section (m)	Volume Weighted Mean (μm)	Size Fraction
Sand Springs	SS-3	2.13–2.16	78.934	Very fine sand
	SS-6	4.12–4.14	45.966	Silt
	SS-7	4.27–4.29	40.617	Silt
	SS-9	4.72–4.76	97.038	Very fine sand
	SS-11	5.03–5.05	126.243	Fine sand
	SS-15	5.71–5.73	149.776	Fine sand
Saddle Butte 1	SB1-3	0.51–0.54	17.398	Silt
	SB1-8	2.88–2.89	16.622	Silt
	SB1-12	4.93–4.97	155.362	Fine sand
	SB1-15	5.87–5.90	31.722	Silt
	SB1-18	6.32–6.36	224.754	Fine sand
	SB1-23	8.64–8.68	69.037	Very fine sand
	SB1-25	9.80–9.85	54.700	Silt
	SB1-26	10.10–10.14	221.484	Fine sand
	SB1-27	10.41–10.45	148.945	Fine sand
	SB1-30	12.17–12.20	158.403	Fine sand
	SB1-34	0.29–0.30	75.280	Very fine sand
	SB1-42	3.33–3.44	154.341	Fine sand

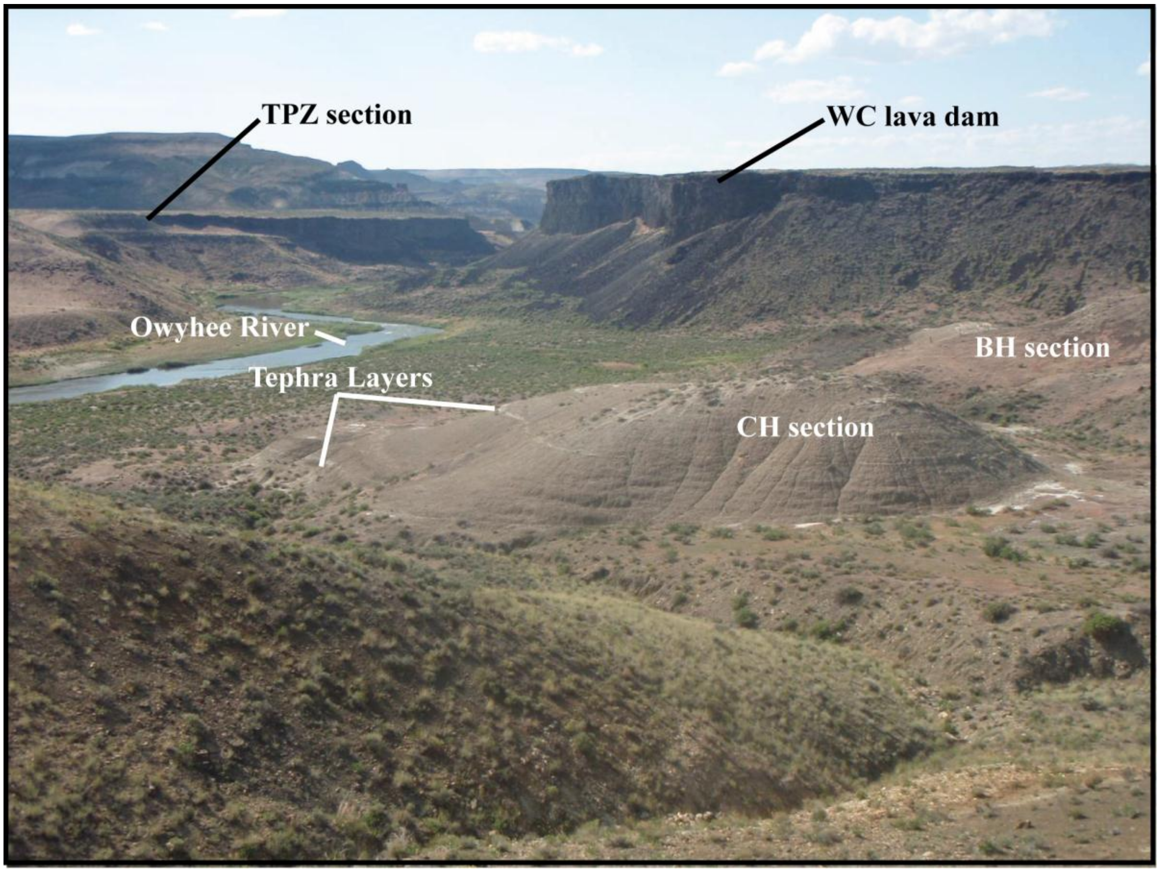

Figure 10. Photograph of the Caitlin's Hill (CH) section with Trapezoid (TPZ) section, Bone Hill (BH) section, front of West Crater (WC) lava dam, and Owyhee River in background. Two tephra layers show up in the Caitlin's Hill (CH) section as prominent white layers.

section sits ~20 m above the modern riverbed. This section consists of one large hill with two steps eroded into the riverward side of the hill. All laminations or other sedimentary features in the section dip very shallowly, toward the location of the modern river.

The CH section includes many different types of sediment and can be separated into three zones based on sediment descriptions and the terraces described above (Fig. 11). The basal zone (0–7.5 m) consists of alternating sand and silt beds that are horizontally continuous throughout the hill. Some of the sandy beds include ripple

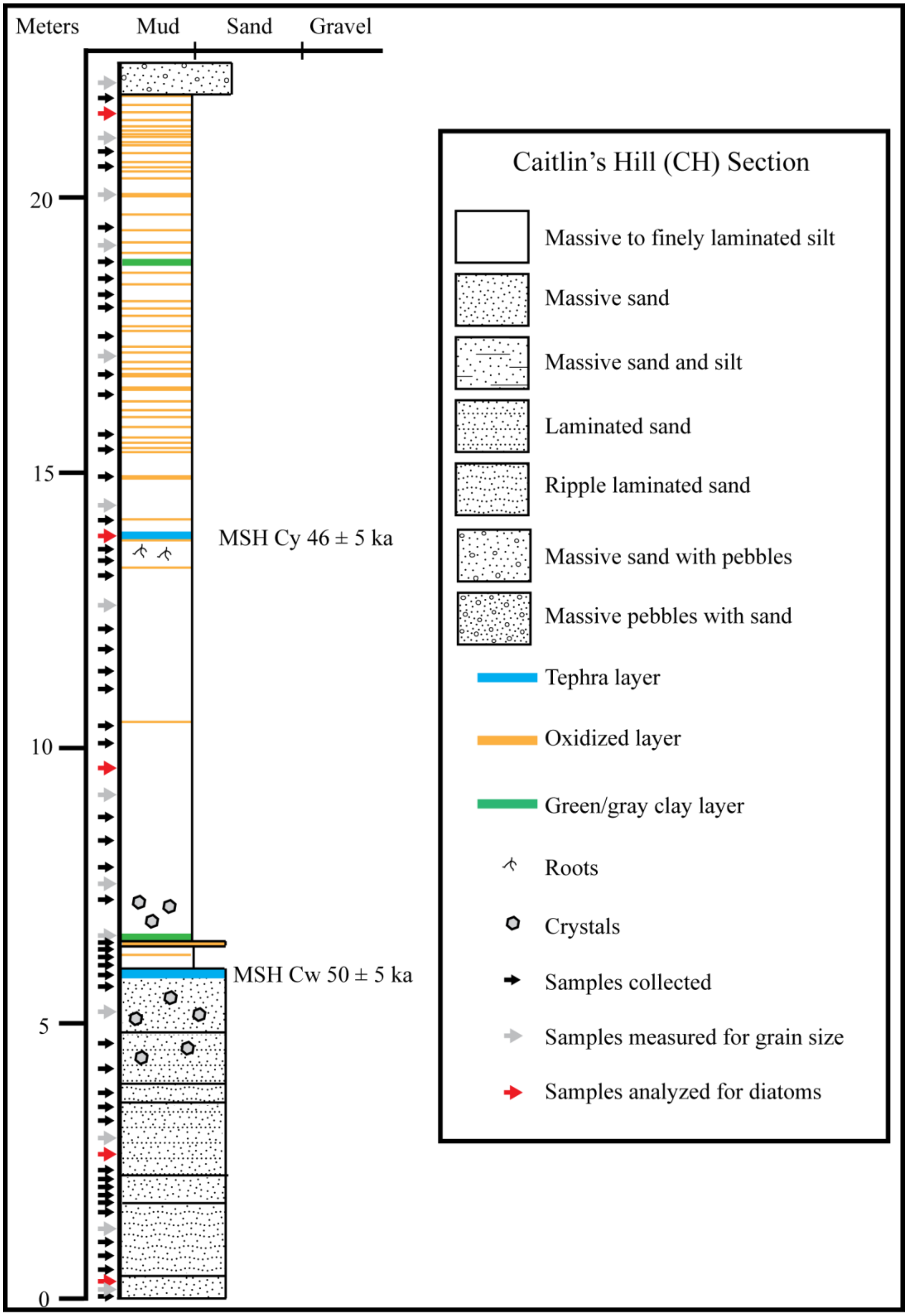

Figure 11. Diagram of the Caitlin's Hill (CH) stratigraphic section with MSH Cy and Cw tephra layers labeled.

laminations (Fig. 12), while some of the silty beds contain gypsum crystals. The upper ~30 cm of this zone contains a thick layer of clayey silt with alternating layers of tan-

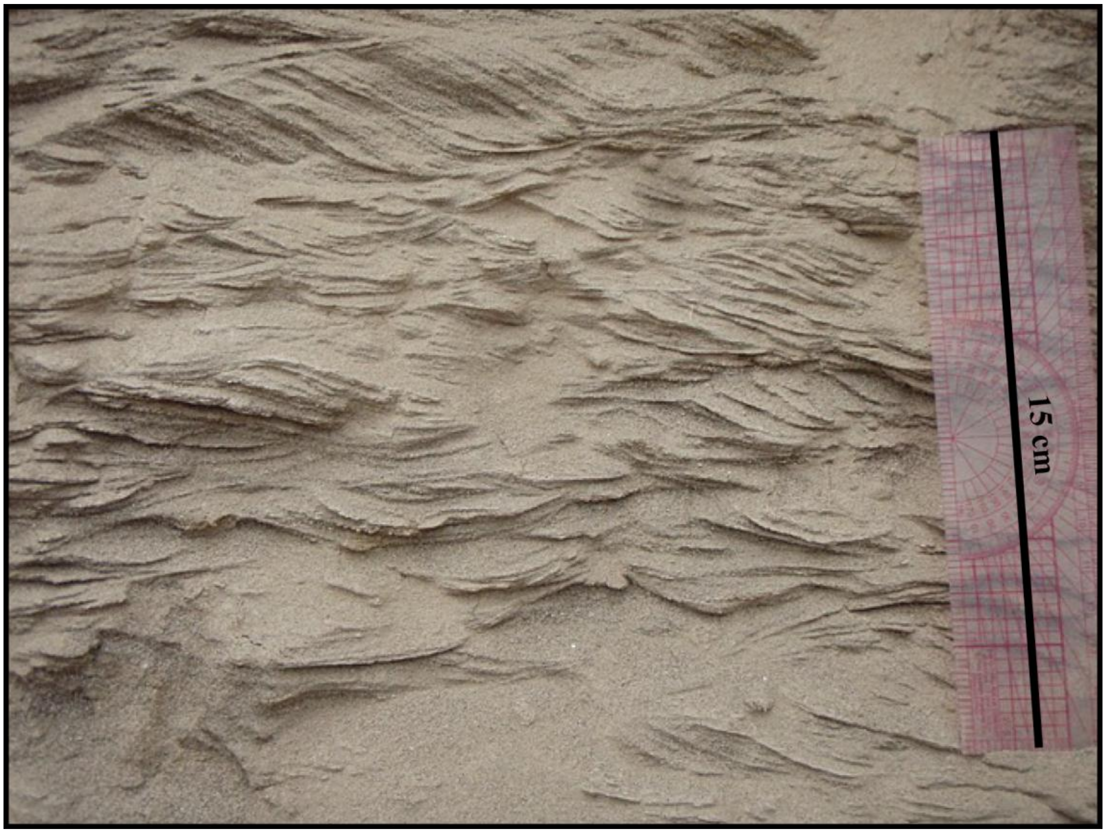

Figure 12. Photograph of cross-bedded, ripple-laminated silty sand layer near the base of the Caitlin's Hill (CH) section.

brown and green sediments (Fig. 13). The alternating layers reach thicknesses of up to ~1 cm. Tan-brown layers are mostly thicker than their green counterparts. Approximately 40 pairs of tan-brown and green layers were counted within the unit. A prominent 15-cm thick tephra layer is located just beneath this green and tan-brown clay layer. The tephra layer shows very fine laminations and has abundant burrow-like features. The middle zone (7.5 -13.5 m) consists of massive, tan to white silt and clayey silt. This middle zone also includes a 1-cm thick tephra deposit near the top (Fig. 11). The tephra layer has

Figure 13. Photograph of the alternating green, brown, and tan laminations of the clayey silt layer within the Caitlin's Hill (CH) section.

many thin orange-brown silt layers on the upper and lower boundaries and is cut by cracks filled with gypsum. Finally, the top zone (13.5 - 22 m) is also composed of massive silt, but includes many orange-brown silt layers not present in the middle zone. This upper zone also includes a thin, 3-cm thick layer of greenish brown clay (18.2 m).

Remnants of gravel that once covered the top of Caitlin's Hill are found along the slopes and at the base of the hill. Only a few rounded gravels remain at the top of the section.

Bone Hill (BH) Section

The BH section is located on river right (Rkm 37.85), ~0.15 km downstream of the WC lava dam and ~20 meters north of the CH section (Fig. 10). This section was not described due to its close proximity to the CH section and similar sediment characteristics, but general observations were made (Fig. 14). It is unclear whether the entire BH section is composed of sediments accumulated behind the WC lava dam. The lower portion of the hill is darker in color and more closely resembles the Tertiary sediments in the nearby canyon wall. Lighter colored, less indurated sediments (similar to the CH sediments) are found in the upper portion, along with a ~5-cm thick tephra layer that may correlate to one of the layers in the CH section. This tephra layer is composed of three distinct layers colored white-yellow/tan-white from top to bottom and includes a few fine laminations of orange-brown silt layers. A cap of gravel is preserved on top of Bone Hill.

Main West Crater (MWC) Section

Unlike the CH and BH Sections the MWC Section is located at a higher elevation and on river left at Rkm 37.55. This section is 15.5 m-thick and is comprised of laterally extensive, alternating silt and sand layers (Fig. 15) that dip very shallowly towards the modern river channel. This section laps on to the edge of the SB2 lava flow (Fig. 16). A 3-cm thick tephra deposit is located near the base of the section. This section is overall tan

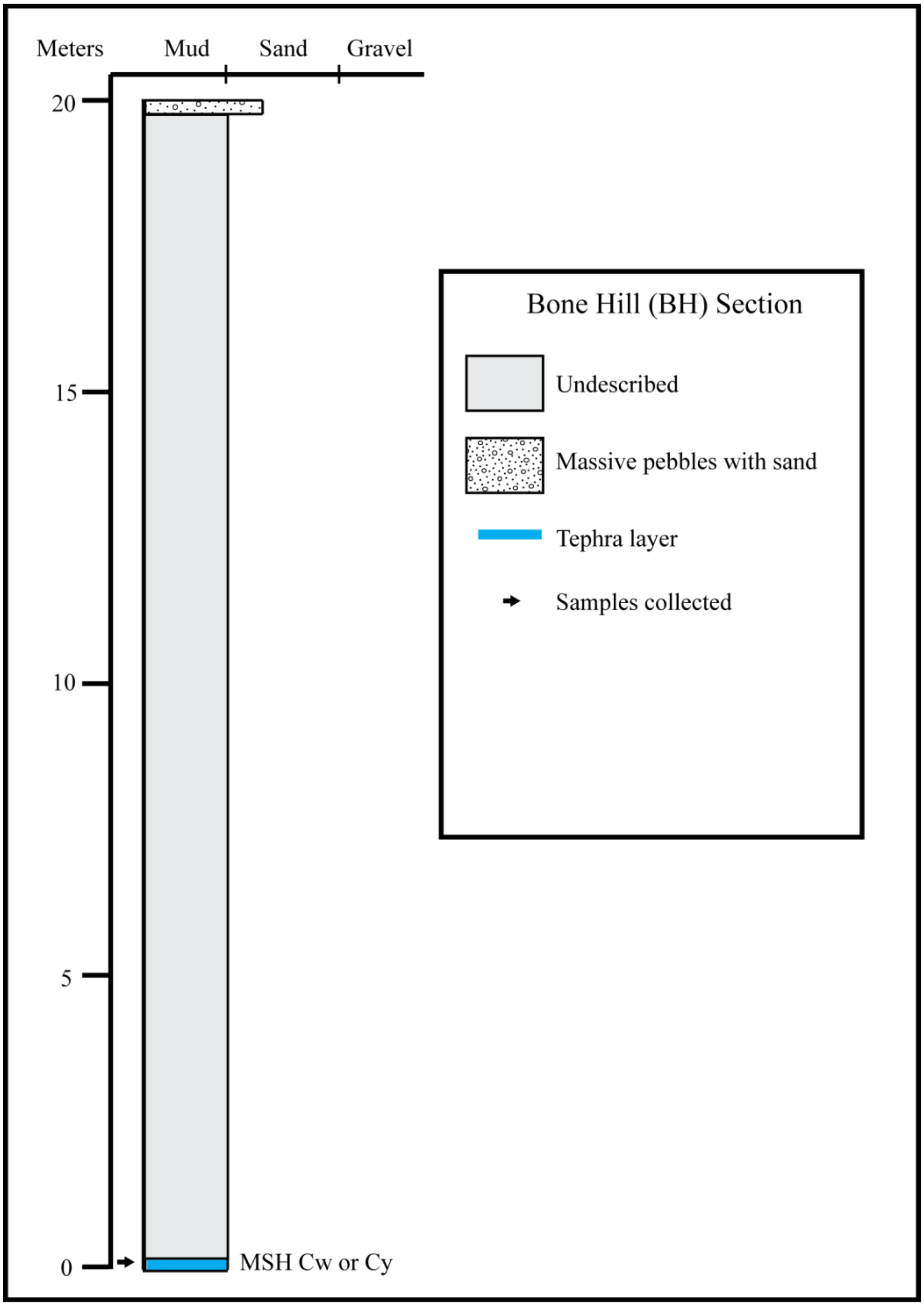

Figure 14. Diagram of the Bone Hill stratigraphic section with basal tephra layer labeled.

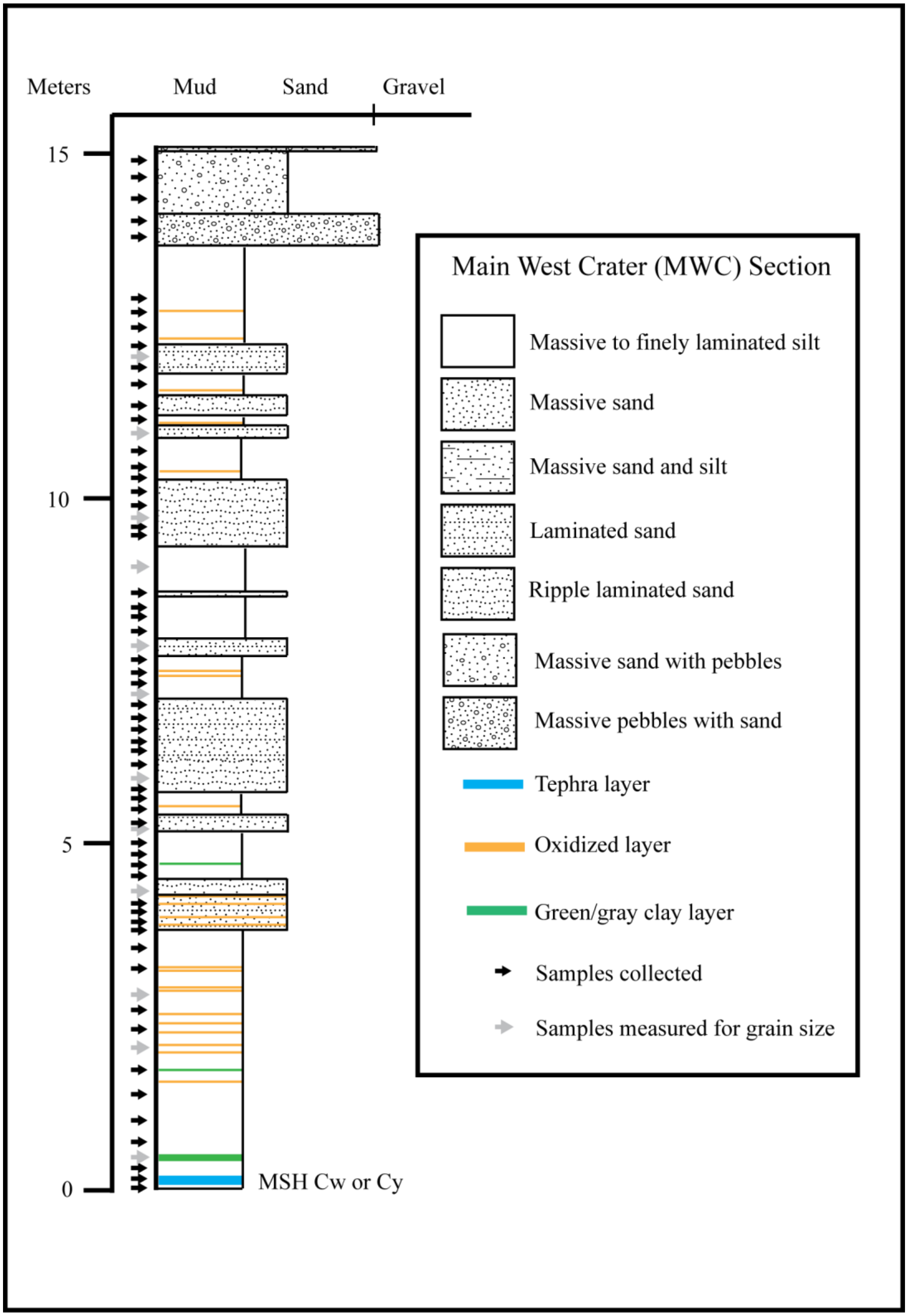

Figure 15. Diagram of the Main West Crater stratigraphic section with basal tephra layer labeled.

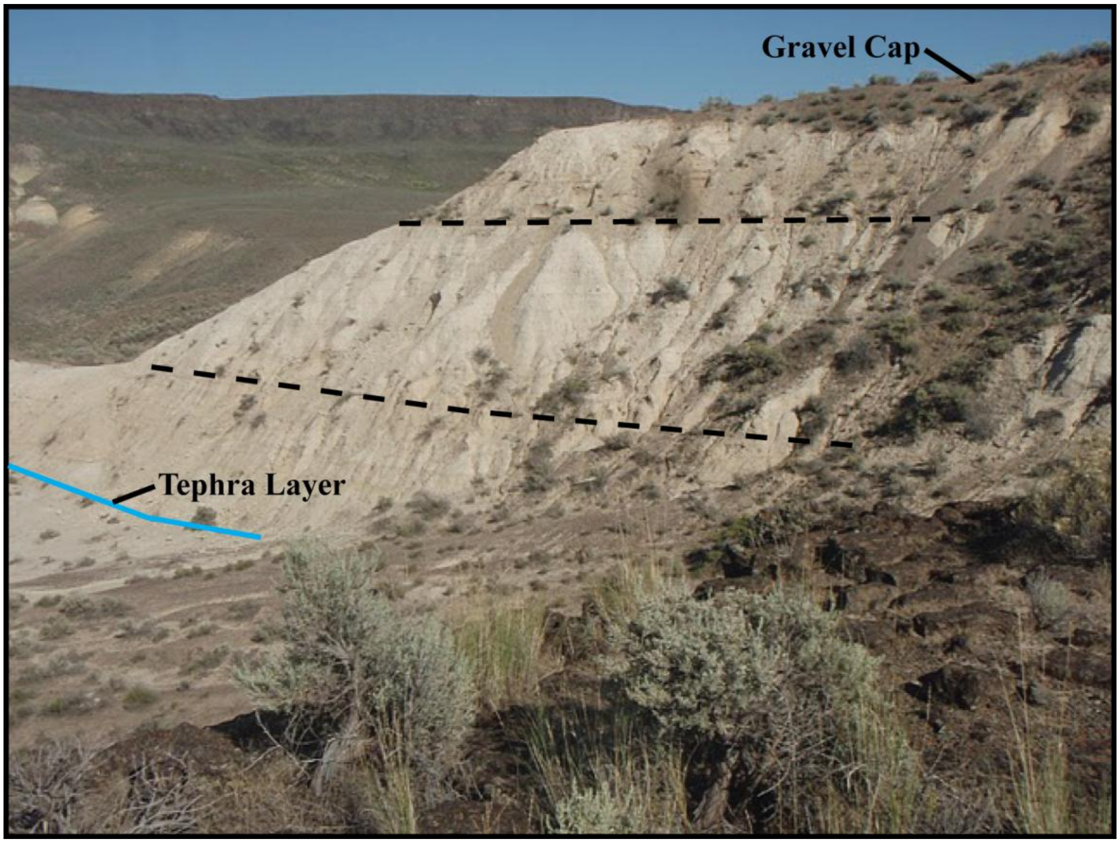

Figure 16. Photograph of the Main West Crater section from top of Saddle Butte 2 basalt flow. Boundaries between three zones in section are outlined in black dashed line. Basal tephra layer is also labeled and marked with blue line.

to white in color, but variations in color distinguish three zones in the outcrop. It is uncertain what the color changes in the outcrop mean, but they are most likely related to changes in sediment source area or to secondary geochemical alteration. This section is capped with a 1.5 m thick gravel and sand layer.

Around the MWC section are many other hills of sediment that may be lacustrine sediment related to the WC lava dam. These hills are eroded, mostly covered in vegetation (grasses) and gravel, and some have terraces cut into them. These hills were not stratigraphically described during this study, but the terraces were measured. These hills sit on the boulder line at ~990 m elevation like the MWC and TPZ sections.

Trapezoid (TPZ) Section

The TPZ section was not described during this project but was identified as Quaternary lacustrine sediment during fieldwork prior to this study. This section is located on river left at Rkm 38, just upstream of the confluence of the Owyhee River and Ryegrass Creek. The TPZ section is the farthest downstream sediment section (Fig. 10). This section is higher in elevation than both the CH and BH sections on river right, and is located above the same boulder line as the MWC section and neighboring sediments.

Although this section was not described in detail, a 3-cm thick tephra layer ~ 3.5 meters from the base was sampled. The TPZ section is primarily silt-sized sediment with some possible sand layers (Fig. 17). The gravel cap on the trapezoid is ~4.4 m thick, much thicker than the gravel caps found on any of the other Quaternary lacustrine sediment sections.

West Crater Top (WCT) Section

The WCT section is a small section ~3.2 m thick that is positioned in what was presumably a low area of the WC lava dam. The section is made up of very light tan-white massive silt and capped with eolian sand (Fig. 18). The section is at an elevation below the WC lava dam crest and appears to be located on top of the WC lava dam, suggesting that the section is related to the WC lava dam. A 1-cm thick tephra layer located at the base of the section challenges this interpretation (see Geochronology section below) and may indicate this section it too old to be related to the WC lava dam.

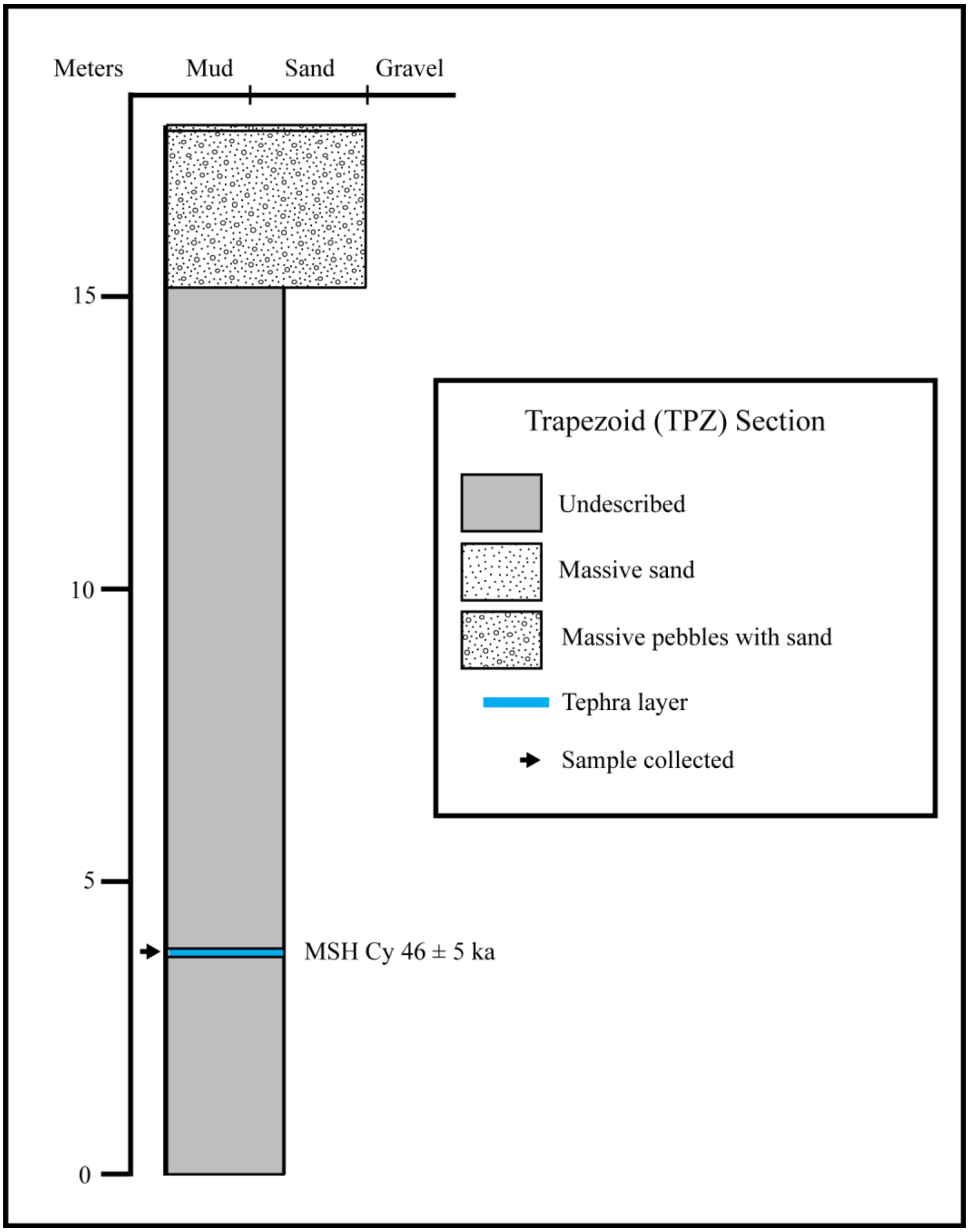

Figure 17. Diagram of the Trapezoid stratigraphic section with MSH Cy tephra layer labeled.

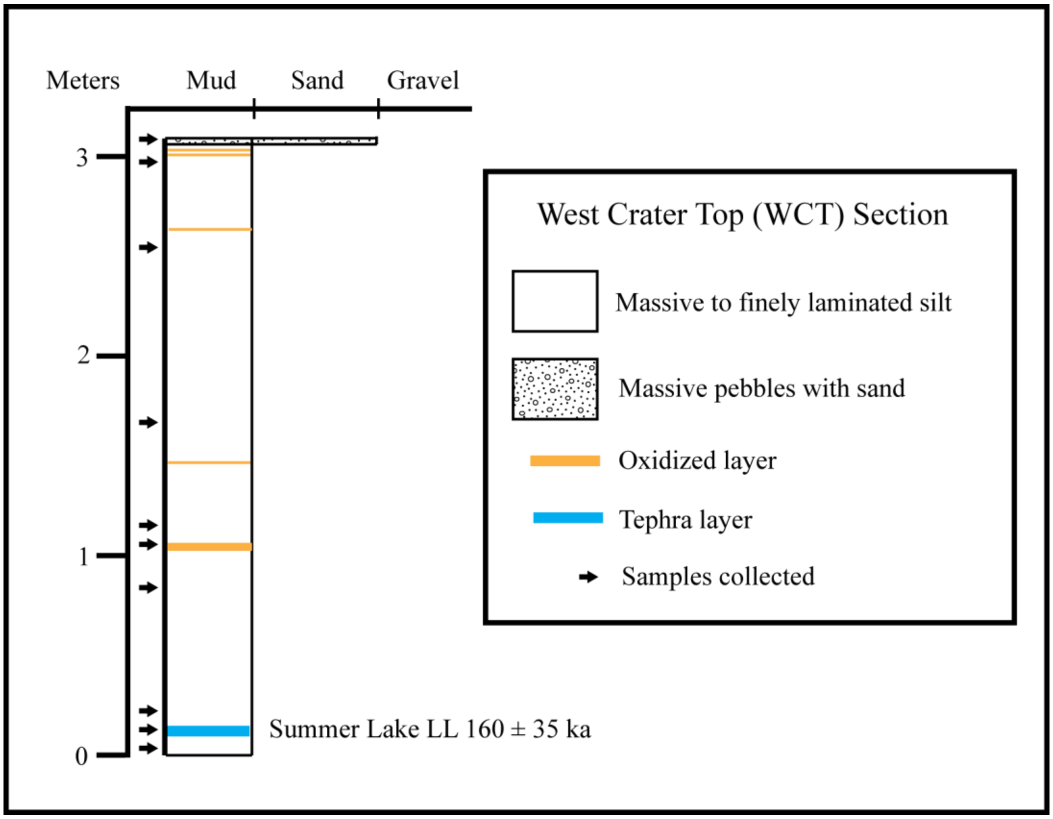

Figure 18. Diagram of the West Crater Top stratigraphic section with Summer Lake LL tephra layer labeled.

The low elevation of the section does show possible relation to the WC lava dam, but there may be complex and unknown stratigraphic relationships below the surface.

Sand Springs (SS) Section

The SS section is located at Rkm 30.5, ~8 km upstream of the WC lava dam and directly upstream of the SB2 lava dam (Fig. 19). The SS section is located in the Sand Springs drainage that parallels the southern border of the SB2 lava dam. The SS section is ~8.6 m thick and comprised of a lower section of massive silt and sand (0-3.5 m) and an upper section of interbedded silt and sand layers with orange-brown colored layers (3.5-

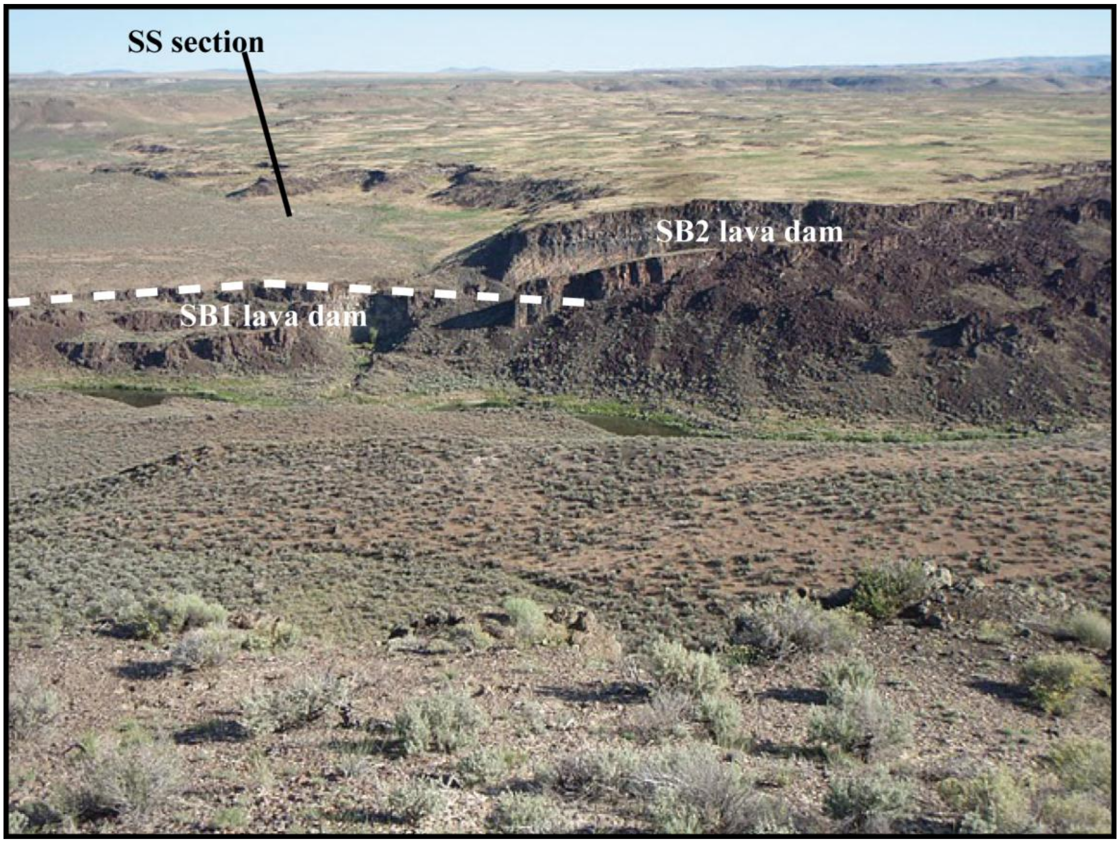

Figure 19. Photograph from river right of the Sand Springs (SS) section and Saddle Butte 2 (SB2) lava dam on river left. Approximate boundary between Saddle Butte 1 (SB1) basalt flow and overlying units shown with white dashed line.

6.25 m) (Fig. 20). The section is capped with 2.35 m of sand with gravel. No tephra layers were found in the SS section.

The SS section sits at the toe of a hill of Tertiary sediment. At first, the section appears to be part of the Tertiary section, but upon further investigation a clear break in sediment characteristics is seen. This break may be depositional, fault, or slump related. Other fine-grained sediments cover the bench created by the SB1 basalt flow and within the Sand Springs Drainage in the immediate area. The sediments located within the drainage, upstream from the SS section, are tan to white massive silts. Some of these

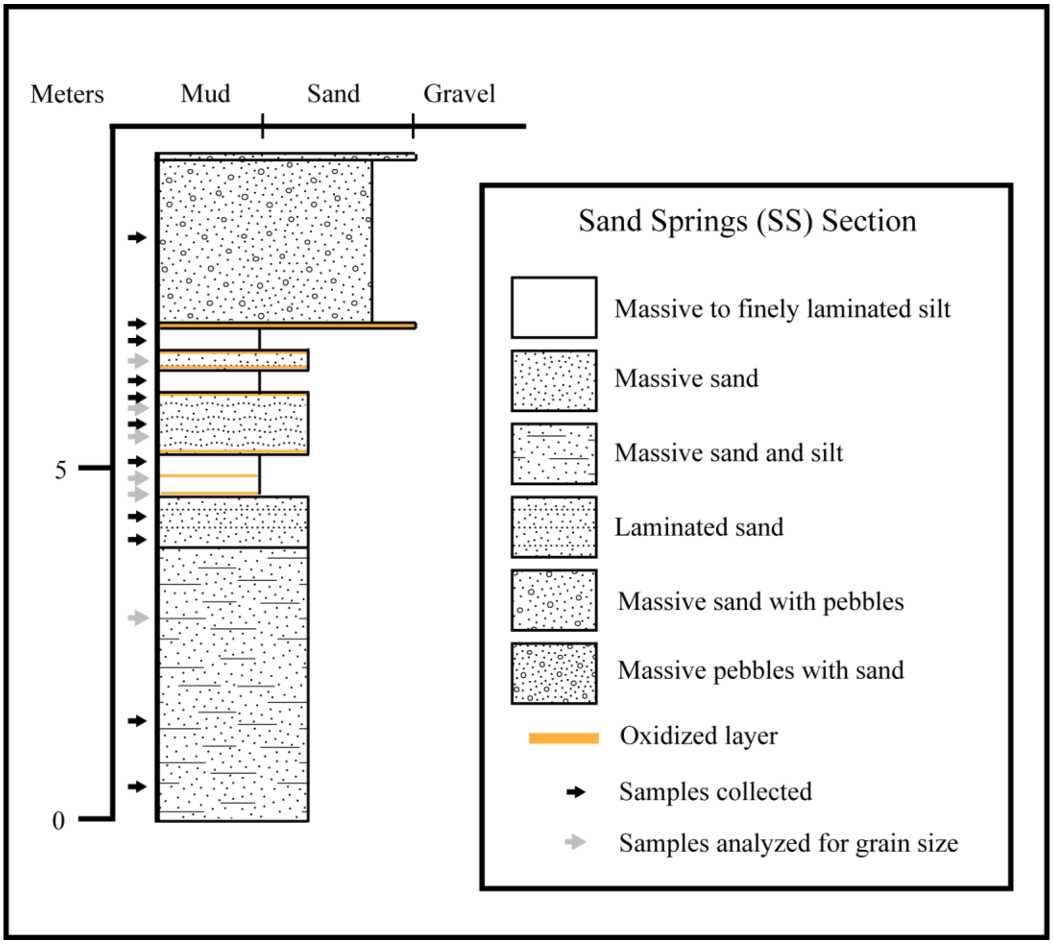

Figure 20. Diagram of the Sand Springs stratigraphic section.

upstream sediments may be related to local drainage deposition and, therefore, may not be related to the lakes formed by the lava dams on the Owyhee River. Other upstream sediments abut and lap onto the SB2 lava dam on the northern side of the drainage showing a direct association with the SB2 lava dam.

Saddle Butte 1 (SB1) Section

Directly across the Owyhee River from the Sand Springs location there is a bench formed by the top of the SB1 basalt flow. This bench, like that in the Sand Springs area, is covered in fine-grained sediments. The SB1 section (Fig. 21) is located on this bench. The SB1 section is located upstream of both the SB2 and the WC lava dams at Rkm

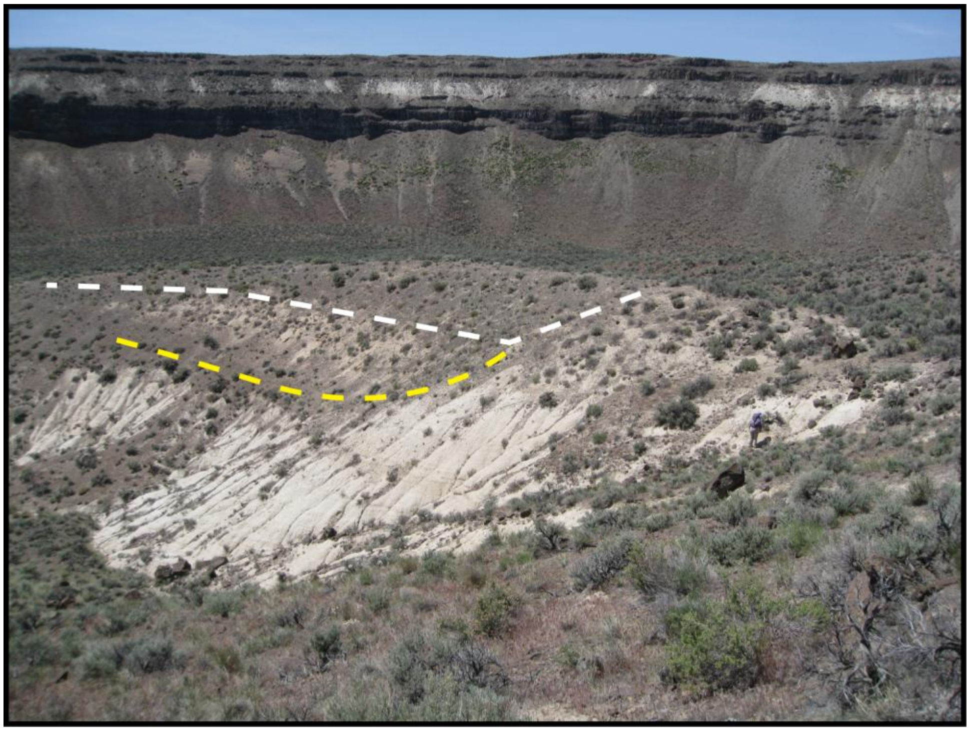

Figure 21. Photograph of the Saddle Butte 1 section with overlying debris flow deposit outlined in white dashed line. Channel incision is also outlined in yellow dashed line.

27.65. The section is ~16-m thick and composed mainly of massive silt with orange-brown colored layers and some sand layers (Fig. 22). Disconformably inset into the west side of the silt section at ~1033 m elevation are massive, laminated, and ripple-laminated gravel and sand deposits (Fig. 23). Both the massive silts and the channel gravels are overlain by a massive, ~3-m thick deposit of silt, sand, and gravel with clasts of basalt and intact blocks of laminated silt (Fig. 24). No tephra deposits were found in the SB1 section.

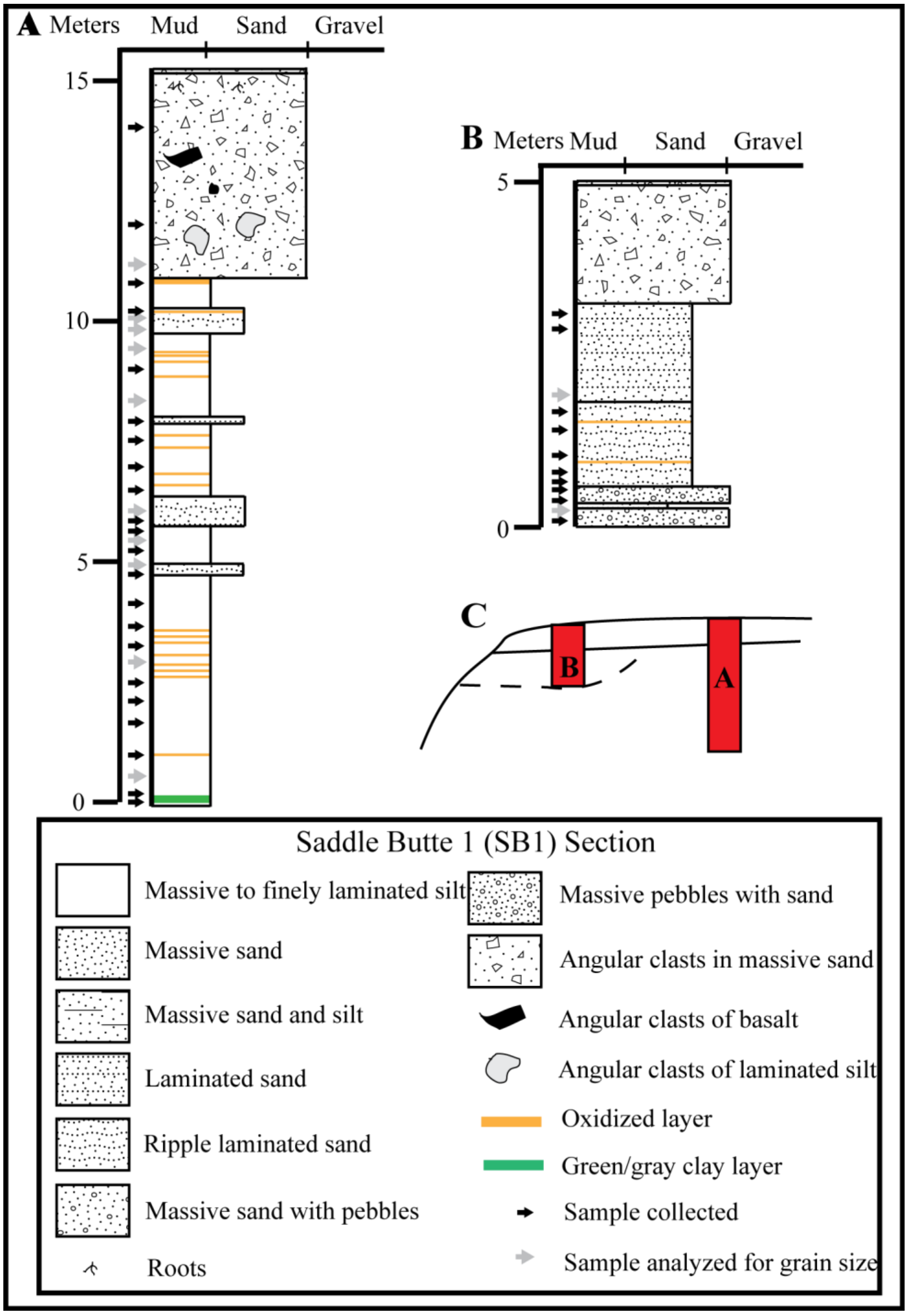

Figure 22. Diagram of the Saddle Butte 1 stratigraphic section, including the (A) fine-grained lacustrine section with overlying debris flow and (B) gravel-filled channel incision. (C) Schematic diagram of relation between sections.

Figure 23. Photograph of channel incision deposit with fluvial gravels and sand with overlying silt and sand deposit.

Terraces

Terrace elevations and locations were measured and described from approximately Rkm 27 to Rkm 47 and in the Rome Valley (Appendix B). Cut-in-fill terraces were usually found in areas of the Owyhee River Canyon where fine-grained Tertiary sediment and/or Quaternary lacustrine sediment were deposited and/or available

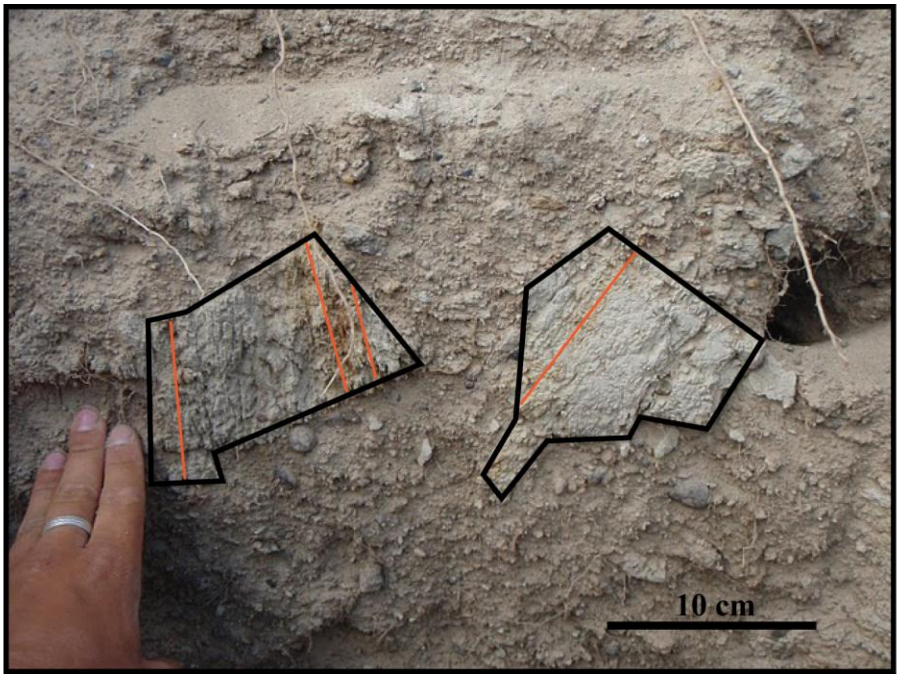

Figure 24. Photograph of intact laminated silt blocks (outlined in black) within debris flow deposit overlying the Saddle Butte 1 section.

for erosion. This preference towards these units resulted in groups of terraces at certain locations where the units outcrop or are preserved along the Owyhee River Canyon.

Many terraces were measured very near the upstream extent of the WC lava dam and ~3 km upstream. Terraces near the dam are made of Quaternary lacustrine sediment and Tertiary lacustrine sediment. Other terraces above the WC lava dam and SB2 lava dams are similar in composition. Some terraces within the Artillery landslide reach (Rkm 34 to 36) of the Owyhee River Canyon have similar elevations (Appendix B) and may correlate. The MWTB terraces are one set of the terraces located upstream of the WC lava dam. The MWTB terraces appear to have lower Tertiary lacustrine sediment boundaries graded to a paleochannel slope with Quaternary lacustrine sediment deposited on top, creating a terrace that thickens downstream. Many terraces related to both the WC lava dam and the SB2 lava dam have overlying gravel units. No terraces related to the WC lava dam and SB2 lava dams were dated in this study.

A suite of terraces within the WC lava dam named the Dog Leg terraces at Rkm ~46-47 were dated previously. There are five terraces (T1-T5) located on the inside bend of the Owyhee River called the Dog Leg (Figure 25). The T5 terrace is made up of fluvially sculpted WC basalt flow and includes abundant boulders and gravel. The T4 terrace is made up of sand and gravel fill overlying the WC basalt flow. Terraces T3, T2, and T1 consist of sand and gravel fill. These terraces have been dated using ^{3}He cosmogenic dating methods (Table 3, C. Fenton unpublished data).

Geochronology

Tephrochronology

All tephra samples from the CH, BH, MWC, and TPZ sections were geochemically correlated to Mount St. Helens (MSH) set C tephra dated at ~46 to 50 ka (Berger and Busacca, 1995; Clynne et al., 2008;Table 4). The tephra layer in the BH section could not be analyzed due to its small grain size, but it was correlated to the MSH set C tephra based on morphological characteristics that were similar to the tephra samples taken from the CH section (F.F. Foit, personal communication, September 2009). Only in the CH section are there two tephra deposits; all other sections only contained one.

The basal tephra sample from the WCT section did not correlate with MSH set C, but instead correlated to Summer Lake tephra LL, dated at 160 ± 35 ka (Berger, 1991; Negrini et al., 2000). This correlation questions the potential identification of this section

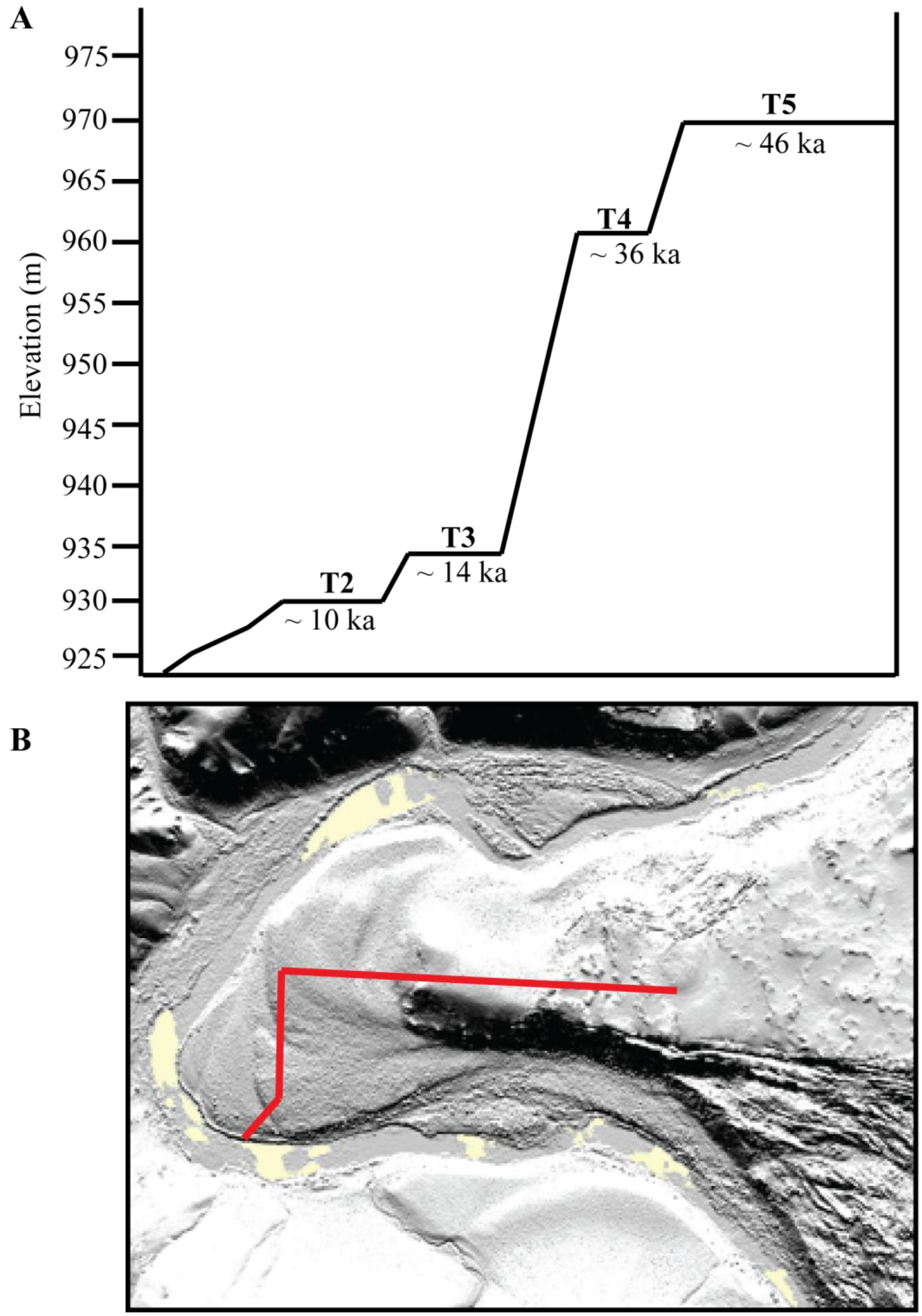

Figure 25. Schematic cross-sectional diagram of Dog Leg terrace elevations and dates (A) (C. Fenton, unpublished data) and plan view LiDAR imagery of the Dog Leg terraces (B) (from Brossy, 2007).

TABLE 3. GEOCHRONOLOGICAL CONSTRAINTS FOR THE INCISION OF THE WEST CRATER LAVA DAM

Feature	River Km	Elevation (m)	Date (ka)	Dating Method
West Crater Lava Dam	38.0	1030	70	$^{40}Ar/^{39}Ar$
Saddle Butte Lava Dam	30.5	1042	144	$^{40}Ar/^{39}Ar$
West Crater Paleochannels	38.0	1030	65 – 54	^{3}He cosmogenics
Dog Leg Terrace 5	45.0 – 47.0	970	46	^{3}He cosmogenics
Dog Leg Terrace 4	45.0 – 47.0	962	36	^{3}He cosmogenics
Dog Leg Terrace 3	45.0 – 47.0	938	14	^{3}He cosmogenics
Dog Leg Terrace 2	45.0 – 47.0	934	10	^{3}He cosmogenics
Dog Let Terrace 1	45.0 – 47.0	928	0	^{3}He cosmogenics
Airplane Point	47.8	946	70	^{3}He cosmogenics
Caitlin's Hill Upper Tephra Cy	37.7	989	46	Geochemical Correlation
Caitlin's Hills Lower Tephra Cw	37.7	981	50	Geochemical Correlation
Main West Crater Tephra	37.7	1012	50 – 46	Geochemical Correlation
Trapezoid Tephra	38.0	999	50 – 46	Geochemical Correlation
Artillery T2 Bar	36.0	962	10 – 20	^{3}He cosmogenics

TABLE 4. TEPHRA GEOCHEMICAL RESULTS AND CORRELATIONS

Samples from Study	Location	SiO_2	Al_2O_3	Fe_2O_3	TiO_2	Na_2O	K_2O	MgO	CaO	Cl	SC	Correlation*
CH-53	Upper CH	77.27	13.67	0.98	0.10	3.59	2.49	0.26	1.55	0.09	0.97+	MSH set Cy[†]
4270801-kh	Lower CH	77.03	13.59	0.99	0.13	3.86	2.36	0.27	1.69	0.08	0.97+	MSH Cw[§]
MWC-2	Lower MWC	77.02	13.67	1.03	0.12	3.74	2.45	0.29	1.60	0.09	0.98	MSH set C[†]
4270801-cb	Lower TPZ	76.84	13.60	1.01	0.12	3.92	2.52	0.27	1.63	0.09	0.98	MSH Cy[#]
WCT-2	Lower WCT	67.25	16.01	3.98	0.69	4.38	2.67	1.21	3.66	0.15	0.97	Summer Lake Tephra LL

Standard Samples	Source	SiO_2	Al_2O_3	Fe_2O_3	TiO_2	Na_2O	K_2O	MgO	CaO	Cl	Date**
MSH Cy Standard	Negrini et al. (2000)	76.68	13.93	1.05	0.11	3.90	2.43	0.27	1.55	0.07	46 ± 5 ka
MSH Cw Standard	Busacca et al. (1992)	71.50	13.20	1.10	0.09	3.50	2.10	0.27	1.58	0.08	50 ± 5 ka
Summer Lake LL	Davis (1985)	66.40	16.10	3.93	0.80	4.90	2.70	1.32	3.60	0.16	160 ± 35 ka

* Dr. Nick Foit at WSU completed all tephra geochemistry analyses and correlations for samples from this study. Geochemical analyses are normalized to 100 weight percent. Similarity coefficients (SC) were calculated using the methods from Borchardt et al. (1972).

[†] Correlated to MSH set C, probably MSH Cy (personal communication with Dr. Nick Foit). Sample CH-53 identified as MSH Cy by stratigraphic relation to sample 4270801-kh.

[§] Correlated to MSH set C, probably MSH Cy (personal communication with Dr. Nick Foit). Of the top matches, the top match and third to top match are correlated to layer Cw by other studies. The second match is to a generic MSH set C standard.

[#] Correlated to MSH set C, probably MSH Cy (personal communication with Dr. Nick Foit). Of the top matches, the top match is a generic MSH set C, but the second and fourth matches are correlated to layer Cy by other studies.

** References and discussion for dates is given in text.

as Quaternary lacustrine sediment related to the WC lava dam. In light of this date, more information is needed before this section of sediment can be thoroughly understood.

MSH set C actually includes 6 separate layers. From oldest to youngest they are Cb, Ct, Cw, Cm, Cy, and Cs (Mullineaux, 1986). The stratigraphic relations of these layers have been described based on many outcrops near MSH by Mullineaux (1986). All MSCH set C tephra deposits are characterized by an abundance of biotite and the presence of cummingtonite (Mullineaux, 1986). The samples collected from the field area were no different, excluding the WCT tephra sample (F.F. Foit, personal communication, September 2009). Geochemical correlation to specific MSH set C layers is difficult due to their similar geochemical signatures. Similarity coefficients (SC) between the various MSH set C layer standards and the samples in this study vary only within 1% or less (Table 2).

Optically Stimulated Luminescence

Although samples for OSL dating methods were taken from different stratigraphic sections (CH, MWC, and SS sections) and stratigraphic positions, the ages do not agree with previous dates on the basalt flows and dates gathered in this study. The OSL ages are all very similar with all ages at ~20 ka. The similarity in ages suggests a systematic error in the ages. The material present in the field area is likely the cause of the systematic error. Also, deposition by fluvial and lacustrine processes may make these samples unsuitable for this dating method.

The most common problems for OSL dating usually result in dates being much older than expected (Aitken, 1998). Older than expected ages can be caused by fluvial and lacustrine sediments not being fully bleached by exposure to sunlight during transport and prior to burial (Aitken, 1998; Forman et al., 2000). The OSL results from this study produce ages younger than expected, which is uncommon. Younger than expected ages may indicate inaccuracies with water moisture estimates, radioactive dose rates, anomalous fading, and changes in sensitivity or traps within the quartz grains (Aitken, 1998; Forman et al., 2000; Walker, 2005).

Microfauna Analysis

Silicic diatom frustules were found throughout the CH section and in other sections, but only those in the CH section were studied further. Those samples in the CH section with diatoms present are indicated in Appendix A. No calcareous fossil material was found in the lacustrine sediment.

A preliminary summary of results (S. Starratt, personal communication, April 2010) indicates that diatoms in the CH section are poorly to moderately preserved and limited to smaller frustrules. Overall, no deep-water diatoms are present in the samples. Most diatoms showed signs of etching that indicates alkaline conditions. All samples contain diatoms that indicate low to moderate nutrient loads and some that are known to have symbiotic relationships with blue-green algae. Some species were slightly silicified suggesting that available silicon in the lake was being used.

Samples CH-3 and CH-14 have low abundances, poor preservation, and low diversity of diatoms. These two samples are located within the basal zone of the CH section and are dominated by epiphytic or epilithic diatom species that attach to surfaces and live in turbid conditions. Samples CH-41, CH-53, and CH-71 have higher abundances and species diversity of diatoms. All three samples include soil diatoms.

CHAPTER IV

DISCUSSION

The discussion and interpretation of results will begin with the preservation and geochronology of the stratigraphic sections. Following the geochronology section, the West Crater, Saddle Butte 2, and Bogus Rim lava dams and lakes will be discussed. Focus will be mainly on the West Crater lava dam due to high preservation of lacustrine sediments and geochronology. Lastly, suggestions for future work in the Owyhee field area and in lava-dammed rivers will be given.

Preservation of Lacustrine Sediments

The location of preserved Quaternary lacustrine sediments within the Owyhee River Canyon is controlled by many factors. Different means of preservation include their proximity to protective resistant features in the canyon, the armoring of the sections by capping gravel deposits, and their elevations above the modern river channel and floodplain.

The large sections of Quaternary lacustrine sediments that are described in this study are found near the lava dam they relate to (Fig. 2) and/or near where tributaries meet the Owyhee River. Basalt-rich areas near the dam are resistant to erosion and may have “protected” the lacustrine sediment from post-lava dam river incision. The proximity of these large lacustrine sections to stream tributaries suggest that these tributaries may be a source of the sediment within the sections. It is normal for lake and reservoir sedimentation to include sediment from the main river input, tributaries, and slope material from the sides of the basin (Foster et al., 1990).

Another mechanism for preservation of the Quaternary lacustrine sediments are the gravel units that overlie the lacustrine sediments. These gravel caps may armor the fine-grained sections from vertical erosion. However, this armoring may be short-lived due to erosion of the gravel units and lateral hillslope retreat of the moderately vegetated slopes.

The location of preserved Quaternary lacustrine sediments may have been affected by flooding in the Owyhee River Canyon. Quaternary lacustrine sediments are found preserved along canyon walls and on top of high-elevation benches. Large floods within the Owyhee River Canyon probably occurred during the outburst floods from Lake Alvord via Crooked Creek. The latest of these floods occurred ~13-14 ka and may have reached discharge levels between 10,000 and 40,000 $m^3 s^{-1}$ (Carter et al., 2006). These outburst and other, more regular, floods would have eroded the Quaternary lacustrine sediments in the lower elevation and axial portions of the Owyhee River Canyon.

Geochronology

Tephrochronology

Tephrochronology served as the main dating method for the lacustrine sediments. All tephra layers sampled in the sections, except for the WCT section, were correlated to MSH set C (Table 2). There are 6 layers included within MSH set C, but only layers Cw, Cy, and Cs are important marker beds distally (Mullineaux, 1986). Mullineaux (1986) indicated that there is uncertainty as to whether or not layers Cy and Cs are the same tephra. Mullineaux (1986) also postulated that the Marble Bluff tephra described by

Davis (1985) in Summer Lake and other sections in the Great Basin is in fact Cs. In later papers the Marble Bluff tephra was identified as layer Cy (Negrini et al., 2000; Kuehn and Foit, 2001).

The correlation of most tephra deposits in the field area to MSH set Cy are sound, but that correlation breaks down in the CH section. In the CH section, two distinct tephra layers are separated by approximately 7.75 meters of massive silt (Fig. 11 and 12). These two tephra deposits do not exhibit any obvious signs of reworking and therefore cannot be the same tephra layer, although they are geochemically very similar (Table 4). If reworking at CH is excluded, then MSH Cw and Cy layers are the only logical option for the identity of the two tephra layers in the CH section. MSH Cy is known from Summer Lake, OR (Negrini et al., 2000; Kuehn and Foit, 2001) and various locations in eastern Washington (Berger, 1991; Berger and Busacca, 1995; Whitlock et al., 2000). The MSH Cw layer has only been found in eastern Washington (Busacca et al., 1992, Berger and Busacca, 1995; Whitlock et al., 2000). Based on stratigraphic relations (Mullineaux, 1986) the upper tephra in CH is Cy and the lower tephra is Cw. The geochemical analysis results summarized in Table 4 show that all although both tephras correlate to MSH set C, they very likely correlate to Cw and Cy.

Dates vary for MSH set C, specifically layers Cw and Cy, due to location, material, and dating method (radiocarbon or thermoluminescence). Radiocarbon dates from Crandell (1981) suggested layers Cw and Cy were deposited 38 ka B.P. and 36 ka B.P, respectively. These radiocarbon dates have been cited and added to by Davis (1985) and Mullineaux (1986). Several authors now question the validity of these radiocarbon dates because they are near the limit of standard radiocarbon methods (Busacca et al., 1992; Berger and Busacca, 1995; Richardson et al., 1997). Clynne et al. (2008) presented recalibrated radiocarbon dates on undifferentiated MSH set C of Crandell (1981) at 47.5 ± 6 ka. Currently the most commonly cited age for MSH set C and layer Cy is 47 ± 2 ka (Negrini et al., 2000; Kuehn and Foit, 2001; Spencer and Knapp, 2010). This is a thermoluminescence date published by Berger and Busacca (1995), but another thermoluminescence date from the same paper, 46 ± 5 ka, may be a more accurate age estimate (G.W. Berger, personal communication, January 2010). Berger and Busacca (1995) dated other tephra layers in eastern Washington, including layer Cw, which they bracketed between 46 ± 6.3 ka and 74.6 ± 6.2 ka. Berger and Busacca (1995) state that although this is a large age range they suspect layer Cw is ~55 ka. Richardson et al. (1997) redated some of the same locations of Berger and Busacca (1995), and produced younger ages, including for some of the Cw layers. Furthermore, Clynne et al. (2008) states that all MSH set C tephra deposits underlie a till in the Lewis River Valley, WA, dated at 50 ka and a radiocarbon date from a possible Cw layer at this location is 49.5 ± 1 ka (Clynne, 2008; Vogel 2005).

This study will use the thermoluminescence date for layer Cy at 46 ± 5 ka. However, the dates for layer Cw vary significantly. In this study an age of 50 ± 5 ka will be used for the age of layer Cw. This age incorporates the age constraints of the thermoluminescence dates for the Cw layer in eastern Washington (Berger and Busacca, 1995) and a radiocarbon date from a possible Cw layer located near MSH (Clynne et al., 2008), as well as stratigraphic evidence in the Lewis River Valley (Clynne et al., 2008).

West Crater Lava Dam and Lacustrine Sediments

The duration of the West Crater Lava Dam and the deposition of the correlating Quaternary lacustrine sediments can be separated into five stages (Fig. 26) (1) Stage 1 (~70 ka) marks the emplacement of the WC lava dam and the filling of WC lake was with water; (2) Stage 2 (~70 to 42 ka) consisted of sedimentation into the WC lake and overflow of the WC lava dam; (3) Stage 3 (~42 ka to perhaps 36 ka) is marked by the incision of the basalt lava dam, the draining of the WC lake, and incision of the Quaternary lacustrine sediments; (4) Stage 4 (perhaps 36 to 15 ka) includes the incision through the Tertiary sediments of the modern canyon, which may have been faster than Stage 3 when incision was through the basaltic dam; (5) Stage 5 (~15 to 0 ka) includes the formation a river gradient similar to the modern river and the formation of the modern canyon.

Stage 1- Lava Dam Emplacement and Lake Formation

The WC basalt flow formed the WC lava dam at ~70 ka (Bondre, 2006; Brossy, 2007) when the flow followed Bogus Creek to the Owyhee River Canyon. As the WC lava flow entered the canyon, it covered the channel of the Owyhee River and the surrounding Tertiary sediments and other units. The lack of large sediment interbeds within the WC basalt flow, and similar paleomagnetic measurements, suggest the WC basalt flow, and therefore the lava dam, were emplaced within a short period of time (Brossy, 2007). Lake formation behind the dam would have begun as soon as the river was blocked.

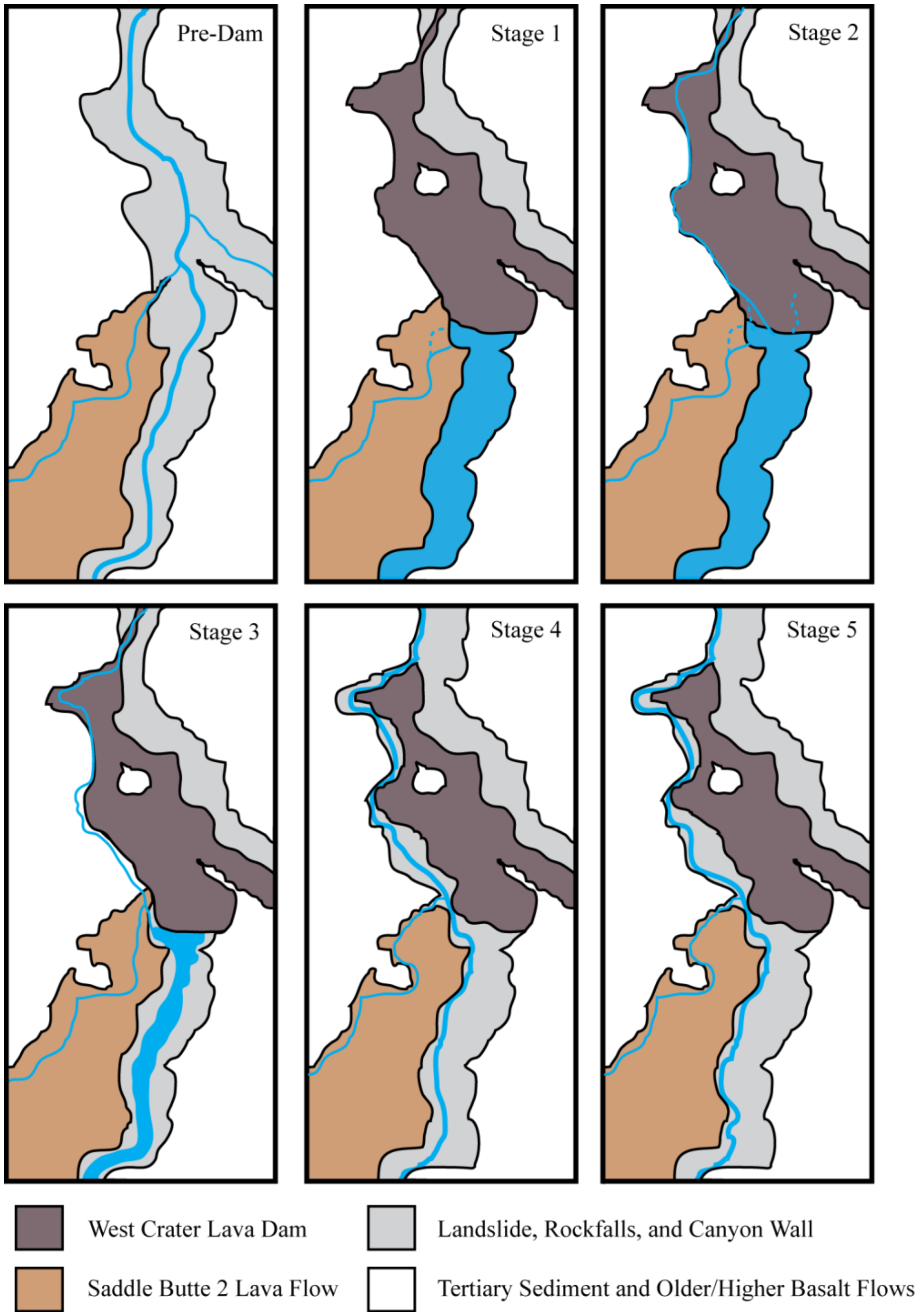

Figure 26. Schematic diagram showing the landscape and Owyhee River pattern of the West Crater lava dam area through time (north to top). The approximate location of Ryegrass Creek west of the Owyhee River, is also shown. Diagrams step through the five different stages of the West Crater lava dam duration and the history of the reestablishment of the river. The five stages are described in the text.

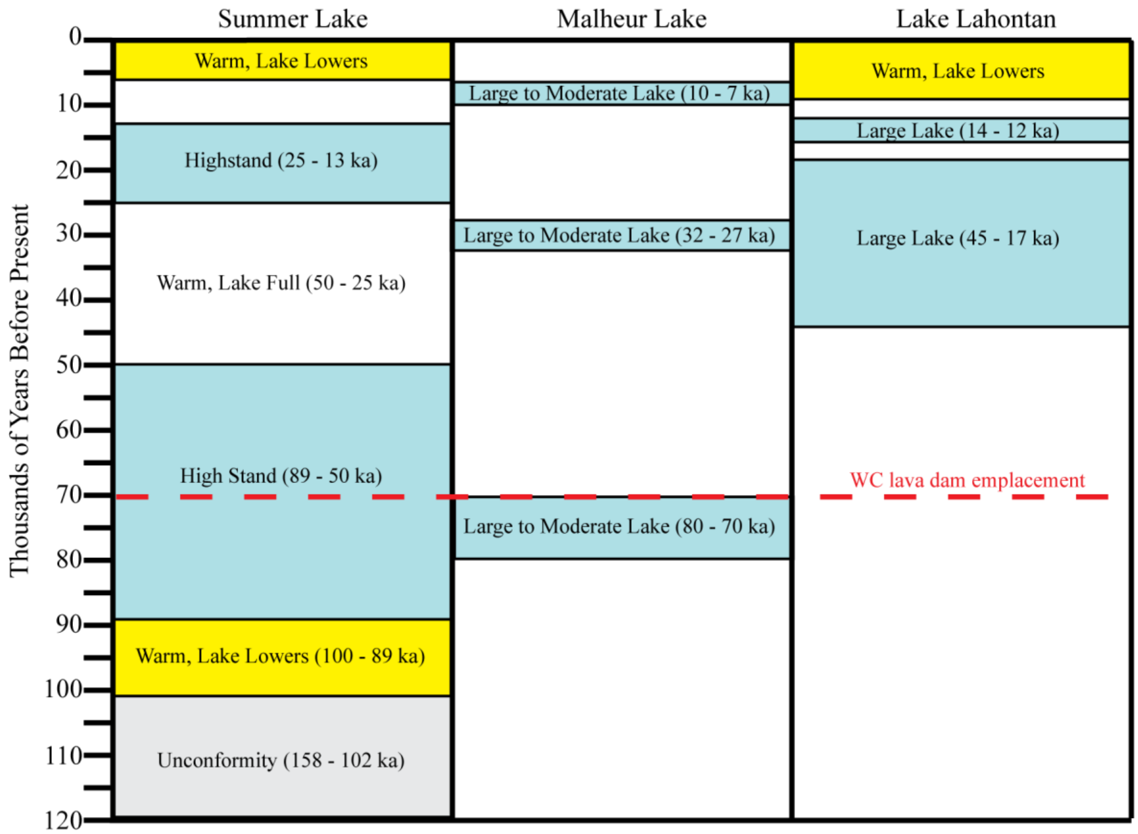

Figure 27. Diagram of lake conditions at Summer Lake (Lake Chewaucan), Malheur Lake, and Lake Lahontan from 120 ka to present (Negrini et al., 2000; Palacios-Fest et al., 1993, Dugas, 1998; Benson and Thompson, 1987; Hostetler et al., 1994). White areas indicate a gap in the record or little data. Blue and yellow show expansion of lake or highstand conditions and shrinking or shallowing of lake, respectively. Timing of emplacement of WC lava dam is also shown.

At 70 ka the climate of the area would have been much wetter than it is today (Fig. 27). Nearby Lake Chewaucan (~230 km west of the Owyhee field area) and Malheur Lake (~80 km west of the field area) experienced highstands at ~70 ka. Lake Chewaucan experienced another highstand at 20-15 ka (Negrini et al., 2000). No one has modeled the climatic conditions needed to sustain a highstand in Lake Chewaucan or Malheur Lake, but it has been done for Lake Lahontan (~190 km south of the Owyhee field area). Lake Lahontan was a much larger lake that underwent highstands at approximately the same time as Lake Chewaucan and other pluvial lakes in the region (Licciardi, 2001). Hypothetical water budgets for Lake Lahontan during its 20-13.5 ka highstand have been calculated by Hostetler and Benson (1990). Hostetler and Benson (1990) proposed a 42% decrease in evaporation, a 1.8x increase in precipitation, and a 2.4x increase in stream discharge from modern mean annual values to maintain the 20-13.5 ka highstand in Lake Lahontan. If these ratios are applied to Lake Chewaucan and Malheur Lake, they create positive water budgets that would also have been able to sustain these lakes at highstand levels.

If the climatic variables proposed by Hostetler and Benson (1990) could sustain highstand conditions at Lake Chewaucan at 20-13.5 ka, then similar conditions likely existed during the earlier 89-50 ka highstand of Lake Chewaucan and the 80-70 ka highstand of Malheur Lake. The correlation between the timing of highstands within these lake basins suggest that conditions were likely similar in the Owyhee River Canyon at the time of emplacement of the WC lava dam (Fig. 27). When the climatic conditions proposed by Hostetler and Benson (1990) are applied to the Owyhee River drainage, the WC lake could have filled to capacity (0.668 km^3) in less than one year (Table 5). Even using modern mean annual discharge measurements for the Owyhee River recorded at Rome, Oregon (Rkm 0; 0.833 km^3 y^{-1}), the time needed to fill the WC lake to full capacity is still less than one year (Table 5). Neither estimate includes additional streamflow from Jordan Creek and Crooked Creek, evaporation from the WC lake, or water leakage through the WC lava dam.

TABLE 5. LAKE EXTENTS AND FILL TIMES

Lake	Volume (km^3)	Surface Area (km^2)	Water Fill Time (yr)
West Crater lake	0.668	N.D.*	<1
Saddle Butte 2 lake	0.574	N.D.*	<1
Bogus Rim lake	N.D.*	1200	N.D.*

* N.D. = not determined.

Malde (1982) cited leakiness of the McKinney lava dam in southern Idaho as being one of the reasons for its long duration and large accumulation of sediments. He speculated that the accumulating sediments eventually plugged the fractures in the McKinney lava dam, allowing water levels to rise and eventually flow over the dam, initiating incision of the dam. It is unknown if large leaks occurred in the WC lava dam that may have prohibited the lake from filling in the calculated time. Leaks may have occurred, but no leaks could have been larger than the discharge of the Owyhee River into the WC lake. If leaks were substantial and larger than the discharge of the Owyhee River, the lake would not have filled. Based on evidence of overflow on top of the WC lava dam (see subsection Stage 2), lacustrine sediments, and the calculated discharges and infilling rates, it is inferred that the WC lake filled and may have done so relatively rapidly.

Stage 2- Lake Sedimentation and Dam Overflow

The change from flowing river to infilling lake should be recorded in the lacustrine sediment record as a change from larger to smaller grain size. This change in sediment type may be recorded at the base of the CH section (Fig. 11). The basal zone of CH contains ~4.7 m of ripple-laminated sands that appear to record several different directions of water flow (Fig. 12). The multiple flow directions could be attributed to eddying and turbidity in the Owyhee River caused by the WC lava dam. This interpretation is contradicted by the lack of gravel in the deposit, which is unlike all other Owyhee River deposits. An alternative explanation is that the ripple-laminated sands at the base of the CH section result from tributary channel flow or underflow currents after lake formation (Reneau and Dethier, 1996). This theory is challenged by the absence of complete sediment packages or depositional discontinuities that suggest turbidity current deposition. Additionally, diatoms in the basal zone of the CH section indicate turbid, shallow water conditions (S. Starratt, personal communication, April 2010) not indicative of deep-water currents. Although these diatoms correspond to a fluvial depositional environment, they would have needed time to establish a population indicating the lake filling may not have been as rapid as previously stated (see subsection Stage 1). It is possible the turbid, shallow water diatoms and sand preserved in the section were carried in by the flow from the upstream portions of the river. Such transport and reworking might explain the moderately to poor preservation of diatom frustrules. Only massive to laminated silts are found above the basal sand layers, indicating a shift to a calm depositional environment brought on by the WC lake (Fig. 11).

As the lake level rose, the delta of the river would have moved upstream until the lake filled to the top of the lava dam and the delta was situated at the inflow point of the Owyhee River. Typical reservoir deposition includes topsets (coarse sediment) that gradually transition to bottomsets (fine sediment) (Fig. 28). Delta deposits, such as topsets, may not have formed due to the quick (<1 yr) filling of the WC lake. The

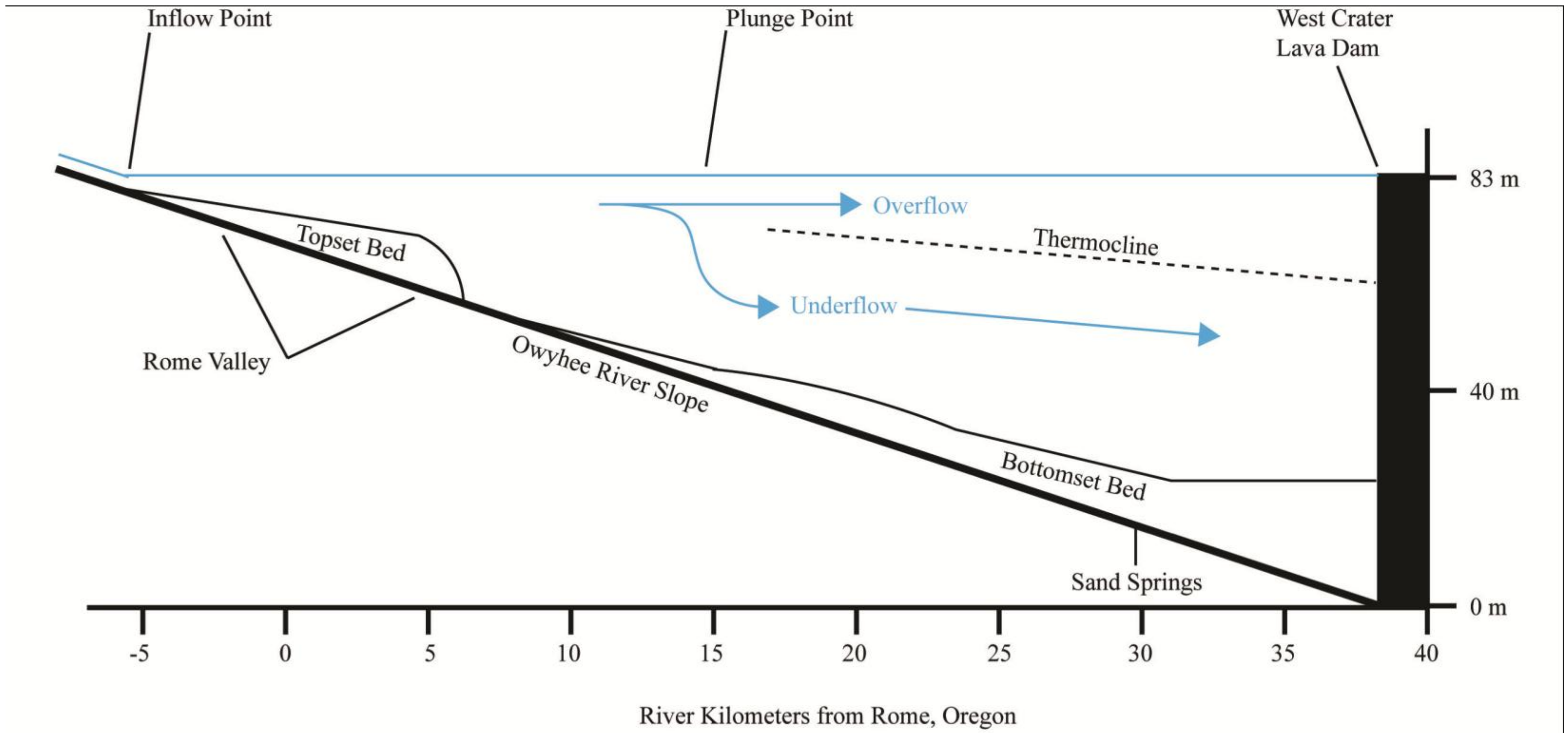

Figure 28. Schematic diagram of the longitudinal profile of West Crater (WC) lake with West Crater (WC) lava dam and possible reservoir sedimentation. West Crater lava dam is represented by a bold box, but it should be noted that the lava dam extends ~13 km downstream from this location. West Crater lake level and speculated thermocline position marked based on approximate annual thermocline depth in Lake Owyhee.

preserved sections of lacustrine sediment impounded behind the WC lake are botttomset sediments (fine-grained). Density currents, which control the path water and sediment takes when it enters the lake, deposit bottomsets. Density currents can be underflow, interflows, or overflows depending on whether they travel below, along, or above the thermocline (Smith et al., 1960). It is unknown which types of density currents were dominant in the WC lake, but all may have occurred due to seasonal variations. When underflows are dominant, sediment moves farther into the lake along the lakebed. When interflows or overflows are dominant, very little mixing in the lake occurs and water spreads across the surface, dropping its sediment load quickly. Overflow processes may play a part in the high levels of suspended sediment load in the epilimnetic layer of the modern Lake Owyhee and may have been equally as effective at moving sediment in the WC lake. Fine-grained sediment has been observed near the lake surface of modern Lake Owyhee ~60 km downstream of the Owyhee River input point (Craft el al., 2000). The ability to transport fine-grained sediments tens of kilometers downstream of the input could account for the dominant grain size in the WC lake sediments. If large amounts of fine-grained sediment were able to make it farther downstream, then classic delta deposits may never have formed at the lake-river junction and the lake would have filled with fine-grained sediments.

Microfauna and Lake Conditions

The absence of calcareous fossil material from the Quaternary lacustrine sediments is peculiar. If a lake existed on a scale of thousands of years in this location, one would expect organisms such as ostracodes, snails, and freshwater mussels to be present. The lack of this material may be explained by stratification and anoxia within the lake.

In order to build calcareous shells or valves, an organism needs to be able to access calcium and bicarbonate from the water or its food (Boggs, 2001). The modern Owyhee River has carbonate-calcium ratios of 0.9 to 1.1 (USGS). This range in ratios would allow for ostracode valve formation, but is it unclear how much calcium and bicarbonate was in the WC lake. Calcium precipitates out of water as calcite at TDS values of ~325 mg/l in many western U.S. rivers (Curry, 1999). Only 9 lacustrine sediment samples out of 250 effervesced when tested with HCl. The low percentage of HCl-reacting samples suggests that the WC lake did not precipitate calcite and therefore possibly had lower than ~325 mg/L TDS. Modern Lake Owyhee is undersaturated with respect to calcium carbonate and has TDS values ranging from 103 to 243 (Craft et al., 2000). Although the modern water chemistry of the Owyhee River and Lake Owyhee are undersaturated with respect to calcium carbonate, organisms are still able to create calcareous shells under these conditions. However, this undersaturation could destroy calcareous shell material after the organism dies and therefore may explain the absence of calcareous shells within the stratigraphic record of the WC lake.

Today's Lake Owyhee is a highly stratified lake with minimal turn over. If the lake that existed behind West Crater lava dam was similar to Lake Owyhee, it may have been stratified and created the same conditions seen in Lake Owyhee. Prolonged stratification in Lake Owyhee results in stagnation of the lower levels, causing anaerobic conditions, high CO_2 levels, and low nutrients (Craft et al., 2000). The characteristics of diatoms found within the CH section suggest low nutrient levels within the WC lake (S. Starratt personal communication, April 2010). Also, if stratification did occur in the WC lake then the potential geochemical conditions at depth could account for the lack of calcareous and silicic benthic species. In contrast, the nutrient-rich, well-mixed surface water in Lake Owyhee plays host to many algal blooms. Some diatoms types found within the CH section are known to be symbiotic with blue-green algae, suggesting the WC lake may have had similar conditions and algae blooms.

Variations in Sedimentation

Sediment source and sedimentation rates vary in each of the sections, specifically between the MWC and the CH sections. The high elevation and the on lapping of the MWC section onto the SB2 lava flow (Fig. 4) suggest that the section records local tributary and slope sedimentation into the WC lake. The low elevation, position, and fine-grained sediments of the CH section suggest the section records deep WC lake sedimentation. Although uncertain, the basal tephra deposit of the MWC section may correlate to the upper tephra in the CH section (Fig. 5). This possible correlation is based on similarities in layer thickness and correlation of the upper tephra in CH to the tephra in the TPZ section (Table 4). The elevation (Appendix B) and position of the TPZ section is very similar to the MWC section, indicating that the basal tephra layers in each section may be the same. If the tephra layers in the MWC and CH sections correlate, these sections may record a full lake record but not from the same depositional environment.

The MWC, CH, and TPZ sections are primarily fine grained, but sand beds can be found within the sections (Figs. 11, 15, and 17). The numerous sand layers within the

MWC section are examples of these sand beds. The sand layers in the MWC section may be the result of sedimentation from small, local tributaries or slope erosion based on the sections proximity to the canyon wall and the slope of the sediment layers towards the axis of the canyon. All preserved sediment sections are situated along the canyon wall and/or near areas where small drainages exist. Many of the tributaries are very small and remain dry for much of the year, but large precipitation events could mobilize sediment. This could be especially true in the past when wetter climate conditions may have created larger, more frequent tributary flows. Another explanation for the sand beds are slope failures of the immediate canyon walls during the existence of the lake, especially of the older Tertiary sediments.

Characteristics of the MWC and CH sections indicate that the types of deposition changed during the duration of the WC lake. Two color changes within the MWC section delineate three zones of the section (Fig. 16) and may indicate a change in local sediment source or geochemistry. Also, the sand layers within the middle zone of the MWC indicate an influx of local sand moved in during higher energy events. Three zones are also evident in the CH section and are marked by changes in bedding, grain size, and other features. The basal zone consists of laminated to rippled sand interpreted as the shift from a fluvial to lacustrine system. The massive to laminated silts and clays of the middle zone are interpreted as a lacustrine, depositional environment. The upper zone in the CH section also consists of massive silt to clays but is extensively crossed by laterally extensive orange-brown oxidation layers that may indicate minor differences in grain size, geochemistry of WC lake water or sediments during deposition, or oxidation reactions occurring after or during the draining of the WC lake. Although there are three zones in both the MWC and CH sections they are markedly different in characteristics including bedding features, grain size, and elevation suggesting they do not correlate.

Different sections record variations in lake sedimentation. Sections such as the MWC record likely record slope and nearby tributary sedimentation, while the CH section records deep lake sedimentation. Differences in sedimentation throughout the sections are marked by changes in grain size, bedding structures, color changes, and slope of sedimentary layers.

Sedimentation Rate

The CH section is the only section with two dated horizons, therefore allowing the calculation of a sedimentation rate. The two MSH tephra horizons Cw and Cy are dated to 50 ± 5 ka and 46 ± 5 ka, respectively (Table 3 and 4), and lie on the upper and lower boundaries of the middle zone of the CH section (Fig. 11). Although the tephra ages overlap in errors, the distance between the two tephra horizons is 7.75 m suggesting there was a reasonably amount of time between deposition of the two tephra layers. An average sedimentation rate for the time period between the two tephra layers is 1.9 ± 1.8 mm y^{-1}. At this rate, the 83 m deep basin created by the WC lava dam could have been filled within ~43,000 years. Using this average sedimentation rate, at least 4,300 more years is necessary to account for the accumulation of 8.4 m of similar massive to laminated silts above the Cy tephra layer in the CH section. When this sedimentation rate is applied to the entire CH section, the sediment record could exceed 50,000 years in length. A record of this length is highly unlikely due to geochronological constraints on the incision of the dam (see Stage 3 subsection below) and indicates that this sedimentation rate may be a minimum estimate.

This average sedimentation rate is within a massive silt deposit where the sedimentation rate could be much different than for other sediments preserved in the section. The calculated sedimentation rate can be viewed as an estimate, but it is important to note that sedimentation into the WC lake varied over time. Although the MWC and CH sections are dominated by mostly massive to finely laminated silt, both sections include higher energy deposits that were probably deposited more rapidly. The massive silt deposit does not include evidence of higher flow rates, larger sediment loads, or larger grain sizes such as occur in basal zone of the CH section or in the middle portion of the MWC section (Figs. 11 and 15). It is likely that this sedimentation rate does not apply to these portions of section and others that include sand and bedding structures indicating a higher sedimentation rate. However, it is likely that the sedimentation rate could be applied to similar massive to laminated silt units such as those in the upper zone of the CH section. Overall, the calculated sedimentation rate represents a minimum estimate of sedimentation rates for sections related to the WC lava dam.

Airfall tephra deposits within the CH and MWC sections represent particularly high sedimentation rates. Airfall tephra deposits have the ability to deposit distinct layers up to meters in thickness within time periods of minutes to days. The lower tephra in the CH section is ~15 cm thick and was deposited in very little time. Other smaller 2 to 4 cm tephra deposits in the upper portion of the CH section and at the base of the MWC section were also deposited as airfall and in very little time. These extremely high sedimentation rates complicate the calculation and use of average sedimentation rates taken over meters of section.

A sedimentation rate of 1.9 ± 1.8 mm y^{-1} can be calculated between the two tephra layers in the CH section. Although this rate is helpful in determining lake sedimentation and duration, the rate should not be applied to the all of the lacustrine sediments. Some lacustrine sediments include bedding structures and larger grain sizes that indicate higher sedimentation rates than the silt-dominated section over which the sedimentation rate was calculated.

Dam Overflow

Erosion of the basaltic WC lava dam possibly started at the moment of water overflow. Based on the distance suspended load travels in modern Lake Owyhee, suspended sediment was probably in the water that overflowed the WC dam. Clear water without sediment only incises through dissolution or flow cavitation, but once sediment is introduced to the streamflow abrasion can begin (Foley, 1980).

Early overflow and erosion of the lava dam sculpted shallow channels over the top of the WC basalt lava dam at an elevation within two meters of the dam surface (Brossy, 2007). Some of these channels include a very small amount of rounded pea-gravels of similar composition to other gravels within the lacustrine sediments, the Tertiary sediments, and the modern Owyhee River. These eroded channel features have been dated to ~59 ka using cosmogenic radionuclides (Table 3; C. Fenton unpublished data), indicating that water was flowing over the dam at this time but major incision had not began.

The Dog Leg terraces also help constrain the timing of overflow of the WC lava dam. The highest Dog Leg T5 terrace formed at ~46 ka. This terrace is a fluvially sculpted surface on the WC lava dam. At the same time that the Dog Leg T5 terrace was formed, sediment was being deposited at the CH and the MWC sections (based on tephrochronology within sections). This observation reveals an interesting characteristic of lava dams; deposition may be occurring behind the dam even as parts of the dam are being sculpted and incised. Even at ~46 ka when sculpting is happening at the Dog Leg terraces, the upstream portions of the dam must still be in place due to the elevation of the top of the MWC section ~13 m below the WC lava dam crest. The minimum age for the tephra at the base of the MWC section is ~46 ka, which means that the deposition of 15.5 m of laminated silts and sands that make up the MWC section (Fig. 15) still had to occur before major incision (more than 13 m) happened in the WC lava dam. If the calculated sedimentation rate for massive to laminated silts is used, then the time needed to deposit the 15.5 m at the MWC section is 8200 yrs and major incision in the dam would not have begun until ~38 ka. This is a maximum estimate for the time needed to deposit these sediments because the MWC section includes sand-sized grains and bedding structures indicating higher deposition rates.

Water began flowing over the WC lava dam shortly after emplacement sculpting paleochannels into the dam’s surface. Some of these channels have been dated at ~59 ka. The highest Dog Leg terrace, T5, is sculpted surface at the downstream end of the dam and has been dated to ~46 ka. Corresponding tephrochronology and sedimentation rate calculations for the WC lacustrine sediments indicate lake sedimentation was occurring until sometime between ~46 and ~38 ka. These dates constrain the timing of the beginning of major incision into the dam to after ~46 ka and the duration of the pre-incision dam to at least 24,000 years.

Stage 3- Incision of WC lava dam

The channels on the top of the WC lava dam indicate that the Owyhee River had begun to flow over the dam before the course of the Owyhee River was established in its present location. Basalt is much more difficult to erode than mudstone and sandstone, and the Owyhee River took the path of least resistance along the western edge of the WC lava dam and formed an epigenetic gorge. The soft Tertiary sediments along the western edge of the WC lava dam would have been more susceptible to erosion than the dam itself, with an erosion potential two magnitudes higher than the basalt lava dam (Sklar and Dietrich, 2001). Although the bed material is important in determining rates of erosion by streams, the sediment load in the stream also controls abrasion rates. Abrasion rates peak at intermediate grain sizes and decrease when the sediment load increases to the point of causing deposition on the channel bed (Sklar and Dietrich, 2001). Abrasion in overflow channels would have been at a minimal in the absence of bedload material in the channels. Once the lake basin filled with sediment or incision cut the dam to the sedimentation level, coarser-grained sediment would have been transported across the finer lacustrine deposits and onto the dam, increasing abrasion and erosion rates (Sklar and Dietrich, 2001). The dam would then experience the “tools effect” described by Sklar and Dietrich (2001). Erosion would have been minimal for a period of time until a supply of coarser sediment grains was accessible at which time erosion would dramatically increase. Although a small amount of gravels exists in the channels on top of the WC lava dam, rounded basalt boulder “tools” are found near where the river incised the modern Owyhee River Canyon adjacent to the WC lava dam. These “basalt bowling balls” suggest that one or more large events with high discharges and stream power flowed over the dam at the location of the present day canyon, with the boulders derived from the incision of the channel.

Fluvial gravel and sand units capping the finer lacustrine sediment sections indicate an end to lake deposition and a reestablishment of river flow through the canyon during the incision of the WC lava dam. The elevation of the river when it flowed over the lacustrine sediments upstream of the dam is controlled by the height the lacustrine sediments reached before the lake was drained. It is uncertain what elevation the lacustrine sediments reached in the WC lake, but the lake basin was probably not completely filled with sediment. Three lines of evidence suggest that the lacustrine sediment did not fill the lake basin behind the WC lava dam before major incision began. Firstly, the estimated minimum sedimentation rate calculated previously (see subsection Stage 2) suggests at least ~43,000 years is needed to fill the lake with sediment. Geochronological constraints indicate that the lake was only able to last at least ~24,000 years before incision into the dam began and the lake was compromised (see subsection Stage 2). Secondly, no lacustrine sediment deposits are preserved that fully confirm that the basin was filled with sediment. Tephra and sediment layers within preserved sections exhibit a slope towards the axis of the WC lake basin, suggesting a concave lake floor bathymetry. Lastly, very little gravel is found on the top of the WC lava dam suggesting bedload was never transported over the top of the dam. If lacustrine sediments had filled the lake basin, the deposits would have made a large plain of sediments for the river to flow over and bedload would have been able to be transported over the lake sediments and into paleochannels on top of the dam. Only a very small amount of bedload is observed in the paleochannels, indicating this was not the case. Based on this interpretation fluvial gravels would not have been available for use as abrasion “tools” on the WC lava dam until incision of the dam reached the elevation of the top of the lacustrine sediments within the WC lake basin.

Terraces and Incision

Terraces upstream and within the WC lava dam help constrain the timing and rate of incision through the dam. Terraces upstream of the dam remain undated but indicate that as the dam was incised the Owyhee River also incised through the lacustrine sediments of the WC lake. There are multiple terraces cut into the Quaternary lacustrine sediments (Fig. 29), each with a gravel and sand cap deposited during the formation of the wide or meandering river channel as it created the planar terrace surface. The gravel and sand caps range from ~0.1 to 4.4 m thick (Appendix B). Variations in thickness may be due to erosion and/or changes in sediment load amount, discharge, or thalweg location during deposition. No systematic relations exist between cap thicknesses and river kilometers or elevation. The thickest cap overlies the TPZ section and is 4.4 m thick (Fig. 17). The source of much of the deposit is likely nearby Ryegrass Creek, but could be

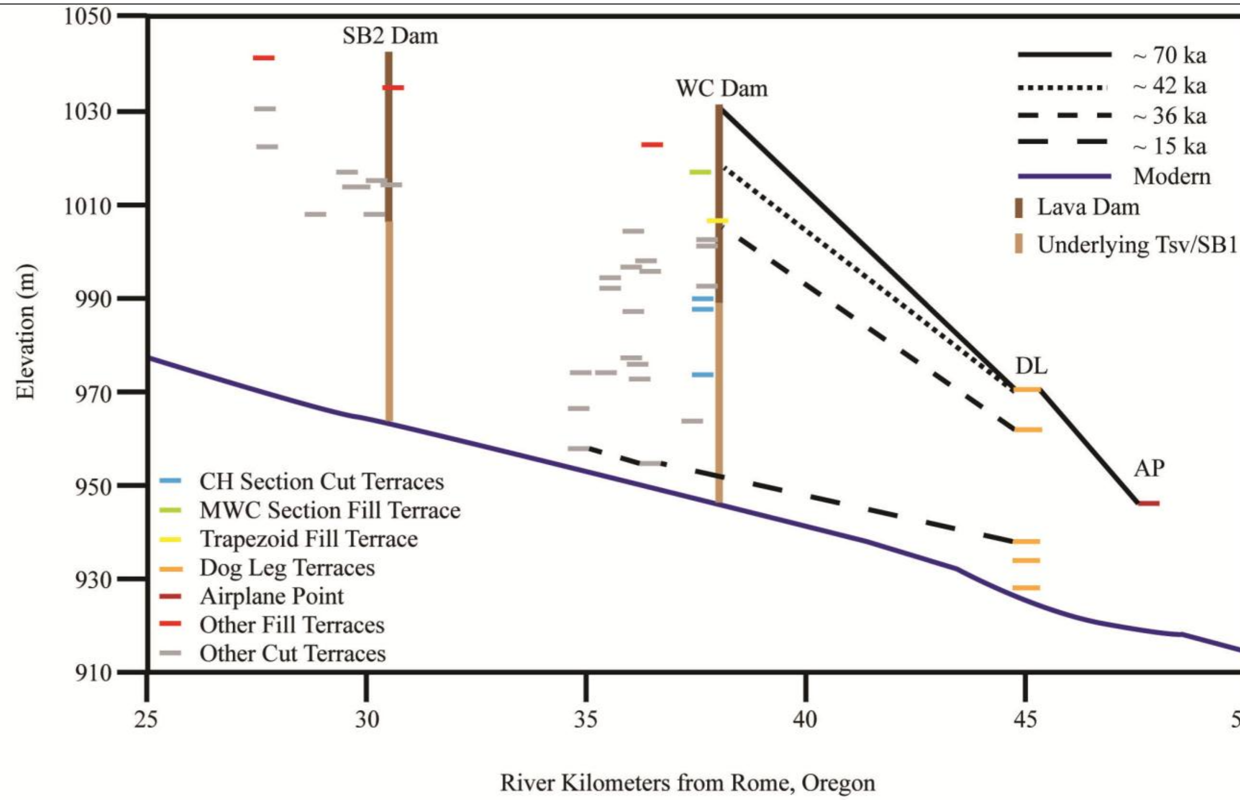

Figure 29. Longitudinal profile of the Owyhee River between RKm 25 and 50. Saddle Butte 2 (SB2) and West Crater (WC) lava dams are shown at their upstream extent. Underlying units for Saddle Butte 2 and West Crater lava dams (SB1 basalt flow and Tertiary sediment, respectively) shown by lighter brown. Terraces, both dated and undated, are also plotted and labeled. Original West Crater lava dam surface correlations shown by solid black line. Estimates of river incision through the West Crater lava dam and underlying Tertiary sediment at ~70, 42, 36, and 15 ka are shown by dashed black lines. Modern river profile shown by dark blue line.

attributed to early deposition of the new fluvial channel of the Owyhee River that may have had large discharge and sediment loads.

Although the Owyhee River eventually followed the western edge of the WC lava dam where it was able to incise both Tertiary sediments and the basalt dam, at Airplane Point the river was forced to incise through the basalt dam (Fig. 3). At Airplane Point basalt filled the canyon between two walls of older rhyolite units (Brossy, 2007). This basalt plug would have been a point of higher resistance and may have acted as the temporary base level for the river upstream, limiting upstream incision rates (Foley, 1980). ^{3}He cosmogenic dates on Airplane Point show that it was emplaced as part of the WC lava dam and water flowed over the top shortly after emplacement at ~70 ka (Fenton unpublished data).

Approximately 1 km upstream of Airplane Point are the Dog Leg terraces (Figs. 3 and 29). Their formation documents pauses in incision at certain times and at certain elevations. The T5 terrace, dated to ~46 ka (C. Fenton, unpublished data), shows sculpting directly into the WC basalt flow, suggesting that overflow of the dam was occurring by this time. No significant incision was occurring at this location at ~46 ka, but incision may already have begun happening downstream at Airplane Point.

The Dog Leg T4 terrace is dated at ~36 ka (C. Fenton, unpublished data) and is the only date that can help constrain the incision of the WC lava dam during this time. By this time the WC dam was presumably being incised at its upstream extent and lacustrine sedimentation at the MWC section had stopped as the lake drained. At this point fluvial incision into the Quaternary lacustrine sediment upstream of the dam would have dominated. It is possible that the pause in incision at ~36 ka during the formation of the T4 terrace occurred when the incision near the front of the WC lava dam came into contact with a tongue of SB2 basalt flow. A tongue of the SB2 basalt flow reaches across the Owyhee River Canyon at Rkm 39. Here the SB2 flow followed a paleochannel of Rye Grass Creek toward the pre-WC lava dam Owyhee River east of this location (Fig. 26). This tongue of basalt is at an elevation of ~990 m and is located underneath the WC lava dam. This elevation is similar to that of the upper portion of the CH section (Fig. 29) where many orange-brown layers are present. These layers may be due to minor fluctuations in the surface of the lake at this approximate elevation.

If the correlation between the T4 surface and SB2 basalt layer slowing river incision is correct, then the WC lava dam may have been removed very quickly (Fig. 30). Incision rates calculated based on this interpretation must account for the removal of the 40 m of the basaltic WC lava dam above the SB2 basalt layer in the time period from ~46 to ~36 ka. Using these measurements an incision rate of 4.00 mm y^{-1} can be calculated for the removal of the WC lava dam (Table 6). This incision rate is high for basalt incision and may indicate either this correlation is incorrect or the WC lava dam may have failed at least partially. No evidence of a large failure is observed today, so it is likely this correlation is incorrect.

It is a possibility that the pause in incision that formed the T4 surface at ~36 ka was caused by the WC lava dam itself. Basalt lava flows inherently include many layers with different flow and jointing structures. It is very likely that during the incision of the WC lava dam, incision rates varied depending on the properties of the basalt.

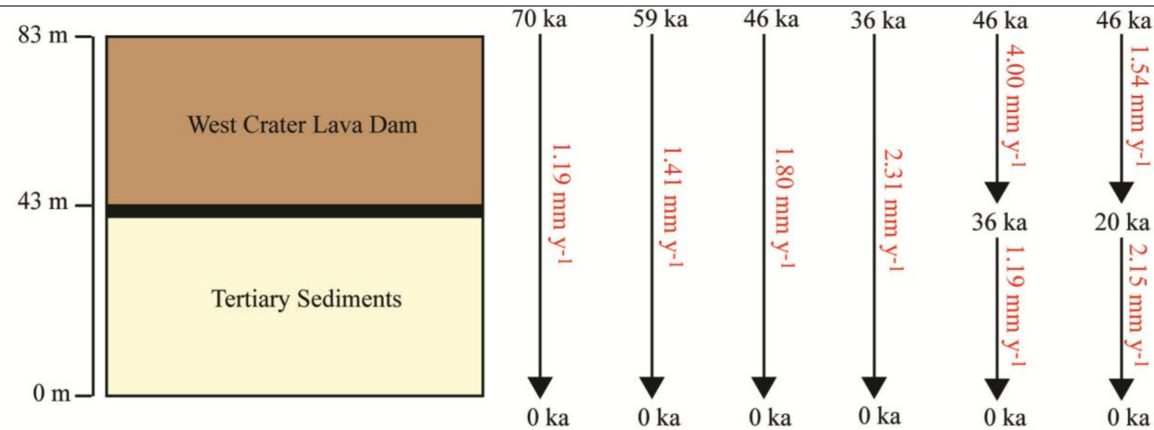

Figure 30. Schematic diagram of incision through the West Crater (WC) lava dam and the Tertiary sediments. Bold line between West Crater lava dam and underlying Tertiary sediments indicates location of Saddle Butte 2 (SB2) lava flow and Ryegrass Creek paleochannel within the geomorphic stratigraphy. Black arrows indicate height, and text on each end of the arrow indicates the time periods, over which incision rate (labeled in red) were calculated. Note two arrow pairs on right include differential incision rates over the West Crater lava dam and the Tertiary sediments. These right-most arrow pairs show the relationship between incision of the West Crater lava dam and the Tertiary sediments, with one being high and the other being low in one scenario and vice versa in the next.

TABLE 6. INCISION RATE ESTIMATES FOR THE WEST CRATER LAVA DAM

Time Period (ka)	Height (m)	Incision Rate (mm y^{-1})	Description
70–0	83	1.19	Dam crest to modern river level
59–0	83	1.41	Paleochannel at dam crest to modern river level
46–0	83	1.80	Dam crest to mrl w/ tephra constraints
36–0	83	2.31	Dam crest to mrl
46–36	40	4.00	Dam crest to SB2 tongue w/ tephra constraints and SB2 tongue-T4 correlation
36–0	43	1.19	SB2 tongue to modern river level w/ speculated SB2 tongue-T4 correlation
46–36	8	0.80	Dog Leg T5 to T4
36–14	24	1.09	Dog Leg T4 to T3
14–10	4	1.00	Dog Leg T3 to T2

Another possibility that by ~36 ka the upstream end of the WC lava dam was not yet incised, and incision through the Dog Leg terrace region was caused by upstream knickpoint migration upstream from the Airplane Point area. Dates on the Dog Leg T3 surface and boulder bars upstream of the dam indicate that the dam was completely incised by ~15 ka (see subsection Stage 5). If knickpoint progression was the dominant process, the WC lava dam would have had to incise from the Dog Leg terraces to the upstream end of the dam (a distance of ~7 km) in ~21 ka, an erosion rate of 0.3 m/yr. It is possible that more than one knickpoint was responsible for incision of the basalt dam.

Stage 4- Incision of Tertiary Sediments

The incision of the Tertiary sediments underlying the WC lava dam was likely much more rapid than that through the WC lava dam. The Tertiary sediments in the reach affected by the WC lava dam are mostly fluviolacustrine mudstones, sandstones, and volcaniclastic sediments. Based on the information above, a number of incision rates can be calculated for the incision through the WC lava dam and the Tertiary sediments (Fig. 30; Table 6). Incision rates range from 1.09 to 4.00 mm y^{-1}. This range of incision rates overlaps and exceeds incision rates calculated for basaltic lava dams in tectonically active areas of 0.098 mm y^{-1} to 1.15 mm y^{-1} (Shao-Ping et al., 2006). This difference may represent incision through a mixture of both basaltic WC lava dam and the underlying and adjacent Tertiary sediments. In addition, many of the higher incision rates are calculated based on the SB2 tongue to T4 terrace correlation and therefore may be overestimates. Rates of incision from the WC lava dam crest to the modern river level, through the WC lava dam and the underlying Tertiary sediments, range from 1.19 to 1.80 mm y^{-1} (Fig. 30; Table 6).

Timing of incision through the WC lava dam and Tertiary sediment is loosely bracketed between ~46 ka and ~0 ka. This time bracket is based on tephrochronology in the sediment sections, sculpting of the WC lava dam top, and the modern river. Also, the total height at the front of the dam from the WC lava dam crest to the modern river level is 83 m. The 83 m of material is roughly split in half between WC lava dam on top (83 to 43 m) and Tertiary sediment below (43 m to 0 m; Fig. 30) With this information some insights can be gained about relative incision rates through the dam at this location. It is possible that very slow incision over the WC lava dam occurred due to the low erosion potential of the basalt and the lack of abrasion tools available. If slow incision occurred through the WC lava dam, then the incision through the Tertiary sediment may have been very quick, making up for the time “lost” working through the harder WC lava dam (Fig. 30). Alternatively, if the WC lava dam was incised quickly and/or failed catastrophically, then incision through the Tertiary sediments may have been gradual. Another possibility is that incision rates remained nearly constant throughout the incision of both the WC lava dam and the Tertiary sediments. A near constant incision rate could have been possible due to the course chose by the Owyhee River, following the western edge of the WC lava dam. By following the edge of the lava dam, erodible Tertiary sediments may have been incised and not the WC lava dam directly. Both constant and rapid incision rates may have been possible and more geochronological constraints are needed to be sure of which scenario is correct.

It is important to note that incision rates based on terrace dates may have errors up to thousands of years due to the character of terrace formation (Hancock and Anderson, 2002). The dates used in this study are on surficial features on terraces, therefore they likely represent the latter stages of terrace surface formation before incision by the Owyhee River continued. Incision rates between terraces or terraces and modern river level are averages and may include thousands of years of very low to nonexistent incision periods. This would suggest that incision rates based on these dates are actually minimum incision rates.

Incision through the Tertiary sediments could have been much faster than through the WC lava dam due to the difference in erosion potential. Incision rates calculated for the Owyhee River are very fast and are higher than even tectonically uplifted regions. High incision rates calculated for incision through the WC lava dam may result from incision actually occurring through the adjacent Tertiary sediments and not the lava dam directly. More geochronological constraints are needed before clear conclusions can be made about the incision through both the WC lava dam and the Tertiary sediments.

Stage 5- Incision to Modern River Level

By ~14 ka, when the Dog Leg T3 terrace formed (C. Fenton, unpublished data), the WC lava dam was incised and the elevation and gradient of the river were similar to those of the modern river (Fig. 29). Additional evidence for the timing of the removal of the WC lava dam are various boulder deposits located on a bar ~2 km upstream from the WC lava dam. These boulders were deposited as upstream landslide dams failed (Othus, 2008), therefore indicating that the river was through-flowing and near the modern river level. Cosmogenic ages of the boulders range from ~10 to 20 ka (C. Fenton, unpublished data) indicating that the Owyhee River was nearly down to its channel elevation by this time and that the WC lake no longer existed.

Saddle Butte 2 Lava Dam and Lacustrine Sediments

Lava Dam Emplacement and Lake Formation

The SB2 basalt flow occurred at ~144 ka (B. Turrin, unpublished data) after the SB1 basalt flow. The SB2 basalt flow entered the canyon via the Sand Springs Drainage and not Granite Creek as the SB1 basalt flow had. The SB1 flow formed a lava dam in the Owyhee River Canyon but the extent to which the SB1 lava dam had incised by the time the SB2 lava dam was emplaced is not known. The crest elevation of the SB2 lava dam is ~1042 m. This elevation is 12 m above the WC lava dam crest elevation (1030 m).

Using the modern discharge of the Owyhee River at 0.833 $km^3\ y^{-1}$ and the approximate volume of the SB2 lake at full capacity (~0.574 km^3), the fill-time would have been less than one year (Table 5). Like the WC lake, this extremely rapid filling of the SB2 lake could have caused overflow, and therefore possibly incision, to begin shortly after the SB2 lava dam was emplaced.

Lake Sedimentation

The SS and SB1 sections (Figs. 20 and 22) are located just upstream from the SB2 lava dam (Fig. 2 and 3). The top of the SS section (~1020 m) is lower in elevation than the crests of both the WC and SB2 lava dams. Without geochronological constraints it is uncertain to which lava-damming event the SS section corresponds. Because of the proximity to the SB2 lava dam and the existence of hills of similar massive silt located less than 1 km up the Sand Springs drainage, the SS section is most likely related to the SB2 lava dam. The upper SS deposits include small hills that on-lap the SB2 lava dam and larger hills that stand isolated in the center of the drainage. These deposits reach elevations higher than the WC lava dam crest elevation, but not higher than the SB2 lava dam crest elevation. The elevation data and geomorphic relations of these upper SS deposits strongly suggest that they correlate to the SB2 lava dam.

The SB1 section sits on a bench created by a remnant of the SB1 lava dam (Fig. 6). This bench is similar in elevation to the SB1 lava dam remnant that the SS section sits on (Fig. 5). The SB1 section is composed of massive to laminated silt and sand with a fluvial channel cut (Fig. 21 and 22). Overlying the section is a debris flow deposit. The section of fine-grained material reaches an elevation of ~1044 m. This elevation is 2 m higher than the estimated SB2 lava dam crest, but within the range of uncertainty and therefore the SB1 section is correlated to the SB2 lava dam.

Although the main section of fine-grained material in the SB1 section can be correlated to the SB2 lava dam due to elevation, the origin of the fluvial channel cut into the section is less clear (Figs. 21 and 22). The base of the fluvial channel is at 1030 m elevation, the same elevation as the WC lava dam crest. It is possible that this channel was cut by stream flow related to the overflow of the WC lava dam, but in order for the additional 4 m of accumulated fluvial gravels to be deposited on top of the channel base the water level must have reached to at least 1034 m. The WC lava dam could not have kept water at this elevation and therefore cannot be responsible for the deposition of gravels and sediments within the channel cut. The low elevation of the WC lava dam would also make it difficult to create the stream flow and channel slope needed for the deposition of the fluvial gravel. Therefore it is likely that the cutting and deposition of the fluvial channel occurred during the incision of the SB2 lava dam. Furthermore, the sediment overlying the basal gravel deposits in the channel includes silt and fine-grained sand (Fig. 23), suggesting a change in sediment source or water flow. These two deposits may have occurred during the evolution of the main channel or by some blockage that occurred during the overflow and incision of the SB2 lava dam.

Two ~6 m-high sections of rounded fluvial gravels located in borrow pits just north of Rome, Oregon may account for some of the deltaic bedload deposits in the SB2 lake based on their elevation. The elevation of the tops of the borrow pits are 1039 to 1041 m indicating they are too high to correlate to the WC lava dam, but may correlate to the SB2 lava dam. These gravels do not exhibit the bedding or imbrication commonly found in deltaic features and topsets. It is possible that the gravel units may not have resulted from the lakes and could be part of a fluvial deposit related to aggradation of sediment in the valley.

The SS and SB1 stratigraphic sections can be correlated to the SB2 lava-damming event based on elevation and geomorphic relations. The fluvial channel cut in the SB1 section likely was formed during the incision of the SB2 lava dam. Gravel deposits in the Rome Valley near Rkm 1 may be deltaic deposits from the SB2 lava dam based on elevation.

Dam Removal and Incision

A number of terraces are located upstream of the SB2 lava dam (Fig. 28). These terraces are cut into Quaternary lacustrine sediment and are situated on the remnants of the SB1 lava dam. Because these terraces are undated and located upstream of both the WC and SB2 lava dams, they could relate to either lava dam. There is also a chance that some of these terraces may represent river incision that predates either of these lava-damming events. These terraces are located directly on top of the SB1 flow, suggesting they are related to the SB2 lava dam and not the later WC lava dam. This suggestion may not be true if the SB2 lake did not collect sediment or all sediment collected was eroded from the top of the SB1 lava dam remnants before the WC lava dam and lake. Other terraces located on the eastern edge of the SB2 lava dam could be remnants of incision initiated by the SB2 lava dam. Without geochronological constraints, the origin of these terraces can only be speculated.

Bogus Rim Lava Dam and Lacustrine Sediments

Although the BR lava dam was not the main focus of this study, its impacts on the landscape would have been extensive. The BR lava dam blocked a much shallower and wider paleo- Owyhee River Canyon ~1.9 Ma (Bondre, 2006), and had a crest elevation of ~1200 m (Fig. 10). The subsequent lake formed by this dam would have covered ~1100 km^2 (applying max water level to modern topography). Unlike the smaller WC and SB lava dams, which were held within the deeply incised Owyhee Rive Canyon, the high elevation of the dam crest and the shallow paleo-canyon allowed this dam to flood a large portion of the surrounding landscape.

Fine-grained sediments and capping gravel deposits extend outward from the rim of the modern canyon in much of the study area. These fine-grained sediments are massive to finely laminated and up to 10 m thick. The capping gravel deposits are up to 3-5 m thick (P. K. House, personal communication, December 2009). Lacustrine sediment related to the BR lava dam and lake was deposited directly onto Tertiary basalts and sediments. The blanketing of the surrounding area with lacustrine sediment filled depressions and leveled topography in this region.

Implications and Comparisons

The Owyhee River was integrated from Northern Nevada to the Snake River ~7 Ma years ago (Beranek et al., 2006) and was interrupted numerous times by lava dams. If the nine intracanyon flows identified thus far (Brossy, 2007; P.K. House, personal communication, December 2009) created lava dams similar to the WC lava dam, in that they lasted ~55,000 years, then the Owyhee River has been directly affected by lava dams for ~7% of its history. It is important to note that these nine intracanyon flows are the youngest flows to impact the Owyhee River and span only the last ~2 million years. Many other older flows, not fully delineated in previous work, exist in the vicinity of the Owyhee River Canyon and compose much of the surrounding rim basalts. These rim basalts likely affected the river prior to, or during the early phases of, the incision of the Owyhee River Canyon. Prior to the incision of the Owyhee River Canyon, a broad plain may have existed for the river to migrate across, but with numerous lava flows emplaced on the plain, the river course may have become increasingly constricted over time. This limiting of lateral incision may have focused stream erosion into a smaller area and subsequently instigated vertical erosion of the Owyhee River Canyon. In addition to constriction of the channel by lava flows, changes in base level and tectonics may have played a part in the incision of the Owyhee River Canyon.

Incision of the Owyhee River Canyon entrenched the river and locked it into a single course. Lava dams that affected the Owyhee River within the canyon then may have had lesser effects on the course of the river. An example might be the diversion of the river around a lava dam. Unless the lava dam filled to the top of the Owyhee River Canyon, the river would stay within the limits of the canyon making a relatively small diversion. Diversions within the canyon may be limited, but each time the river was diverted around a lava dam and forced to incise the adjacent bedrock, the canyon was widened.

The limited scope of this project prevents the use of the WC lava dam as a representative case study of all lava dams on the Owyhee River. In addition, the lack of detailed studies of lava dams on other rivers, makes it difficult to compare the results of this study to other lava-damming events. The best example of a similar lava dam, based on the limited information available, is the McKinney lava dam and the Yahoo Clay of the Snake River described by Malde (1982). This lava dam was similar to the WC lava dam in that the dam was of similar basaltic composition and it was emplaced within the Snake River Canyon whose walls are made up of bedrock units similar to those of the Owyhee River Canyon. It is also important to note that the climate of the Snake River Plain is similar to that of the Owyhee Uplands. The McKinney lava dam (183 m) was much higher than the WC lava dam (83 m) and the lacustrine sediment unit associated with it, the Yahoo Clay, accumulated to the top of the lava dam. This may mean that incision processes in the two dams was different. The McKinney lava dam was emplaced at ~52 ka (Tauxe et al., 2004) and therefore had to be completely incised in less time than the WC lava dam (~55,000 years). The shorter duration of the McKinney lava dam is surprising since the dam was much larger than the WC lava dam. This might indicate that size is not the most important factor when determining how long a lava dam may last before the river reestablishes its course. Other factors that might explain the shorter duration of the McKinney lava dam are the higher stream discharge and power and possibly larger sediment loads in the Snake River, which would have caused the lake to quickly fill with sediment.

Although there are similarities between the McKinney lava-damming event and the WC lava dam, there are many differences including the duration of the lava dams. One could hypothesize that depending on numerous variables (e.g. size, emplacement style, composition, structural strength, stream size and type, climate, and bedrock lithologies), the effects and duration of lava dams and their lakes will be unique to each dam.

CHAPTER V

CONCLUSIONS

This study explored an area of the Owyhee River Canyon that has been affected by lava dams over the course of the Quaternary. An approximate chronology of the WC lava dam was deduced from $^{40}Ar/^{39}Ar$ and ^{3}He cosmogenic dates, tephrochronology, stratigraphy of the lacustrine sediments, and geomorphic relations found in the field. The chronologies of the SB2 and BR lava dams were not determined in this study due to the lack geochronology and preservation of features associated with them.

The lacustrine sediments that accumulated behind the lava dams were helpful in understanding details about the history of the lava dam and their correlating lakes. In general, the lacustrine sediments were located near the lava dams, along the canyon walls, and near small tributaries. Stratigraphic descriptions and microfauna analysis of the lacustrine sediments helped in understanding lake sedimentation and possible lake levels. Dating of the Quaternary lacustrine sediments proved to be problematic due to the lack of organics for radiocarbon dating, inaccurate OSL ages, and questions concerning MSH set C tephra ages. Tephra layers MSH Cw, MSH Cy, and Summer Lake Tephra LL provided some of the few dates on the stratigraphic sections.

Terraces located and described in this study were also helpful in understanding the incision of the WC lava dam. Terraces were located in areas where Quaternary lacustrine sediments have been preserved, where Tertiary sediments crop out, and within the WC lava dam. Previously obtained ^{3}He cosmogenic dates (Brossy, 2007) on sculpted paleochannels on top of the dam and the Dog Leg T5 and T4 terraces were immensely important in discerning the elevation of the Owyhee River during incision of the WC lava dam. Additionally, ^{3}He cosmogenic dates on the Dog Leg T3 and T2 terraces and boulder bars within the Artillery landslide reach provided a time estimate for the establishment of the modern river channel.

Results from this study indicate that the duration of the WC lava dam can be separated into five stages (Fig. 29). Stage 1 includes the emplacement of the WC lava dam at ~70 ka and the filling of the lake basin with water. Modern stream discharge rates could have easily filled the lake in < 1 year. In addition, paleoclimate record from nearby pluvial lakes indicate stream discharge was probably higher than modern ~70 ka. During Stage 2, the WC lava dam remained mostly intact with only minor sculpting from water overflow while sediments were deposited into the lake basin until after ~46 ka. In the absence of similar lava dams and lakes, Lake Owyhee proved to be a helpful analog for understanding possible lake conditions and sediment transport in the WC lake.

During Stage 3, incision may have begun sometime after ~46 ka and the dam may have been nearly incised by ~36 ka or later. The WC lake was probably drained during Stage 3. Paleoclimate records indicate greater effective moisture during time of incision, suggesting stream discharge was probably not a limiting factor in the incision of the WC lava dam. Stage 4 spans from the end of Stage 3 to ~15 ka in which the Owyhee River gradually incised the Tertiary sediments below the WC lava dam and the upstream Quaternary lacustrine sediments. Incision rates calculated for the WC lava dam and the underlying Tertiary sediments range from 1.19 to 1.80 mm y^{-1}. These rates are high for incision into basalt and may indicate incision was predominantly through the Tertiary sediments. More geochronological constraints are needed before incision of the Owyhee River Canyon around the WC lava dam can be fully understood and quantified. Possible factors influencing the rate of incision through the dam include the so-called “tools effect”, in which major incision could not start until material was available at the overflow elevation of the lava dam. Other factors affecting incision rates included differences between the erosion potential on the basalt lava dam versus the adjacent and underlying Tertiary sediments, and changes in the location of the incision channel in relation to these units.

By ~15 ka the Owyhee River was near the modern river gradient and Stage 5 began. During Stage 5, the river incised for at least another ~10 ky to reach its current elevation. Overall, the WC dam lasted a minimum of ~24,000 years before major incision occurred. Once incision of the dam was completed, it took another ~31,000 years for the Owyhee River to reach a near-modern river gradient. Taken as a whole, the Owyhee River was influenced directly for ~55,000 years by the WC lava-damming event.

The Owyhee River was likely integrated sometime after 7 Ma (Beranek et al., 2006). At least nine intracanyon flows have affected the Owyhee River over its history. If these lava flows dammed the river and the duration of the WC lava dam is representative of these dams, then at least 7% of the history of the Owyhee River has been directly affected by lava dams. There are many more lava flows in the vicinity of the Owyhee River that possibly encroached on the course of the paleo-Owyhee River and may have caused changes in incision. Over time, lava flows may have controlled the morphology and course of the Owyhee River.

The conclusions stated here are specific to the WC lava dam and may not be representative of other lava dams. Variations in size, composition, emplacement style, adjacent units, stream size, and climate may affect the life of individual lava dams. Smaller and larger lava dams may be easier or harder to remove or incise, respectively, although stream discharge, and therefore climate, may be controlling factors. Also, some dams may be structurally weak or strong due to emplacement style, composition, and adjacent units. Examples of structurally weak lava dams are those located in the Grand Canyon that are known to have catastrophically failed due to weak supporting units (Fenton et al., 2004; Fenton et al., 2006). Some similarities do exist between the WC lava dam on the Owyhee River and other lava dams described in the literature. The most similar case is that of the McKinney lava dam and the Yahoo Clay unit in southern Idaho (Malde, 1982). The McKinney lava dam is located in a similar climate regime, with similar basalt composition, with similar Tertiary bedrock sediment units, and was incised in less than 52,000 years. These similarities suggest that the effects and duration of lava dams on rivers in the Snake River Plain and the Owyhee Uplands may be similar.

Many future projects could involve further investigation of the Owyhee Uplands, specifically its stratigraphy, surficial processes, and geochronology. As few data sets exist for the modern Owyhee River, increased research and monitoring are also needed to fully understand this river system and provide background data for future studies. In general, more detailed research on lava dams, their lakes, and the resulting lacustrine sediments on rivers other than the Owyhee River are needed in order to understand the large number of effects lava dams can have on river systems. In these future studies, lacustrine sediments should be thoroughly investigated and used as a valuable resource. Of course, to fully employ the lacustrine sediments in understanding the lava dam and fluvial incision history, more dating techniques need to be used and the existing techniques must be improved.

REFERENCES

Abbott, W. H., 1972, Micropaleontology and paleoecology of Miocene non-marine diatoms from the Harper District, Malheur County, Oregon [M.S. thesis]: Monroe, Northeast Louisiana University, 86 p.

Aitken, M.J., 1998, An introduction to optical dating: New York, Oxford University Press, 267 p.

Benson, L.V., Lund, S.P., Burdett, J.W., Kashgarian, M., Rose, T.P., and Schwartz, M., 1998, Correlation of Late-Pleistocene lake-level oscillations in Mono Lake, California, with North Atlantic climate events: Quaternary Research, v. 49, p. 1-10.

Benson, L.V., and Thompson, R.S., 1987, Lake-level variation in the Lahontan Basin for the past 50,000 years: Quaternary Research, v. 28, p. 69-85.

Beranek, L.P., Link, P.K., and Fanning, C.M., 2006, Miocene to Holocene landscape evolution of the western Snake River Plain region, Idaho: Using the SHRIMP detrital zircon provenance record to track eastward migration of the Yellowstone hotspot: Geological Society of America Bulletin, v. 118, p. 1027-1050.

Berger, G.W., 1991, The use of glass for dating volcanic ash by thermoluminescence: Journal of Geophysical Research, v. 96, p. 19,705-19,720.

Berger, G.W., 2010, personal communication, January.

Berger, G.W., and Busacca, A.J., 1995, Thermoluminescence dating of late Pleistocene loess and tephra from eastern Washington and southern Oregon and implications for the eruptive history of Mount St. Helens: Journal of Geophysical Research, v. 100, p. 22,361-22,374.

Birkeland, P.W., 1963, Pleistocene volcanism and deformation of the Truckee area, north of Lake Tahoe, California: Geological Society of America Bulletin, v. 74, p. 1453-1464.

Boggs, S., Jr., 2001, Principles of sedimentology and stratigraphy: Upper Saddle River, New Jersey, Prentice-Hall, 726 p.

Bondre, N.R., 2006, Field and geochemical investigation of basaltic magmatism in the western United States and western India [Ph.D. thesis]: Oxford, Miami University, 263 p.

Borchardt, G.A., Aruscavage, P.J., and Millard, H.T., Jr., 1972, Correlation of the Bishop Ash, a Pleistocene marker bed using instrumental neutron activation analysis: Journal of Sedimentary Research, v. 42, p. 301-306.

Bouchard, D.P., Kaufman, D.S., Hochberg, A., and Quade, J., 1998, Quaternary history of the Thatcher Basin, Idaho, reconstructed from the $^{87}Sr/^{86}Sr$ and amino acid composition of lacustrine fossils: implications for the diversion of the Bear River into the Bonneville Basin: Paleogeography, Paleoclimatology, Paleoecology, v. 141, p. 95-114.

Bradbury, J.P., Colman, S.M., and Dean, W.E., 2004, Limnological and climatic environments at Upper Klamath Lake, Oregon during the past 45 000 years: Journal of Paleolimnology, v. 31, p. 167-188.

Brand, B.D., and White, C.M., 2007, Origin and stratigraphy of phreatomagmatic deposits at the Pleistocene Sinker Butte Volcano, Western Snake River Plain, Idaho: Journal of Volcanology and Geothermal Research, v. 160, p. 319-339.

Breckenridge, R.M., and Sprenke, K.F., 1997, An overdeepened glaciated basin, Lake Pend Oreille, northern Idaho: Glacial Geology and Geomorphology, rp01/1997 http://ggg.qub.ac.uk/ggg/papers/full/1997/rp011997/rp01.htm.

Brossy, C.C., 2007, Fluvial response to intra-canyon lava flows, Owyhee River, southeastern Oregon [M.S. thesis]: Ellensburg, Central Washington University, 109 p.

Bryan, K., 1929, Geology of reservoir and dam sites with a report on the Owyhee irrigation project, Oregon: U.S. Geological Survey Water-Supply Paper 597-A, 72 p.

Busacca, A.J., Nelstead, K.T., McDonald, E.V., and Purser, M.D., 1992, Correlation of distal tephra layers in loess in the Channeled Scabland and Palouse of Washington State: Quaternary Research, v. 37, p. 281-303.

Capra, L., 2007, Volcanic natural dams: identification, stability, and secondary effects: Natural Hazards, v. 43, p. 45-61.

Carter, D.T., Ely, L.L., O’Connor, J.E., and Fenton, C.R., 2006, Late Pleistocene outburst flooding from pluvial Lake Alvord into the Owyhee River, Oregon: Geomorphology, v. 75, p.346-367.

Central Snake Projects, 1994, Owyhee Reservoir Resource Management Plan, April 1994: U.S. Bureau of Reclamation, 261 p.

Clynne, M.A., Calvert, A.T., Wolfe, E.W., Evarts, R.C., Fleck, R.J., and Lanphere, M.A., 2008, The Pleistocene eruptive history of Mount St. Helens, Washington, from 300,000 to 12,800 years before present: U.S. Geological Survey Professional Paper 1750, p. 593-627.

Cohen, A.S., Palacios-Fest, M.R., Negrini, R.M., Wigand, P.E., and Erbes, D.B., 2000, A paleoclimate record for the past 250,000 years from Summer Lake, Oregon, USA: II. Sedimentology, paleontology and geochemistry: Journal of Paleolimnology, v. 24, p. 151-182.

Craft, D., Cannon, N., Zimmer, D., Krill, K., and DiMattia, L., 2000, Water quality and mercury in Lake Owyhee, southeastern Oregon: U.S. Department of the Interior Bureau of Reclamation, p. 279.

Crandell, D. R., Mullineaux, D.R., Meyer, R., Spiker, E., and Kelley, M.L., 1981, Radiocarbon dates from volcanic deposits at Mount St. Helens, Washington: U.S. Geological Survey Open File Report 81-844, 10 p.

Crow, R., Karlstrom, K.E., McIntosh, W., Peters, L., and Dunbar, N., 2008, History of Quaternary volcanism and lava dams in western Grand Canyon based on lidar analysis, ^{40}Ar/^{39}AR dating, and field studies: Implications for flow stratigraphy, timing of volcanic events, and lava dams: Geosphere, v. 4, p. 183-206.

Cummings, M.L., Evans, J.G., Ferns, M.L., and Lees, K.R., 2000, Stratigraphic and structural evolution of the middle Miocene synvolcanic Oregon-Idaho graben: Geological Society of America Bulletin, v. 112, p. 668-682.

Curry, B.B., 1999, An environmental tolerance index for ostracodes as indicators of physical and chemical factors in aquatic habitats: Palaeogeography, Palaeoclimatology, Palaeoecology, v. 148, p, 51-63.

Davis, J.O., 1985, Correlation of late Quaternary tephra layers in a long pluvial sequence near Summer Lake, Oregon: Quaternary Research, v. 23, p. 38-53.

Downing, K.F., and Park, L.E., 1998, Geochemistry and early diagenesis of mammal-bearing concretions from the Sucker Creek Formation (Miocene) of Southeastern Oregon: Palaios, v. 13, p. 14-27.

Duffield, W., Riggs, N., Kaufman, D., Champion, D., Fenton, C., Forman, S., McIntosh, W., Hereford, R., Plescia, J., and Ort, M., 2006, Multiple constraints on the age of a Pleistocene lava dam across the Little Colorado River at Grand Falls, Arizona: Geological Society of America Bulletin, v. 118, p. 421-429.

Dugas, D.P., 1998, Late Quaternary variations in the level of Paleo-Lake Malheur, Eastern Oregon: Quaternary Research, v. 50, p. 276-282.

ESRI, 2006, ArcMap 9.2, Redlands, CA.

Fenton, C.R., Poreda, R.J., Nash, B.P., Webb, R.H., and Cerline, T.E., 2004, Geochemical discrimination of five Pleistocene lava-dam outburst flood deposits, Western Grand Canyon, Arizona: Journal of Geology, v. 112, p. 91-120.

Fenton, C.R., Webb, R.H., and Cerling, T.E., 2006, Peak discharge of a Pleistocene lava-dam outburst flood in Grand Canyon, Arizona, USA: Quaternary Research, v. 65, p. 324-335.

Fenton, C.R., Webb, R.H., Pearthree, P.A., Cerling, T.E., Poreda, R.J., and Nash, B.P., 2000, Cosmogenic 3He dating of western Grand Canyon basalts: Implications for Quaternary Incision of the Colorado River, *in* Young, R.A., and Spamer, E.E., eds., Colorado River: Origin and evolution: Grand Canyon, Arizona, Grand Canyon Association, p. 147-152.

Ferns, M.L., Evans, J.G., and Cummings, M.L., 1993, Geologic map of Mahogany Mountain 30 x 60 Minute Quadrangle, Malheur County, Oregon, and Owyhee County, Idaho: Oregon Department of Mineral Industries Geological Map Series GMS-78, scale 1:100,000, 1 sheet, 12 p. text.

Foit, F.F., 2009, personal communication, September.

Foley, M.G., 1980, Bed-rock incision by streams: Geological Society of America Bulletin, v. 91, p. 577-578.

Forman, S.L., Pierson, J., and Lepper, K., 2000, Luminescence geochronology, *in* Noller, J.S., Sowers, J.M., and Lettis, W.R., eds., Quaternary geochronology methods and applications: Washington, D.C., American Geophysical Union, p. 157-176.

Foster, I.D.L., Dearing, J.A., Grew, R., and Orend, K., 1990, The sedimentary data base: an appraisal of lake and reservoir sediment based studies of sediment yield, *in* Walling, D.E., Yair, A., and Berkowicz, S., eds., Erosion, transport, and deposition processes: IAHS Publication no. 189, p. 19-43.

Freeth, S.J., and Rex, D.C., 2000, Constraints on the age of Lake Nyos, Cameroon: Journal of Volcanology and Geothermal Research, v. 97, p. 261-269.

Global Mapper LLC, 2007, Global Mapper 8.03, Parker, CO.

Godchaux, M.M, Bonnichsen, B., and Jenks, M.D., 1992, Types of phreatomagmatic volcanoes in the western Snake River Plain, Idaho, USA, *in* Geist, D.J., and White, C.M., eds., Special issue in honour of Alexander R. McBirney: Journal of Volcanology and Geothermal Research, v. 52, p. 1-25.

Granger, D.E., and Muzikar, P.F., 2001, Dating sediment burial with in situ-produced cosmogenic nuclides: theory, techniques, and limitations: Earth and Planetary Science Letters, v. 188, p. 269-281.

Hamblin, W.K., 1994, Late Cenozoic lava dams in the western Grand Canyon: Geological Society of America Memoir 183, p. 139.

Hancock, G.S., and Anderson, R.S., 2002, Numerical modeling of fluvial strath-terrace formation in response to oscillating climate: Geological Society of America Bulletin, v. 114, p. 1131-1142.

Hardy, M.A., Maret, T.R., and George, D.L., 2003, Reconnaissance of chemical and biological quality in the Owyhee River from the Oregon state line to the Owyhee Reservoir, Oregon, 2001-02: U.S. Geological Survey Water Resources Investigations Report 03-4327, p. 49.

Hart, W.K., and Mertzman, S.A., 1983, Late Cenozoic volcanic stratigraphy of the Jordan Valley area, southeastern Oregon: Oregon Geology, v. 45, p. 15-19.

Hostetler, S., and Benson, L.V., 1990, Paleoclimatic implications of the high stand of Lake Lahontan derived from models of evaporation and lake level: Climate Dynamics, v. 4, p. 207-217.

Hostetler, S.W., Giorgi, F., Bates, G.T., and Bartlein, P.J., 1994, Lake-atmosphere feedbacks associated with paleolakes Bonneville and Lahontan: Science, v. 263, p. 665-668.

House, P.K., 2009, personal communication, December.

Howard, K.A., Shervais, J.W., and McKee, E.H., 1982, Canyon-filling lavas and lava dams on the Boise River, Idaho, and their significance for evaluating downcutting during the last two million years, *in* Bonnichsen, B. and Breckenridge, R.M., eds., Cenozoic geology of Idaho: Idaho Bureau of Mines and Geology Bulletin, no. 26, p. 629-641.

Huscroft, C.A., Ward. B.C., Barendregt, R.W., Jackson, L.E., Jr., and Opdyke, N.D., 2004, Pleistocene volcanic damming of Yukon River and the maximum age of the Reid Glaciation, west-central Yukon: Canadian Journal of Earth Science, v. 41, p. 151-164.

Kaufman, D.S., O'Brien, G. Mead, J.I., Bright, J., and Umhoefer, P., 2002, Late Quaternary spring-fed deposits of the Grand Canyon and their implications for deep lava-dammed lakes: Quaternary Research, v. 58, p. 329-340.

Kittleman, L.R., 1965, Cenozoic stratigraphy of the Owyhee region, southeastern Oregon: Bulletin of the Museum of Natural History, University of Oregon, no. 1, 45 p.

Komatsu, G., Arzhannikov, S.G., Gillespie, A.R., Burke, R.M., Miyamoto, H., and Baker, V.R., 2008, Quaternary paleolake formation and cataclysmic flooding along the upper Yenisei River: Geomorphology, v. 104, p. 143-164.

Krebs, W.N., Bradbury, J.P., and Theriot, E., 1987, Neogene and Quaternary lacustrine diatom biochronology, Western USA: Palaios, v. 2, pp. 505-513.

Kuehn, S.C., and Foit, F.F., Jr., 2001, Updated tephra stratigraphy at Summer Lake, Oregon, a sub-basin of pluvial Lake Chewaucan, *in* Negrini, R., Pezzopane, S., and Badger, T., eds., Quaternary Studies near Summer Lake, Oregon: Guidebook for the Friends of the Pleistocene Ninth Annual Pacific Northwest Cell Field Trip, pp. SK1-SK9.

Licciardi, J.M., 2001, Chronology of latest Pleistocene lake-level fluctuations in the pluvial Lake Chewaucan basin, Oregon, USA: Journal of Quaternary Science, v. 16, p. 545-553.

Malde, H.E., 1982, The Yahoo Clay, a lacustrine unit impounded by the McKinney Basalt in the Snake River Canyon near Bliss, Idaho, *in* Bonnichsen, B. and Breckenridge, R.M., eds., Cenozoic geology of Idaho: Idaho Bureau of Mines and Geology Bulletin, no. 26, p. 617-628.

Malde, H.E., 1987, The Montini Volcano; A lava dam on the ancestral Snake River, southwest Idaho, *in* Beus, S.S., eds., Rocky Mountain Section of the Geological Society of America Centennial Field Guide, vol. 2, p. 127-130.

Mock, C.J., and Bartlein, P.J., 1994, Spatial variability of Late-Quaternary paleoclimates in the Western United States: Quaternary Research, vol. 44, p. 425-433.

Mullineaux, D.R., 1986, Summary of pre-1980 tephra-fall deposits erupted from Mount St. Helens, Washington State, USA: Bulletin of Volcanology, v. 48, p. 17-26.

Negrini, R.M., Erbes, D.B., Faber, K., Herrera, A.M., Roberts, A.P., Cohen, A.S., Wigand, P.E., and Foit, F.F., Jr., 2000, A paleoclimate record for the past 250,000 years from Summer Lake, Oregon, USA: I. Chronology and magnetic proxies for lake level: Journal of Paleolimnology, v. 24, p. 125-149.

Nott, J., Young, R., and McDougall, I., 1996, Wearing down, wearing back, and gorge extension in the long-term denudation of a highland mass: Quantitative evidence from the Shoalhaven catchment, southeast Australia: The Journal of Geology, v. 104, p. 224-232.

Othus, S.M., 2008, Comparison of landslides and their related outburst flood deposits, Owyhee River, southeastern Oregon [M.S. thesis]: Central Washington University, 136 p.

Ouimet, W.B., Whipple, K.X., Crosby, B.T., Johnson, J.P., and Schildgen, T.F., 2008, Epigenetic gorges in fluvial landscapes: Earth Surface Processes and Landforms, v. 33, p. 1993-2009.

Palacios-Fest, M.R., Cohen, A.S., Ruiz, J., and Blank, B., 1993, Comparative paleoclimate interpretations from nonmarine ostracodes using faunal assemblages, trace elements, shell chemistry, and stable isotope data: Climate Change in Continental Isotopic Records, AGU Geophysical Monograph 78, p. 179-190.

Peterson, N.V., and Groh, E.A., 1970, Geologic tours of Cove Palisades State Park near Madras, Oregon: The Ore Bin, v. 32, p.141-168.

Pietsch, T.J., Olley, J.M., and Nanson, G.C., 2008, Fluvial transport as a natural luminescence sensitizer of quartz: Quaternary Geochronology, v. 3, p. 365-376.

Pratt-Sitaula, B., Garde, M., Burbank, D.W., Oskin, M., Heimsath, A., and Gabet, E., 2007, Bedload-to-suspended load ratio and rapid bedrock incision from Himalayan landslide-dam lake record: Quaternary Research, v. 68, p. 111-120.

Reneau, S.L., and Dethier, D.P., 1996, Late Pleistocene landslide-dammed lakes along the Rio Grande, White Rock Canyon, New Mexico: Geological Society of America, v. 108, p. 1492-1507.

Reynolds, R.L., Rosenbaum, J.G., Rapp, J., Kerwin, M.W., Bradbury, J.P., Colman, S., and Adam, D., 2004, Record of late Pleistocene glaciation and deglaciation in the southern Cascade Range. I. Petrological evidence from lacustrine sediment in Upper Klamath Lake, southern Oregon: Journal of Paleolimnology, v. 31, p. 217-233.

Richardson, C.A., McDonald, E.V., and Busacca, A.J., 1997, Luminescence dating of loess from the northwest United States: Quaternary Science Reviews, v. 16, p. 403-415.

Righter, K., and Carmichael, I.S.E., 1992, Hawaiites and related lavas in the Atenguillo graben, western Mexican Volcanic Belt: Geological Society of America Bulletin, v. 104, p. 1592-1607.

Rittenour, T.M., Goble, R.J., and Blum, M.D., 2005, Development of an OSL chronology for Late Pleistocene channel belts in the lower Mississippi valley, USA: Quaternary Science Reviews, v. 24, p. 2539-2554.

Schnurrenberger, D., Russell, J., and Kelts, K., 2003, Classification of lacustrine sediments based on sedimentary components: Journal of Paleolimnology, v. 29, p. 141-154.

Shao-Ping, C., Chuan-You, L., and Qui-Zhi, Y., and Shi-Wei, Z., 2006, Differentiating Pleistocene tectonically driven and climate-related fluvial incision: the Sanggan River, Datong Basin, North China: Geological Magazine, v. 143, p. 393-410.

Sklar, L.S., and Dietrich, W.E., 2001, Sediment and rock strength controls on river incision into bedrock: Geology, v. 29, p. 1087-1090.

Smith, W.O., Vetter, C.P., and Cummings, G.B., and others, 1960, Comprehensive survey of sedimentation in Lake Mead 1948-49: U.S. Geological Survey Professional Paper 295, 254 p.

Spencer, P.K., and Knapp, A.N., 2010, New stratigraphic markers in the late Pleistocene Palouse loess: novel fossil gastropods, absolute age constraints and non-aeolian facies: Sedimentology, v. 57, p. 41-52.

Sperazza, M., Moore, J.N., and Hendrix, M.S., 2004, High-resolution particle size analysis of naturally occurring very fine-grained sediment through laser diffractometry: Journal of Sedimentary Research, v. 74, p. 736-743.

Starratt, S., 2010, personal communication, April.

Tauxe, L., Luskin, C., Selkin, P., Gans, P., and Calvert, A., 2004, Paleomagnetic results from the Snake River Plain: Contribution to the time-averaged field global database: Geochemistry, Geophysics, Geosystems, v. 5, doi 10.1029/2003GC000661.

Trimble, D.E., and Carr, W.J., 1961, Late Quaternary history of the Snake River in the American Falls Region, Idaho: Geological Society of America Bulletin, v. 72, p. 1739-1748.

U. S. Geological Survey, 2008, Water-data report 2008 13181000 Owyhee River near Rome, OR, http://wdr.water.usgs.gov/wy2008/pdfs/13181000.2008.pdf (Retrieved November 22, 2009).

Vacco, D.A., Clark, P.U., Mix, A.C., Cheng, H., and Edwards, R.L., 2005, A speleothem record of Younger Dryas cooling, Klamath Mountains, Oregon, USA: Quaternary Research, v. 64, p. 249-256.

Visceras, C., Fernandez, J., Garcia-Garcia, F., Soria, J.M., Calvache, M.L., and Jauregui, P., 2009, Dynamics of sedimentary environments in the accelerated siltation of a reservoir: the case of Alhama de Granada, southern Spain: Environmental Geology, v. 56, 1353-1369.

Vogel, M.S., 2005, Quaternary geology of the lower Lewis River Valley, Washington: influence of volcanogenic sedimentation following Mt. St. Helens eruptions [M.S. thesis]: Pullman, Washington State University, 146 p.

Walker, M., 2005, Quaternary dating methods: West Sussex, England, John Wiley and Sons Ltd., p. 93-120.

Waters, A.C., 1973, The Columbia River Gorge: Basalt stratigraphy, ancient lava dams, and landslide dams: State of Oregon Department of Geology and Mineral Industries, v. 77, p, 133-162.

Whitock, C., Sarna-Wojcicki, A.M., Bartlein, P.J., and Nickmann,. R.J., 2000, Environmental history and tephrostratigraphy at Carp Lake, southwestern Columbia Basin, Washington, USA: Palaeogeography, Palaeoclimatology, Palaeoecology, v. 155, p. 7-29.

Wolf, K.H., and Ellison, B., 1971, Sedimentary geology of the zeolitic volcanic lacustrine Pliocene Rome Beds, Oregon, 1: Sedimentary Geology, v. 6, p. 271-302.

Zielinski, G.A., and McCoy, W.D., 1987, Paleoclimatic implications of the relationship between modern snowpack and late Pleistocene equilibrium-line altitudes in the mountains of the Great Basin, Western U.S.A.: Arctic and Alpine Research, v. 19, p. 127-134.

APPENDIXES

Appendix A

Field Descriptions of Quaternary Lacustrine Sediment Samples

Sample	Description
Caitlin's Hill Section (listed bottom to top)	
CAO-OW-0609-CH-1	Dark gray and tan, horizontally to sub-horizontally, very thinly laminated, medium to fine-grained sand, with light tan silt. Diatoms present. Height above base of section is .20–.24 m.
CAO-OW-0609-CH-2	Light tan, massive, clayey silt. Diatoms present. Height above base of section is .29–.32 m.
CAO-OW-0609-CH-3	Grayish green, subhorizontal wavy/irregular very thin bed of clayey silt. Diatoms present, sent for identification. Height above base of section is .36–.37 m.
CAO-OW-0609-CH-4	Dark gray and tan, ripple laminated, medium to fine-grained, silty sand. Diatoms present. Height above base of section is .55–.58 m.
CAO-OW-0609-CH-5	Light tan, massive and blocky, clayey silt. Diatoms present. Height above base of section is .68–.72 m.
CAO-OW-0609-CH-6	Dark gray and tan, ripple laminated, medium to fine-grained, silty sand, with climbing ripple structures. Diatoms present. Height above base of section is .91–.94 m.

Sample	Description
Caitlin’s Hill Section Cont’d (listed bottom to top)	
CAO-OW-0609-CH-7	Light tan, massive to faintly laminated, clayey silt. Diatoms present. Height above base of section is 1.12–1.15 m.
CAO-OW-0609-CH-8	Dark gray and tan to white, ripple laminated, medium to fine grained, silty sand, with < 3 cm balls of white clastic material. Diatoms present. Height above base of section is 1.40–1.45 m.
CAO-OW-0609-CH-9	< 3 cm balls of white clastic material with dark gray to black spots. Diatoms not present. Height above base of section is 1.42–1.45 m.
CAO-OW-0609-CH-10	Gray to tan, very thinly laminated, sandy silt, with areas of orange oxidation. Diatoms present. Height above base of section is 1.66–1.71 m.
CAO-OW-0609-CH-11	Tan to white, very thinly laminated, sandy silt. Diatoms present. Height above base of section is 1.74–1.78 m.
CAO-OW-0609-CH-12	Light tan, massive and blocky, clayey silt. Diatoms present. Height above base of section is 1.96–2.00 m.
CAO-OW-0609-CH-13	Dark gray and tan, horizontally to sub-horizontally, very thinly laminated, medium to fine-grained sand, with light tan silt. Diatoms present. Height above base of section 2.09–2.13 m.

Sample	Description
Caitlin’s Hill Section Cont’d (listed bottom to top)	
CAO-OW-0609-CH-14	Dark gray and tan to white, very thinly laminated, medium to fine grained, silty sand, with < 1 cm balls of white clastic material. Diatoms present, sent for identification. Height above base of section 2.50–2.54 m.
CAO-OW-0609-CH-15	Tan to white, very thinly laminated, sandy silt. Diatoms present. Height above base of section is 2.69–2.74 m.
CAO-OW-0609-CH-16	Tan to white, very thinly laminated to massive, sandy silt. Diatoms present. Height above base of section is 2.92-2.96 m.
CAO-OW-0609-CH-17	Dark gray, very finely laminated, clayey silt, underlying and overlying a light tan, very finely laminated, clayey silt. Diatoms present. Height above base of section is 3.12–3.16 m.
CAO-OW-0609-CH-18	Tan to white, very thinly laminated, sandy silt. Diatoms present. Height above base of section is 3.28–3.32 m.
CAO-OW-0609-CH-19	Dark gray and tan to white, ripple laminated, medium to fine grained, silty sand. Diatoms not present. Height above base of section is 3.65–3.70 m.

Sample	Description
Caitlin’s Hill Section Cont’d (listed bottom to top)	
CAO-OW-0609-CH-20	Tan to white, very thinly laminated, sandy silt with approximately < 3 mm gypsum crystals and possible bioturbation marks. Diatoms not present. Height above base of section is 4.10-4.14 m.
CAO-OW-0609-CH-21	Tan to white, very thinly laminated, sandy silt with approximately < 3 mm gypsum crystals and possible bioturbation marks. Diatoms not present. Height above base of section is 4.46–4.50 m.
CAO-OW-0609-CH-22	Light tan, massive and blocky, clayey silt, with < 3 mm gypsum crystals and very thin red mineral concretion laminations. Diatoms not present. Height above base of section is 4.90–4.94 m.
CAO-OW-0609-CH-23	Light tan, massive, silty clay, with possible burrow or root cavities filled with white tephra infilling the space. Diatoms not present. Height above base of section is 5.43–5.47 m.
CAO-OW-0609-CH-24	White tephra ash layer with burrow or root cavities filled with tan silty clay. Diatoms not present. Height above base of section is 5.64–5.69 m.

Sample	Description
Caitlin’s Hill Section Cont’d (listed bottom to top)	
CAO-OW-0609-CH-25	Light tan, massive, silty clay, with small component of intermixed tephra. Height above base of section is 5.81–5.84 m.
CAO-OW-0609-CH-33	Dark red to orange, very fine lamination of possible oxidized organics. Diatoms present. Height above base of section is 5.85–5.86 m.
CAO-OW-0609-CH-26	Dark tan to gray, very finely laminated to massive, silty clay with alternating dark and light layers. Diatoms present. Height above base of section is 5.86–5.89 m.
CAO-OW-0609-CH-27	Dark tan to gray, massive, silty clay. Diatoms not present. Height above base of section is 6.02–6.05 m.
CAO-OW-0609-CH-28	Tan to orange, massive, silty sand layer with possible oxidation causing coloring. Diatoms not present. Height above base of section is 6.06–6.11 m.
CAO-OW-0609-CH-29	Alternating dark green and tan (alternating light and dark), very fine laminations of silty clay. Diatoms not present. Height above base of section is 6.12–6.16 m.
CAO-OW-0609-CH-30	Alternating dark green and tan (alternating light and dark), very fine laminations of silty clay. Diatoms present. Height above base of section is 6.22–6.25 m.

Sample	Description
Caitlin’s Hill Section Cont’d (listed bottom to top)	
CAO-OW-0609-CH-31	Light tan, massive, clayey silt, with occasional red dots (< 3 mm) of mineralization, possibly manganese oxide. Diatoms not present. Height above base of section is 6.69–6.73 m.
CAO-OW-0609-CH-32	Light tan, massive, clayey silt, with occasional red dots (< 3 mm) of mineralization, possibly manganese oxide. Diatoms present. Height above base of section is 7.14–7.17 m.
CAO-OW-0609-CH-34	Brownish tan, massive and blocky, clayey silt with lenses of light colored clay material. This layer possible pinches out under sample CAO-OW-0609-CH-29. Diatoms present. Height above base of section is 6.16–6.20 m.
CAO-OW-0609-CH-35	Correlates to CAO-OW-0609-CH-29 and 30. Diatoms present. Height above base of section is 6.49–6.53 m.
CAO-OW-0609-CH-36	Correlates to CAO-OW-0609-CH-31 and 32. Diatoms present. Height above base of section is 6.71–6.75 m.
CAO-OW-0609-CH-37	Gray to tan, massive and blocky, clayey silt. Diatoms present. Height above base of section is 6.95–6.98 m.
CAO-OW-0609-CH-38	Gray to tan, massive and blocky, clayey silt. Diatoms present. Height above base of section is 7.65–7.69 m.

Sample	Description
Caitlin’s Hill Section Cont’d (listed bottom to top)	
CAO-OW-0609-CH-39	Gray to tan, massive and blocky, clayey silt. Diatoms present. Height above base of section is 7.88–7.92 m.
CAO-OW-0609-CH-40	Gray to tan, massive and blocky, clayey silt. Diatoms present. Height above base of section is 8.28–8.31 m.
CAO-OW-0609-CH-41	Gray to tan, massive and blocky, clayey silt. Diatoms present, sent for identification. Height above base of section is 8.68–8.71 m.
CAO-OW-0609-CH-42	Gray to tan, massive and blocky, clayey silt. Diatoms present. Height above base of section is 9.30–9.34 m.
CAO-OW-0609-CH-43	Gray to tan, massive and blocky, clayey silt. Diatoms present. Height above base of section is 9.66–9.70 m.
CAO-OW-0609-CH-44	Gray to tan, massive and blocky, clayey silt, below 1 cm thick orange oxidation layer. Diatoms present. Height above base of section is 10.10–10.14 m.
CAO-OW-0609-CH-45	Gray to tan, massive and blocky, clayey silt. Diatoms present. Height above base of section is 10.65–10.69 m.
CAO-OW-0609-CH-46	Gray to tan, massive and blocky, clayey silt. Diatoms present. Height above base of section is 10.92–10.96 m.
CAO-OW-0609-CH-47	Gray to tan, massive and blocky, clayey silt. Diatoms present. Height above base of section is 11.41–11.44 m.

Sample	Description
Caitlin’s Hill Section Cont’d (listed bottom to top)	
CAO-OW-0609-CH-48	Gray to tan, massive and blocky, clayey silt. Diatoms present. Height above base of section is 11.67–11.71 m.
CAO-OW-0609-CH-49	Gray to tan, massive and blocky, clayey silt. Diatoms present. Height above base of section is 12.07–12.11 m.
CAO-OW-0609-CH-50	Gray to tan, massive and blocky, clayey silt with some manganese oxide spots and very thin laminations of orange oxidation layers. Diatoms present. Height above base of section is 12.66–12.70 m.
CAO-OW-0609-CH-51	Gray to tan, massive and blocky, clayey silt. Diatoms present. Height above base of section is 13.14–13.18 m.
CAO-OW-0609-CH-52	Gray to tan, massive, clayey silt, with flakey/platey texture. Diatoms present. Height above base of section is 13.30–13.34 m.
CAO-OW-0609-CH-53	White tephra layer with basal tan/orange layer overlying rooted, loose clayey silt layer. Diatoms present, sent for identification. Height above base of section is 13.42–13.45 m.
CAO-OW-0609-CH-54	Gray to tan, massive and blocky, clayey silt. Diatoms present. Height above base of section is 13.55–13.59 m.

Sample	Description
Caitlin's Hill Section Cont'd (listed bottom to top)	
CAO-OW-0609-CH-55	Gray to tan, massive and blocky, clayey silt. Diatoms present. Height above base of section is 13.89–13.93 m.
CAO-OW-0609-CH-56	Orange and brown stained, ~ 5 cm thick layer of clayey silt. Diatoms present. Height above base of section is 14.42–14.45 m.
CAO-OW-0609-CH-57	Gray to tan, massive and blocky, clayey silt. Diatoms present. Height above base of section is 14.81–14.85 m.
CAO-OW-0609-CH-58	Gray to tan, massive and blocky, clayey silt, including very thin layer of orange oxidized material. Diatoms present. Height above base of section is 15.22–15.26 m.
CAO-OW-0609-CH-59	Gray to tan, massive and blocky, clayey silt. Diatoms present. Height above base of section is 15.74–15.78 m.
CAO-OW-0609-CH-60	Orange and brown stained, ~ 5 cm thick layer of clayey silt. Diatoms present. Height above base of section is 16.19–16.22 m.
CAO-OW-0609-CH-61	Gray to tan, massive and blocky, clayey silt. Diatoms present. Height above base of section is 16.46–16.50 m.
CAO-OW-0609-CH-62	Gray to tan, massive and blocky, clayey silt. Diatoms present. Height above base of section is 16.97–17.01 m.

Sample	Description
Caitlin's Hill Section Cont'd (listed bottom to top)	
CAO-OW-0609-CH-63	Gray to tan, massive and blocky, clayey silt. Diatoms present. Height above base of section is 17.25–17.28 m.
CAO-OW-0609-CH-64	Orange to brown, massive, clayey silt, coloring partially only on surface, but also effecting the actual sediment. Diatoms present. Height above base of section is 17.53–17.56 m.
CAO-OW-0609-CH-65	Gray to tan, massive and blocky, clayey silt. Diatoms present. Height above base of section is 17.88–17.93 m.
CAO-OW-0609-CH-66	Gray to green, flakey and massive, very thin lamination of silty clay. Diatoms present. Height above base of section is 18.19–18.20 m.
CAO-OW-0609-CH-67	Gray to tan, massive and blocky, clayey silt. Diatoms present. Height above base of section is 18.43–18.47 m.
CAO-OW-0609-CH-68	Gray to tan, massive and blocky, clayey silt. Diatoms present. Height above base of section is 18.96–18.99 m.
CAO-OW-0609-CH-69	Gray to tan, massive and blocky, clayey silt, including very thin layer of orange oxidized material. Diatoms present. Height above base of section is 19.46–19.50 m.
CAO-OW-0609-CH-70	Gray to tan, massive and blocky, clayey silt. Diatoms present. Height above base of section is 19.94–19.99 m.

Sample	Description
Caitlin’s Hill Section Cont’d (listed bottom to top)	
CAO-OW-0609-CH-71	Gray to tan, massive and blocky, clayey silt, including very thin layer of orange oxidized material. Diatoms present. Height above base of section is 20.47–20.51 m.
CAO-OW-0609-CH-72	Gray to tan, massive and blocky, clayey silt. Diatoms present. Height above base of section is 20.66–20.70 m.
CAO-OW-0609-CH-73	Gray to tan, massive and blocky, clayey silt. Diatoms present, sent for identification. Height above base of section is 20.96–21.00 m.
CAO-OW-0609-CH-74	Gray to tan, massive and blocky, clayey silt, including very thin layer of orange oxidized material. Diatoms present. Height above base of section is 21.23–21.27 m.
CAO-OW-0609-CH-75	Gray to tan, massive and blocky, clayey silt. Diatoms present. Height above base of section is 21.51–21.56 m.
Main West Crater Section (listed bottom to top)	
CAO-OW-0709-MWC-1	Dark gray to black, very thin lamination of consolidated mineral, possibly organic material. Height above base of section is .02–.03 m.
CAO-OW-0709-MWC-2	White, very thin lamination of soft tephra ash layer, with sharp contacts. Height above base of section is .03–.06 m.

Sample	Description
Main West Crater Section Cont'd (listed bottom to top)	
CAO-OW-0709-MWC-3	Tan to whitish gray, massive and blocky, clayey silt, with brown specks. Height above base of section is .24–.28 m.
CAO-OW-0709-MWC-4	Dark green, very thin lamination of silty clay. Height above base of section is .40–.42 m.
CAO-OW-0709-MWC-5	Tan to whitish gray, massive and blocky, clayey silt. Height above base of section is .60–.64 m.
CAO-OW-0709-MWC-6	Tan to whitish gray, massive and blocky, clayey silt. Height above base of section is .98–1.02 m.
CAO-OW-0709-MWC-7	Tan to whitish gray, massive and blocky, clayey silt. Height above base of section is 1.40–1.44 m.
CAO-OW-0709-MWC-8	Dark green, very thin lamination of silty clay. Height above base of section is 1.80–1.81 m.
CAO-OW-0709-MWC-9	Tan-gray, massive and blocky, clayey silt, overlying a very thin lamination of orange, oxidized sediment. Height above base of section is 2.05–2.07 m.
CAO-OW-0709-MWC-10	Tan to whitish gray, massive and blocky, clayey silt. Height above base of section is 2.34–2.38 m.
CAO-OW-0709-MWC-11	Orange, massive and blocky, clayey silt, with brown specks above and below. Height above base of section is 2.71–2.75 m.

Sample	Description
Main West Crater Section Cont’d (listed bottom to top)	
CAO-OW-0709-MWC-12	Tan to whitish gray, massive and blocky, clayey silt. Height above base of section is 2.92–2.96 m.
CAO-OW-0709-MWC-13	Dark gray, flakey, clayey silt, with dark brown and green, very thin laminations above and below. Height above base of section is 3.26–3.30 m.
CAO-OW-0709-MWC-14	Tan to whitish gray, massive and blocky, clayey silt. Height above base of section is 3.61–3.65 m.
CAO-OW-0709-MWC-15	White to tan, very thin lamination of clayey silt with brown specks throughout. Height above base of section is 3.92–3.93 m.
CAO-OW-0709-MWC-16	Grayish tan, very finely laminated, sandy silt. Height above base of section is 3.95–3.98 m.
CAO-OW-0709-MWC-17	White, very thin lamination of clayey silt, with overlying orange oxidation layer. Height above base of section is 4.04–4.05 m.
CAO-OW-0709-MWC-18	White, very thin lamination of clayey silt, with overlying orange oxidation layer. Height above base of section is 4.19–4.20 m.
CAO-OW-0709-MWC-19	Tan to whitish gray, massive and blocky, clayey silt. Height above base of section is 4.23–4.26 m.

Sample	Description
Main West Crater Section Cont'd (listed bottom to top)	
CAO-OW-0709-MWC-20	White, very thin lamination of clayey silt, with overlying orange oxidation layer. Height above base of section is 4.38–4.40 m.
CAO-OW-0709-MWC-21	Tan to gray, very finely, irregularly laminated, fine-grained, silty sand. Height above base of section is 4.40–4.42 m.
CAO-OW-0709-MWC-22	White, very fine lamination of clayey silt. Height above base of section is 4.43–4.45 m.
CAO-OW-0709-MWC-23	Tan to whitish gray, massive and blocky, clayey silt. Height above base of section is 4.74–4.78 m.
CAO-OW-0709-MWC-24	White, very fine lamination of silty clay, with irregular contacts with very thin brown layers above and below. Height above base of section is 4.99–5.00 m.
CAO-OW-0709-MWC-25	Gray to tan, fine-grained silty sand grading into massive clayey silt, underlain by thin brown layer. Height above base of section is 5.05–5.06 m.
CAO-OW-0709-MWC-26	Gray to tan, very finely laminated, fine-grained sand and silt that is normally graded. Height above base of section is 5.14–5.17 m.

Sample	Description
Main West Crater Section Cont'd (listed bottom to top)	
CAO-OW-0709-MWC-27	White, thinly laminated, indurated, very thin lamination of silty clay. Height above base of section is 5.45–5.46 m.
CAO-OW-0709-MWC-28	Tan to whitish gray, massive and blocky, clayey silt. Height above base of section is 5.76–5.81 m.
CAO-OW-0709-MWC-29	White, soft, clayey sandy silt, with brown specks. Height above base of section is 6.03–6.05 m.
CAO-OW-0709-MWC-30	Gray to whitish tan, horizontal and wavy, very finely laminated, fine-grained sand and silt. Height above base of section is 6.06–6.08 m.
CAO-OW-0709-MWC-31	Gray to whitish tan, irregular and wavy, very finely laminated, fine-grained sand and silt. Height above base of section is 6.12–6.15 m.
CAO-OW-0709-MWC-32	Gray to whitish tan, irregular and wavy, very finely laminated, fine-grained sand and silt. Height above base of section is 6.19–6.22 m.
CAO-OW-0709-MWC-33	Gray to whitish tan, massive, clayey silt. Height above base of section is 6.22–6.25 m.
CAO-OW-0709-MWC-34	Gray to whitish tan, irregular and wavy, very finely laminated, fine-grained sand and silt. Height above base of section is 6.25–6.28 m.

Sample	Description
Main West Crater Section Cont'd (listed bottom to top)	
CAO-OW-0709-MWC-35	Gray to whitish tan, massive, clayey silt. Height above base of section is 6.50–6.54 m.
CAO-OW-0709-MWC-36	White, very fine lamination of silty clay. Height above base of section is 6.57–6.58 m.
CAO-OW-0709-MWC-37	Gray to whitish tan, normally graded, irregular and wavy, very finely laminated, fine-grained sand and silt. Height above base of section is 6.60–6.63 m.
CAO-OW-0709-MWC-38	White, very fine lamination of silty clay. Height above base of section is 6.63–6.65 m.
CAO-OW-0709-MWC-39	Gray to whitish tan, normally graded, irregular and wavy, very finely laminated, fine-grained sand and silt, with blebs of cleaner fine-grained sand. Height above base of section is 6.96–6.98 m.
CAO-OW-0709-MWC-40	Tan to whitish gray, massive and blocky, clayey silt. Height above base of section is 7.40–7.43 m.
CAO-OW-0709-MWC-41	Tan to whitish gray, massive and blocky, clayey silt. Height above base of section is 7.75–7.78 m.
CAO-OW-0709-MWC-42	Tan to whitish gray, laminated to massive, sandy silt. Height above base of section is 8.00–8.04 m.

Sample	Description
Main West Crater Section Cont'd (listed bottom to top)	
CAO-OW-0709-MWC-43	Tan to whitish gray, massive and blocky, clayey silt. Height above base of section is 8.32–8.36 m.
CAO-OW-0709-MWC-44	Tan to whitish gray, very thinly laminated fine-grained silt, with dark gray to white, fine-grained sand. Height above base of section is 8.43–8.46 m.
CAO-OW-0709-MWC-45	Tan to whitish gray, massive and blocky, clayey silt. Height above base of section is 8.71–8.75 m.
CAO-OW-0709-MWC-46	Tan to whitish gray, very thinly laminated fine-grained silt, with dark gray to white, fine-grained sand. Height above base of section is 8.86–8.89 m.
CAO-OW-0709-MWC-47	Tan to whitish gray, massive and blocky, sandy silt. Height above base of section is 9.24–9.28 m.
CAO-OW-0709-MWC-48	Gray to whitish tan, normally graded, irregular and hummocky, very finely laminated, fine-grained sand and silt. Height above base of section is 9.62–9.65 m.
CAO-OW-0709-MWC-49	Tan to whitish gray, massive and blocky, clayey silt. Height above base of section is 9.81–9.84 m.
CAO-OW-0709-MWC-50	Reddish orange, unconsolidated, very thinly laminated, fine-grained sand with white concretionary blebs (<2 mm). Height above base of section is 9.88–9.92 m.

Sample	Description
Main West Crater Section Cont'd (listed bottom to top)	
CAO-OW-0709-MWC-51	Gray to whitish tan, irregular and hummocky, very finely laminated, fine-grained sand interbedded with tan silt. Height above base of section is 10.06–10.11 m.
CAO-OW-0709-MWC-52	Gray to whitish tan, irregular and very finely laminated, fine-grained sand and silt. Height above base of section is 10.24–10.27 m.
CAO-OW-0709-MWC-53	Tan to whitish gray, massive and blocky, clayey silt. Height above base of section is 10.56–10.60 m.
CAO-OW-0709-MWC-54	Gray to whitish tan, irregular and very finely laminated, fine-grained sand and silt. Height above base of section is 10.93–10.97 m.
CAO-OW-0709-MWC-55	Tan to whitish gray, massive and blocky, clayey silt. Height above base of section is 11.06–11.10 m.
CAO-OW-0709-MWC-56	Reddish orange, unconsolidated, very thinly laminated, fine-grained sand. Height above base of section is 11.36–11.42 m.
CAO-OW-0709-MWC-57	Gray to whitish tan, irregular and very finely laminated, fine-grained sand and silt. Height above base of section is 11.61–11.65 m.

Sample	Description
Main West Crater Section Cont’d (listed bottom to top)	
CAO-OW-0709-MWC-58	Tan to whitish gray, massive and blocky, clayey silt. Height above base of section is 11.81–11.85 m.
CAO-OW-0709-MWC-59	Gray to whitish tan, irregular and very finely laminated, fine-grained sand and silt. Laminations visibly thicken and slope towards river. Height above base of section is 11.95–11.98 m.
CAO-OW-0709-MWC-60	Gray to whitish tan, irregular and very finely laminated, fine-grained sand and silt. Height above base of section is 12.07–12.11 m.
CAO-OW-0709-MWC-61	Gray to whitish tan, massive and blocky, clayey silt. Height above base of section is 12.61–12.65 m.
CAO-OW-0709-MWC-62	Brown to tan, massive, clayey silt bounded on top and bottom with indurated orange oxidation beds. Height above base of section is 12.93–12.98 m.
CAO-OW-0709-MWC-63	Gray to whitish tan, massive and blocky, clayey silt. Height above base of section is 13.20–13.24 m.
CAO-OW-0709-MWC-64	Gray to whitish tan, massive and blocky, clayey silt. Height above base of section is 13.41–13.45 m.
CAO-OW-0709-MWC-65	Gray to whitish tan, massive and blocky, clayey silt. Height above base of section is 14.04–14.08 m.

Sample	Description
Main West Crater Section Cont'd (listed bottom to top)	
CAO-OW-0709-MWC-66	Possible caliche layer. Height above base of section is 14.16–14.21 m.
CAO-OW-0709-MWC-67	Gray to whitish tan, massive silty sand with gravels up to 4 cm intermixed. Height above base of section is 14.93–14.98 m.
CAO-OW-0709-MWC-68	Gray to whitish tan, massive silty sand. Height above base of section is 14.71–14.75 m.
CAO-OW-0709-MWC-69	Gray to whitish tan, massive and blocky, clayey silt. Height above base of section is 14.85–14.88 m.
CAO-OW-0709-MWC-70	Laminated sand and pea gravel. Height above base of section is 14.92–14.96 m.
CAO-OW-0709-MWC-71	Gray to whitish tan, thinly laminated, silty sand. Height above base of section is 15.09–15.04 m.
West Crater Top Section (listed bottom to top)	
CAO-OW-0609-WCT-1	Gray, massive and blocky, clayey silt with some oxidation or mineralization along cracks between blocks. Height above base of section is .10–.16 m.
CAO-OW-0609-WCT-2	White tephra ash layer, distinct contacts. Height above base of section is.16–.17 m.

Sample	Description
West Crater Top Section Cont'd (listed bottom to top)	
CAO-OW-0609-WCT-3	Gray, massive and blocky, clayey silt with some oxidation or mineralization along cracks between blocks. Height above base of section is .42–.45 m.
CAO-OW-0609-WCT-4	Gray, massive and blocky, clayey silt with some oxidation or mineralization along cracks between blocks. Height above base of section is .80–.84 m.
CAO-OW-0609-WCT-5	Pale peach, massive and blocky, clayey silt bounded at the top and bottom by orange oxidation layers. Height above base of section is 1.17–1.19 m.
CAO-OW-0609-WCT-6	Gray, massive and blocky, clayey silt with some oxidation or mineralization along cracks between blocks. Height above base of section is 1.36–1.39 m.
CAO-OW-0609-WCT-7	Gray, massive and blocky, clayey silt with some oxidation or mineralization along cracks between blocks and roots. Height above base of section is 1.89–1.92 m.
CAO-OW-0609-WCT-8	Gray, massive and blocky, clayey silt with some oxidation or mineralization along cracks between blocks and roots. Height above base of section is 2.54–2.56 m.

Sample	Description
Main West Crater Section Cont'd (listed bottom to top)	
CAO-OW-0609-WCT-9	Gray, massive and blocky, clayey silt with some oxidation or mineralization along cracks between blocks and roots. Height above base of section is 2.93–2.96 m.
CAO-OW-0609-WCT-10	Grayish tan, unconsolidated, sand probably from eolian features covering the section. Height above base of section is 3.16–3.20 m.
Sand Springs Section (listed bottom to top)	
CAO-OW-0709-SS-1	Tan, fine-grained, massive, unconsolidated sand, possibly slope wash deposit. Height above base of section is .61–.65 m.
CAO-OW-0709-SS-2	Tan, fine-grained, massive, unconsolidated sand, possibly slope wash deposit. Height above base of section is 1.14–1.17 m.
CAO-OW-0709-SS-3	Tan, fine-grained, massive, unconsolidated sand, possibly slope wash deposit. Height above base of section is 2.13–2.16 m.
CAO-OW-0709-SS-4	Gray, very finely laminated with few very small cross-beds, fine-grained, sand, with tan silt. Height above base of section is 3.46–3.50 m.

Sample	Description
Sand Springs Section Cont'd (listed bottom to top)	
CAO-OW-0709-SS-5	Tan, very finely laminated, flakey, clayey silt. Height above base of section is 3.80–3.84 m.
CAO-OW-0709-SS-6	Rusty orange, massive, indurated, thin lamination of clayey silt. Height above base of section is 4.12–4.14 m.
CAO-OW-0709-SS-7	Gray tan, very finely laminated, silt. Height above base of section is 4.27–4.29 m.
CAO-OW-0709-SS-8	Orange, massive, indurated, thin lamination of clayey silt. Height above base of section is 4.40–4.41 m.
CAO-OW-0709-SS-9	Gray to whitish tan, very finely and irregularly laminated, fine-grained sand with tan silt, and blobs of massive sand and silt. Height above base of section is 4.72–4.76 m.
CAO-OW-0709-SS-10	Orange, thinly laminated, indurated, thin lamination of clayey silt. Height above base of section is 4.92–4.96 m.
CAO-OW-0709-SS-12	Tan and gray, unconsolidated, massive, clayey silt blob with gravel next to sample CAO-OW-0709-SS-11. Height above base of section is 4.96–5.00 m.
CAO-OW-0709-SS-11	Gray to whitish tan, very finely laminated, cross-bedded, fine-grained sand and tan silt. Height above base of section is 5.03–5.05 m.

Sample	Description
Sand Springs Section Cont’d (listed bottom to top)	
CAO-OW-0709-SS-13	Light gray to tan, very thinly laminated, blocky, clayey silt. Height above base of section is 5.15–5.19 m.
CAO-OW-0709-SS-14	Gray to whitish tan, faintly laminated to massive, blocky, clayey silt. Height above base of section is 5.36–5.40 m.
CAO-OW-0709-SS-15	Gray to whitish tan, very finely laminated, cross-bedded in places, fine-grained sand, with unconsolidated massive blobs of silt, sand, and gravels that laminations do not deform around. Height above base of section is 5.71–5.73 m.
CAO-OW-0709-SS-16	Gray to whitish tan, faintly laminated to massive, blocky, clayey silt. Height above base of section is 6.05–6.09 m.
CAO-OW-0709-SS-17	Red (probably from oxidation), unsorted, gravels with sand and silt. Height above base of section is 6.23–6.28 m.
CAO-OW-0709-SS-18	Gravel, sand, silt, and basalt pieces up to 10 cm across, probably a type of slope wash covering deposit. Height above base of section is 7.11–7.16 m.
Saddle Butte 1 Section (main)	
CAO-OW-0609-SB1-1	Gray to whitish tan, massive and blocky, clayey silt, with roots and oxidized areas of orange and red. Height above base of section is .06–.10 m.

Sample	Description
Saddle Butte 1 Section (main) Cont'd (listed bottom to top)	
CAO-OW-0609-SB1-2	Light brown with tan to white swirls, thin lamination of silty clay. Height above base of section is .11–.13 m.
CAO-OW-0609-SB1-3	Gray to whitish tan, massive and blocky, clayey silt, with roots and oxidized areas of orange and red. Height above base of section is .51–.54 m.
CAO-OW-0609-SB1-4	Gray to whitish tan, massive and blocky, clayey silt, with roots and oxidized areas of orange and red. Height above base of section is 1.02–1.06 m.
CAO-OW-0609-SB1-5	Gray to whitish tan, massive and blocky, clayey silt, with few oxidized areas of orange and red. Height above base of section is 1.61–1.65 m.
CAO-OW-0609-SB1-6	Gray to whitish tan, massive and blocky, clayey silt, with few oxidized areas of orange and red. Height above base of section is 2.11–2.15 m.
CAO-OW-0609-SB1-7	Gray to whitish tan, massive and blocky, clayey silt, with few oxidized areas of orange and red. Height above base of section is 2.55–2.60 m.
CAO-OW-0609-SB1-8	Rusty orange, very thin lamination of clayey silt, probably an oxidized layer. Height above base of section is 2.88 –2.89 m.

Sample	Description
Saddle Butte 1 Section (main) Cont’d (listed bottom to top)	
CAO-OW-0609-SB1-9	Gray to whitish tan, massive and blocky, clayey silt, with few oxidized areas of orange and red. Height above base of section is 3.36–3.39 m.
CAO-OW-0609-SB1-10	Gray to whitish tan, massive and blocky, clayey silt, with few oxidized areas of orange and red. Height above base of section is 3.91–3.94 m.
CAO-OW-0609-SB1-11	Gray to whitish tan, faintly laminated to massive, clayey silt. Height above base of section is 4.46–4.49 m.
CAO-OW-0609-SB1-13	Gray to whitish tan, massive and blocky, clayey silt. Height above base of section is 4.89–4.93 m.
CAO-OW-0609-SB1-12	Gray to whitish tan, very fine and wavy laminations, sometimes cross-bedded, fine-grained sand with tan silt. Height above base of section is 4.93–4.97 m.
CAO-OW-0609-SB1-14	Gray to whitish tan, massive and blocky, clayey silt. Height above base of section is 5.44–5.48 m.
CAO-OW-0609-SB1-15	Gray to whitish tan, massive and blocky, clayey silt. Height above base of section is 5.87–5.90 m.
CAO-OW-0609-SB1-16	Orange, massive, sandy silt thin lamination. Height above base of section is 6.03–6.07 m.

Sample	Description
Saddle Butte 1 Section (main) Cont’d (listed bottom to top)	
CAO-OW-0609-SB1-17	Gray to whitish tan, irregular lamination of fine-grained sand. Height above base of section is 6.15–6.17 m.
CAO-OW-0609-SB1-18	Gray to whitish tan, very thinly laminated, fine-grained sand and silt, with concretions of rusty orange and red sand. Height above base of section is 6.32–6.36 m.
CAO-OW-0609-SB1-19	Gray to whitish tan, massive and blocky, clayey silt. Height above base of section is 6.48–6.52 m.
CAO-OW-0609-SB1-20	Gray to whitish tan, massive and blocky, clayey silt. Height above base of section is 7.09–7.13 m.
CAO-OW-0609-SB1-21	Gray to whitish tan, massive and blocky, clayey silt. Height above base of section is 7.78–7.82 m.
CAO-OW-0609-SB1-22	Grayish tan, very finely laminated, fine-grained, sand with thin stripe of orange through the middle. Height above base of section is 8.16–8.18 m.
CAO-OW-0609-SB1-23	Gray to whitish tan, massive and blocky, clayey silt. Height above base of section is 8.64–8.68 m.
CAO-OW-0609-SB1-24	Gray to whitish tan, massive and blocky, clayey silt. Height above base of section is 9.25–9.29 m.
CAO-OW-0609-SB1-25	Gray to whitish tan, massive and blocky, clayey silt. Height above base of section is 9.80–9.85 m.

Sample	Description
Saddle Butte 1 Section (main) Cont’d (listed bottom to top)	
CAO-OW-0609-SB1-26	Gray to whitish tan, silt, sand, and pea gravel with very thin laminations that dip ~ 10 degrees towards the river (west). Height above base of section is 10.10–10.14 m.
CAO-OW-0609-SB1-28	Gravels from sample CAO-OW-0609-SB1-26 grade upward into sand with few small pea gravels and white balls of clastic material. Height above base of section is 10.30–10.34 m.
CAO-OW-0609-SB1-27	Tan, very finely laminated, fine-grained sand. Height above base of section is 10.41–10.45 m.
CAO-OW-0609-SB1-29	Gray to whitish tan, massive and blocky, clayey silt. Height above base of section is 11.04–11.08 m.
CAO-OW-0609-SB1-30	Light tan, massive, unconsolidated, silty sand with angular pieces of basalt up to 10 cm across and smaller carbonate covered gravels. Height above base of section is 12.17–12.20 m.
CAO-OW-0609-SB1-31	Light tan, massive, unconsolidated, silty sand with few gravel. Height above base of section is 12.87–12.90 m.
CAO-OW-0609-SB1-32	Pea gravel above very thin silty clay lamination, possibly a small channel. Height above base of section is 14.16–14.20 m.

Sample	Description
Saddle Butte 1 Section (incised section) Cont’d (listed bottom to top)	
CAO-OW-0609-SB1-33	Thinly laminated and shallowly cross-bedded pea gravels and sand that fines towards center of bed. Height above base of incised section is .21–.24 m.
CAO-OW-0609-SB1-34	Grayish tan, massive, interfingering lense of clayey silt into the sand of CAO-OW-0609-SB1-33. Height above base of incised section is .29–.30 m.
CAO-OW-0609-SB1-35	Thinly laminated and shallowly cross-bedded pea gravels and sand that fines upward. Height above base of incised section is .40–.44 m.
CAO-OW-0609-SB1-36	Gray to tan, very thinly laminated and sometimes cross-bedded, sandy silt. Height above base of incised section is .81–.85 m.
CAO-OW-0609-SB1-37	Gray to tan, very thinly laminated and sometimes cross-bedded, sandy silt. Height above base of incised section is 1.30–1.34 m.
CAO-OW-0609-SB1-38	Thinly laminated and shallowly cross-bedded pea gravels and sand that fines upward. Height above base of incised section is 1.81–1.85 m.
CAO-OW-0609-SB1-39	Thinly laminated and cross-bedded pea gravels and sand. Height above base of incised section is 2.12–2.16 m.

Sample	Description
Saddle Butte 1 Section (incised section) Cont’d (listed bottom to top)	
CAO-OW-0609-SB1-40	Thinly laminated and cross-bedded pea gravels and sand. Height above base of incised section is 2.40–2.44 m.
CAO-OW-0609-SB1-41	Tan, very finely laminated, fine-grained, silty sand. Height above base of incised section is 2.94–2.99 m.
CAO-OW-0609-SB1-42	Tan, very finely laminated, fine-grained, silty sand. Height above base of incised section is 3.33–3.44 m.
CAO-OW-0609-SB1-43	Light tan, very finely laminated, fine-grained, silty sand with the occasional > 1 cm pea gravel. Height above base of incised section is 3.86–3.91 m.
CAO-OW-0609-SB1-44	Tan, very finely laminated, fine-grained, silty sand. Height above base of incised section is 4.03–4.06 m.

Appendix B

Elevation Data: Lava Dams, Stratigraphic Sections, Terraces, and Other Features

Feature	Description	River Km	Elevation GPS (m)	Elevation LiDAR (m)
Lava Dams				
WC Lava Dam	Crest	38	1030.0	1030
SB2 Lava Dam	Crest	30.5	1042.0	1042
SB1 Lava Dam	Top Surface	29.6	1017.1	1014
		28.8		1008
BR Lava Dam	Crest	51.5	1200.0	
Stratigraphic Sections				
CH Section	Section top	37.65	997.0	990
	Section base	37.65	974.5	
MWC Section	Gravel cap top	37.55	1017.7	1017
	Fine seds top	37.55	1016.2	
	Section base	37.55	1002.2	
TPZ Section	Gravel cap top	38	1012.0	1007
	Fine seds top	38	1007.6	
WCT Section	Section top	38	1029.0	1023
	Section base	38	1025.7	
SS Section	Gravel cap top	30.5	1019.0	1014
	Fine seds top	30.5	1017.1	
	Section base	30.5	1012.2	
Upper SS	Fine seds top	30.5	1042.4	
SB1 Section	Fine seds top	27.65	1044.2	1040
	Section base	27.65	1028.0	
	Channel base	27.65	1032.9	1030
SB2 Precarious Section	Gravel cap top	36.5	1021.3	1022
	Fine seds top	36.5	1021.0	

Feature	Description	River Km	Elevation	
			GPS (m)	LiDAR (m)
Stratigraphic Sections				
Artillery Sediment Pods	1 Gravel cap top	35.5	996.0	992
	1 Fine seds top	35.5	995.9	
	2 Gravel cap top	35.5	997.3	994
Rome Valley Borrow Pits	1 Gravel top	1	1039.0	
	1 Gravel base	1	1034.8	
	2 Gravel top	1	1041.2	
	2 Gravel base	1	1035.1	
Terraces				
CH Levels	Step 1	37.65	979.3	974
	Step 2	37.65	993.6	988
	Step 3	37.65	997.3	990
Levels near MWC	Hill1 Gravel cap top	37.7	1006.1	1001
	Hill1 Fine seds top	37.7	1004.6	
	Hill2 Gravel cap top	37.7	1006.1	1002
	Hill2 Fine seds top	37.7	1004.0	
	Hill3 Gravel cap top	37.7	997.6	993
	Hill3 Fine seds top	37.7	996.0	
	4 Gravel cap top	37.4–37.8	966.5	964
Boulder Line near MWC	Boulder deposit top	37.7	992.4	986
Boulder Line near TPZ	Boulder deposit top	38	994.5	990
Boulder Line near RGC	Boulder deposit top	38.7		980
MWTB Levels	Gravel cap top	35.7–35.9	995.4	987
	Fine seds top	35.7–35.9	977.0	
Levels north of MWTB	1 Gravel cap top	36		1004
	2 Gravel cap top	36		997
	3 Gravel cap top	36.1		976
	4 Gravel cap top	36.2		973
	5 Gravel cap top	36.3		998
	6 Gravel cap top	36.35		996
	7 Gravel cap top	36.42		955

Feature	Description	River Km	Elevation	
			GPS (m)	LiDAR (m)
Terraces				
Levels south of MWTB	1 Gravel cap top	34.8–35.3		958
	2 Gravel cap top	34.8–35.3		966
	3 Gravel cap top	34.8–35.3		974
Artillery Levels	Mid. Gravel cap top	35.4–35.9	978.0	974
	N. Gravel cap top	35.4–35.9	981.0	975
	S. Gravel cap top	35.4–35.9	978.0	976
SB1 Level	Gravel cap top	27.7–29.5		1022
SS Levels	A	29.2–29.3		1020
	A1	29.3–29.5		1022
	B	29.5–30		1017
	B1	30.2		1015
	B2	30.2–30.5		1015
	C	29.8–30		1014
	D	30.2–30.5		1008
Dog Leg Terraces	T5	44.7–46.85		970
	T4 Gravel cap top	44.7–46.85		962
	T3	44.7–46.85		938
	T2	44.7–46.85		934
	T1	44.7–46.85		928